Abstract

SYNTHESIS OF NON-NATURAL FMOC-PROTECTECTED AMINO ACIDS TO PROVIDE NOVEL FLUORESCENT ANION PROBES AND THEIR INCORPORATION INTO SYNTHETIC PEPTIDES

by

David Percy Farrell

June 2015

Director of Thesis: Dr. William E. Allen

Major Department: Chemistry

Cystic fibrosis is a genetic disorder caused by mutations of the cystic fibrosis transmembrane conductance regulator (CFTR) protein. CFTR serves to control the gradient of chloride and bicarbonate ions across the cellular membrane of epithelial tissues (e.g., mucosa, intestinal walls, and lungs). Excess chloride on the inside of epithelial cells causes mucus in the lungs to become very thick. This thickening is responsible for a patients' characteristic thick sputum, coughing, and trouble breathing. The thick mucus also creates an ideal environment for opportunistic bacteria like Pseudomonas aeruginosa and Mycobacterium tuberculosis to take residence and proliferate. Very little is known about the transmembrane structure of CFTR, but with current therapies a single mutation can shorten a person's life by about 50%.

Many researchers have attempted to bypass the CFTR protein and synthesize anion shuttle transporters or transmembrane pores. The research presented here focuses on the synthesis of anion-responsive amino acids, for eventual incorporation into membrane-spanning peptides. Amino acids **2.1** and **2.2** were successfully synthesized from commercially available Fmoc-Glu-OtBu and Fmoc-Asp-OtBu through the conversion of an acid azide into an isocyanate via a Curtis Rearrangement. An *N*-substituted-4-amino-naphthalimide was chosen as the

chromophore due to its ability to absorb and emit light at a significantly longer wavelength than those produced by naturally occurring amino acids. The fluorescence provides an indirect insight into the binding strength of the novel amino acids, and eventually designer peptides, to various biologically relevant anions. The fluorescence can also be used by a researcher to learn more about a peptides concentration, location, microenvironment, structure, and mechanism of action. The presence of a fluorenylmethyloxycarbonyl (Fmoc) protecting group allows a researcher to use standard solid phase peptide synthesis protocols to produce either a known peptide or any imaginable variation. Fluorescent amino acids are useful tools in grasping a better understanding of protein channelopathies such as cystic fibrosis. One day, the use of synthetic peptide ion channels will be an effective therapy to alleviate the many symptoms and even the causes of death that afflicts the many patients suffering from channelopathies today.

(2.1)

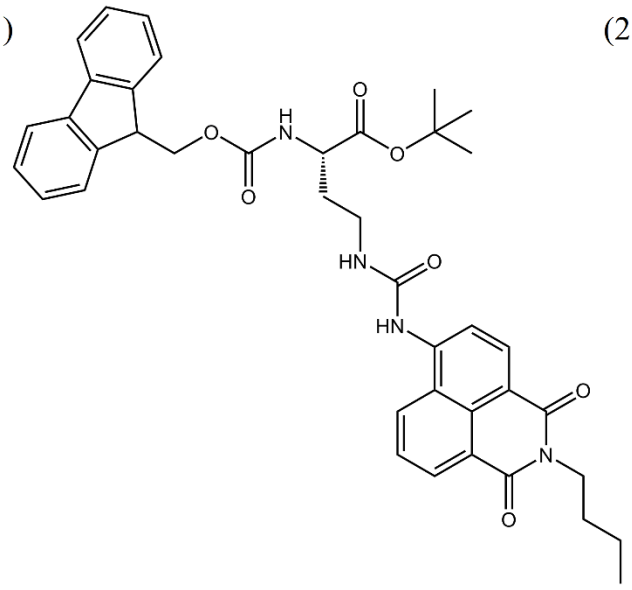

(2.2)

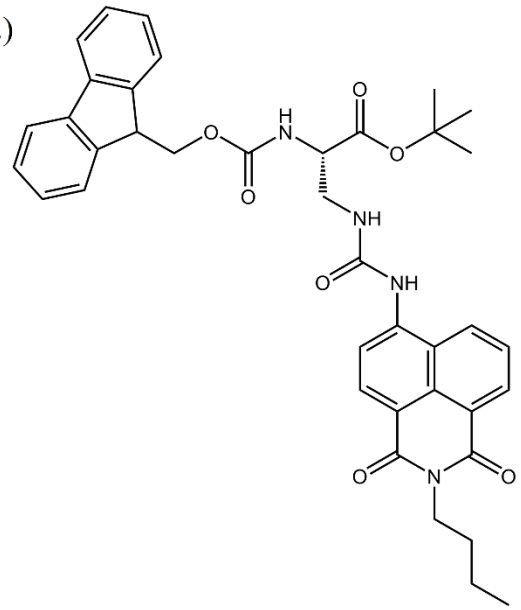

SYNTHESIS OF NON-NATURAL FMOC-PROTECTECTED AMINO ACIDS TO PROVIDE NOVEL FLUORESCENT ANION PROBES AND THEIR INCORPORATION INTO SYNTHETIC PEPTIDES

A Thesis

Presented to

the Faculty of the Department of Chemistry

East Carolina University

In Partial Fulfillment

of the Requirements for the Degree

Master of Science in Chemistry

by

David Percy Farrell

June, 2015

SYNTHESIS OF NON-NATURAL FMOC-PROTECTECTED AMINO ACIDS TO PROVIDE NOVEL FLUORESCENT ANION PROBES AND THEIR INCORPORATION INTO SYNTHETIC PEPTIDES

by

David Percy Farrell

APPROVED BY:

DIRECTOR OF THESIS: _____
Dr. William E. Allen, PhD

COMMITTEE MEMBER: _____
Dr. Colin S. Burns, PhD

COMMITTEE MEMBER: _____
Dr. Anthony M. Kennedy, PhD

COMMITTEE MEMBER: _____
Dr. Paul W. Hager, PhD

CHAIR OF THE DEPARTMENT OF CHEMISTRY:

_____
Dr. Andrew T. Morehead, PhD

DEAN OF THE GRADUATE SCHOOL:

_____
Dr. Paul J. Gemperline, PhD

ACKNOWLEDGEMENTS

I would like to express my greatest gratitude to my thesis director, Dr. William (Toby) E. Allen, for his guidance throughout this rewarding experience. I would like to thank the Allen group members: Ryan, Ruby, Ashley, Jenna, Amanda, Jordan, Sarah, Ber and Maddie for their support and encouragement. Also, special thanks to my thesis committee for sharing their knowledge and experience.

To my family and those I love, thank you.

Finally, I would like to thank ECU, the Department of Chemistry, and the Burroughs-Wellcome Foundation for the financial support received during my tenure in the master's program.

TABLE OF CONTENTS

LIST OF TABLES

LIST OF FIGURES

LIST OF SCHEMES

LIST OF EQUATIONS

LIST OF ABBREVIATIONS

CHAPTER 1: SYNTHETIC ION TRANSPORTERS AND TREATING ION CHANNEL PATHOLOGIES

1.1 Membrane Transport of Anions and Cystic Fibrosis

To function properly, cells must maintain proper concentration gradients of small anions such as chloride (Cl^-) and bicarbonate (HCO_3^-) across their membranes. However, these charged species cannot cross the nonpolar membrane core on their own. When protein-mediated ion transport across lipid bilayers has been altered to the point of causing disease, a "channelopathy" occurs. Cystic fibrosis is perhaps the best-known. It burdens pediatric patients with serious complications and a 50% chance of death before the age of 12 without immediate and constant medical care.[1,2] Cystic fibrosis is caused by a genetic mutation that leads to a fatal change to the chloride channel protein *cystic fibrosis transmembrane conductance regulator* (CFTR). CFTR is a 1480 residue membrane protein that is part of the ATP-binding cassette superfamily of proteins. It is made up of two transmembrane portions (TMD), two nucleotide binding domains (NBD) that sit just on the inside of a cellular bilayer, and a regulatory domain.

Many mutations have been implicated as the cause for this disease but the most common is the deletion of a phenylalanine at the 508th position in the N-terminus NBD. This deletion causes the protein to improperly fold, leading to dysfunction and eventual premature degradation by the cell.[3,4] The key role of F508 in cystic fibrosis was deduced by the Thomas group out of the University of Texas at Dallas. They performed multiple missense mutations at the F508 position producing several mutant proteins with replacement residues instead of a phenylalanine.[5] At lower temperatures the replacement of phenylalanine with other amino acids provided a sequence that would fold into a tertiary structure similar to the wild type protein, and

function as such; with exception to tryptophan. The group also performed Western blot experiments to deduce the ability for the mutant NBD's to associate with the other domains that make up the total CFTR protein. These results along with other data led them to conclude that delF508 results in not only poor folding of the NBD, but also disruption to the surface of the NBD superstructure and thus the inability for it to associate with the other components of CFTR, specifically the transmembrane channel. If the nucleotide binding domain is unable to associate with and activate the TMD then the channel will not open for chloride transport.

What can be lost in the complex biology of the many causes of cystic fibrosis is the macro-physiology. A patient with cystic fibrosis has a dysfunctional chloride channel that when operable is responsible for the balance of ions in tissues that produce mucus, sweat, saliva, tears, and digestive enzymes.(6) The cysts that form on pancreatic tissue of patients with CF were so severe that it would inevitably lead to scarring or fibrosis and thus originated the name cystic fibrosis. Unfortunately, in the 19th century the scarring was only noticed during the autopsies performed on young children. In the 17th century children were 'cursed and destined for death' upon kissing the brow of a newborn and tasting salt. The connection that children with CF had saltier sweat led to the sweat test for diagnosis of CF in 1952 by Paul di Sant' Agnese. The most recognizable symptom of patients with cystic fibrosis is the difficulty they have with breathing and the thick sputum that they often cough up. Functional, wild-type CFTR allows for the flow of chloride back-and-forth across the cell membrane of lung epithelial tissue in response to the need for increased or decreased fluidity of the mucus. The trouble with breathing and the thick sputum are a direct result from the proteins' inability to transport chloride out of the cell into the extracellular matrix. As the chloride concentration increases on the inside of the cell so does the osmotic pressure; drawing water into the cell and causing the extracellular mucus to become very

thick. While, alone, the trouble breathing can be a life complicating symptom, it is tolerable and not deadly; however, the thick mucus is full of peptides, carbohydrates, minerals, and salts which make it a perfect medium for bacterial growth. In modern times, patients with cystic fibrosis can live well into their 30's with some making 40 or even 50, but this typically requires constant medical care and invasive procedures like lung transplantation.[2-6] While the symptoms are manageable, prophylactic antibiotic treatments breed ever stronger and more resistant opportunistic pathogens, eventually leading to an incurable infection and death.

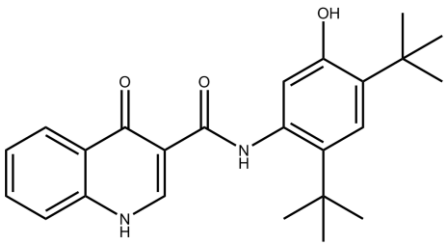

Figure 1.1: Ivacaftor

The development of small molecule therapies for channelopathies like cystic fibrosis is of ever increasing importance. Currently, only one pharmaceutical, Ivacaftor, is available on the market as a CFTR modulator, which targets the underlying cause of CF; a few other formulations are currently in phase III of clinical trials.[5,6] Ivacaftor acts to restore the CFTR proteins ability to transport chloride; however, until recently it was only available to patients with the G551D mutation, making up only a small percentage of the patient population.[6] Ivacaftor has recently been made available by the FDA to nine additional mutations, but these still fail to add up to anything greater than 3.0 % of the patient population. Several research groups have simply bypassed the CFTR protein and attempted to synthetically restore chloride transport using small molecular shuttles or pore forming cyclic peptides.

1.2 Synthetic Anion Transporters

1.2.1 Shuttles

Busschaert et. al. have developed a tripodal tris(2-ureidoethyl)amine moiety that is able to act as a chloride/bicarbonate antiporter shuttle.[1,7] Urea is a commonly used hydrogen-bond donor in the production of neutral anion receptors. The shuttle produced by Busschaert is able to slide through the non-polar portion of a bilayer by simply forming a cage around the anion, and effectively masking the charge.

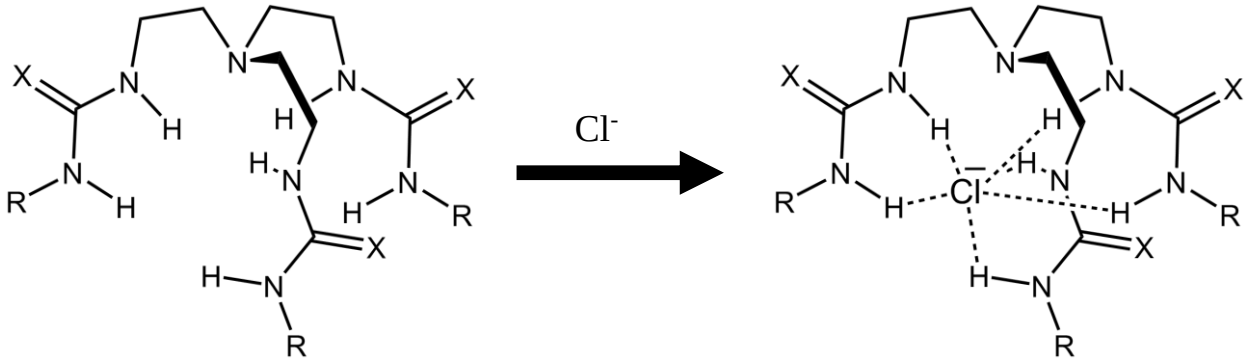

Figure 1.2: A representation of how a tris(2-amino-ethyl)amine based urea or thiourea derivative forms a cage around a chloride atom and conceals its charge as the complex shuttles across a lipid bilayer.

Another genre of anion shuttles made popular out of the University of Texas at Austin by the Sessler group are calix[4]pyrroles (Figure 1.3).[8,9] Again the molecule masks the charge of the anion and acts as a shuttle to transport the anion across a lipid bilayer. In this case the calix[4]pyrrole forms a cup and stabilizes the anion through hydrogen bonding. A paper published in 2006 by Sessler and coworkers used isothermal titration calorimetry and nuclear magnetic resonance to determine how differences in solvents and countercations could affect the ability for the calices to bind to an anion.[30] The group was able to extract K_{assoc} constants for

meso-octamethylcalix[4]pyrrole, **6**, binding with chloride through their ITC experiments. In acetonitrile the K_{assoc} was found to be $1.9 \pm 0.4 \times 10^5$ and $2.2 \pm 0.2 \times 10^5$ M^{-1} for tetraethylammonium chloride and tetrabutylammonium chloride, respectively. The researchers found that it was difficult to develop a pattern for whether tetrabutylammonium or tetraethylammonium was the better countercation for forming the calix + anion complex. They also found it difficult to see a pattern in how the polarity of the solvent affected complexation. Nonetheless, Gale et. al. were able to provide significant evidence that calix[4]pyrrole and its derivatives are very effective binders to chloride and are great transporters of the anion across lipid bilayers. The calix[4]pyrrole system has been expanded on to include additional bridged anion binding moieties, such as triazole rings,[10] and now include calix[4]thiophenes and calix[4]furans.[11]

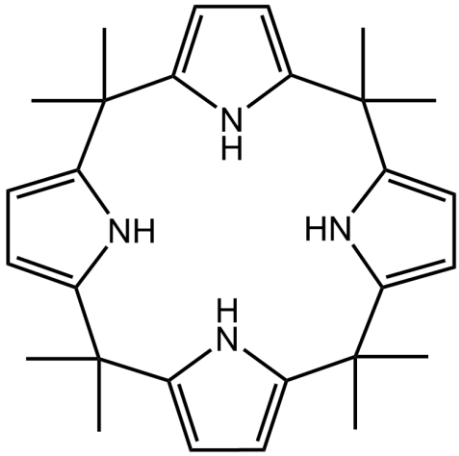

Figure 1.3: *meso*-octamethylcalix[4]pyrrole

1.2.2 Transmembrane Structures

Ideally, an anion transporting therapeutic would come in the form of an inhalant. Cystic fibrosis patients have an increased concentration of chloride on the inside of epithelial cells and thus a therapeutic would need to have the ability to encourage anion transport whilst originating on the exterior of a cellular matrix. While anion shuttles provide a mechanism for the transport of selective anions, they lack a sense of permanency. If they were to be used for the treatment of cystic fibrosis, patients would have to be constantly dosed with the drug because free-floating

shuttles lack an ability to control localization; and this opens questions as to how rapidly these molecules will diffuse through tissue and no longer remain in the most exterior epithelial cells of respiratory tissues. Another class of anion transporting structures are known as self-assembling transmembrane superstructures or channels.

Dr. Steven L. Regen at Lehigh University synthesized one of the earliest attempts at anion transport using a mimic of the antimicrobial sterol squalamine (Figure 1.4).[12,13] The compound showed surprising sensitivity for anions as well as membrane selectivity. The experiment was carried out using liposomes made from phosphatidylglycerol and phosphatidylcholine lipids hydrated in buffer containing sodium chloride, pyranine and HEPES buffer (pH 7.0). Using the fluorescent, pH-sensitive dye pyranine the Regen group was able to indirectly observe a change in pH after introduction of the squalamine-like derivative (Figure 1.4(b)). By trapping the water soluble fluorophore on the inside of liposomes the group could measure the rate at which the pH changed through a rate of change in fluorescence. To ensure that the pH change was not due to sodium transport $^{23}Na^{+}$-NMR experiments were performed on liposomes with $^{23}NaCl$. No transport of sodium was seen and thus the group was able to conclude that the change in pH across the lipid bilayers was a result of either H^{+}/Cl^{-} symporter or Cl^{-}/OH^{-} antiporter activity.

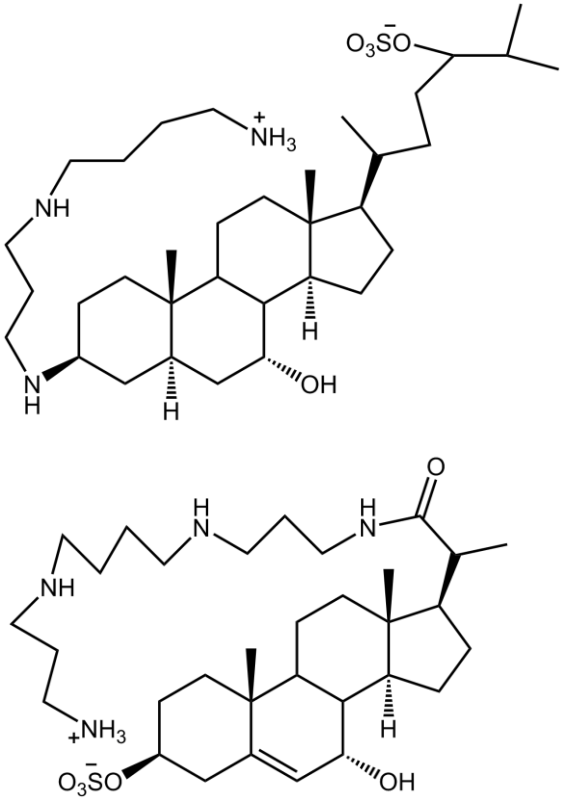

Figure 1.4: (a) Squalamine and (b) anion transporter derivative

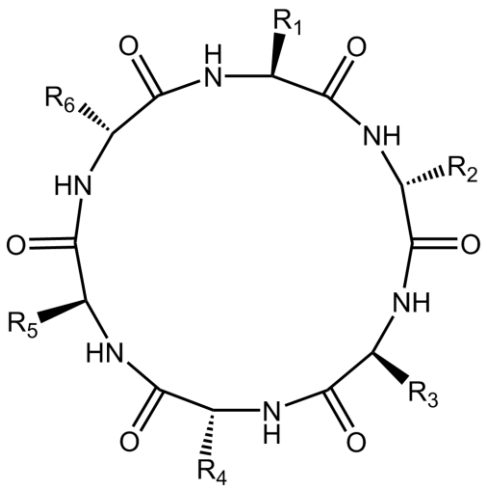

Figure 1.5: Generic example of a cyclic peptide that contains alternating D- and L-amino acids.

The Ghadiri group at The Scripps Research Institute have produced cyclic peptides with all of the side chains radiating out from the center by alternating the amino acid sequence with D and L stereoisomers. An example of a single ring is represented in Figure 1.5. The resulting peptides can self-assemble into nanotubes through a synthetic lipid bilayer by means of several β-sheetlike backbone hydrogen bonds that stabilize the structure without the formation of a net dipole that is commonly known to occur in α-helical peptide species.[14,15] The Ghadiri group found that with charge modification (net + or -) of the terminal cyclic rings led to some level of selectivity for cation transport. From a paper published in 2001 by Ghadiri et. al. it appears that the only method for anion selectivity is mediated through pore diameter; which is achieved by simply decreasing or increasing the number of amino acid residues that are used to make the original ring.[16,17]

What anion shuttles lack in permanency they make up for in selectivity and where nanotubes have the potential as a long term channel they lack selectivity for anions. The work of Jessen et. al. have expanded on the idea that urea moieties make effective hydrogen bond receptors for anions and incorporated them into a fluorescent pseudo-lipid molecule.[18]

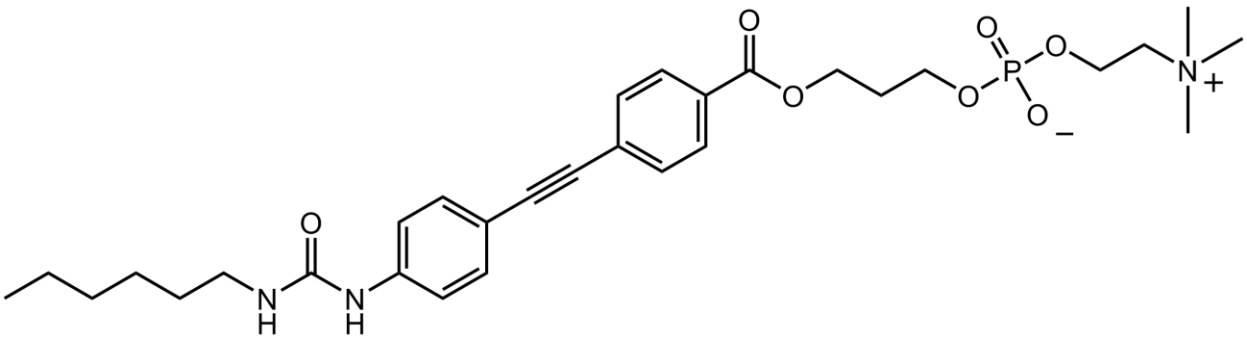

Figure 1.6: The pseudo-lipid, diarylacetylene fluorophore designed by Jessen et. al. to spontaneously incorporate into a synthetic lipid bilayer.

This structure was designed to spontaneously incorporate into a liposomal membrane in a fashion that would localize the ureido, neutral anion receptor inside the nonpolar region of the bilayer. The urea moiety has the potential to stabilize and conceal the negative charge of an anion during its transition through a lipid bilayer.[1] The fluorescence aspect can be used as evidence to signal whether the compound had localized into the lipid bilayer or remained in the aqueous solution due to solvatochromism. Finally, the fluorescence was also used as a technique to measure the novel molecules ability to bind to a series of anions. Jessen and coworkers found that the pseudo lipid had a strong affinity for several anions (K_{assoc} (M^{-1})): bicarbonate (>10^5), dihydrogen phosphate (3.7 x 10^5), chloride (2.9 x 10^5), and nitrate (1.0 x 10^5).[18]

1.3 Membrane-spanning peptides

A relatively new method for the transport of ions across lipid bilayers is the de-novo design of helical peptides.[19,20] Merrifield SPPS opened the door to the production of nearly an endless library of peptides that is limited by available building blocks and an experimenters' imagination. Attempting to synthesize a novel peptide that will form a helix that will spontaneously insert into a cellular membrane requires attention to several factors such as

residue sequence, polarity, length of peptide, and efficiency of synthesis (not all sequences are created equal).[19,20] When a peptide interacts with the interior, non-polar portion of a lipid bilayer, it must conceal the backbone groups capable of hydrogen bonding. In order to do this, transmembrane peptides must take on secondary structure, the most common of which is an alpha-helix. With the backbone of a helix stabilized the next consideration is the many residue sidechains that radiate outwards from the central axis of the helical tube. The amino acid residues of a transmembrane peptide, especially those that interact with the non-polar interior of a lipid bilayer, must be made-up of mostly non-polar residues. When deciding which residues should be used to cap the N and C terminus of a novel peptide it is recommenced that aromatic residues are used at the interface between the non-polar lipid tails and polar head groups of a bilayer; polar residues are used for those directly interacting with the head groups or solvent.[21]

Dr. Krishna Kumar at Tufts University has worked on producing transmembrane α-helical peptides that will spontaneously form dimer and tetramer bundles. This was done by transforming natural leucine residues into hexa-fluorinated leucine.[22] The novel peptide, studded with newly fluorinated residues, will form aggregates due to the unique propensity of poly-fluorinated substances to spontaneously associate. Dr. Kumar was able to control the size of the respective bundles by how often in the primary sequence a natural leucine was substituted with a hexa-fluorinated derivative. When Dr. Christian Anfinsen first demonstrated the reversible unfolding of ribonuclease A it became very apparent that tertiary structure is vitally linked to the primary sequence of a protein, Anfinsen's dogma.[23] Alpha helices are often represented on a

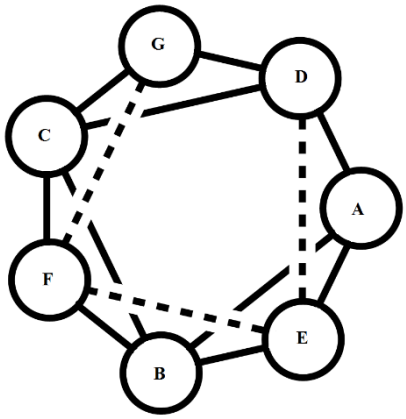

Figure 1.7: Example of an α-helical wheel diagram.

two dimensional plane using a flat representation known as a wheel diagram. One is represented in Figure 1.7. The wheel diagram provides a good representation of the fact that an alpha helix contains different sides or faces, and because of this property a researcher can control the characteristics of a face by substituting various residues at every full turn of the helix. Dr. Kumar did just this by placing all of his poly-fluorinated leucine residues at one face of the peptide.

Dr. William Degrado's research group at the University of California SF developed a transmembrane peptide that spontaneously formed a four-helix bundle and was capable of selectively transporting Zn^{2+} across a lipid bilayer, named 'Rocker'.[(24)] The 'Rocker' peptide's namesake stems from a rocking mechanism that occurs when one end of the peptide bundle initially binds to an atom of zinc (II). This causes the peptide collection to squeeze more closely together at one end while spreading apart at the opposite end of the bundle. As the zinc (II) atom travels across the lipid bilayer the peptide structure rocks to accommodate the movement of the cation. This eventually causes the the once spread apart end of the bundle to come closer together and the opposite, previously close end, to spread apart. The activity of this peptide was done by picking the specific amino acids that would form the faces of the transmembrane alpha helix. On one face, **Side A**, the peptide had several aromatic residues (tyrosine and phenylalanine), and on another face, **Side C**, contains several alanine residues. These specific residues allowed for the individual peptides to aggregate into the desired tetramer, as well as leaves space for the rocking mechanism to occur. As for the transporting mechanism, Dr. Degrado placed histidine, serine, and glutamic acid residues on the face, **Side B**, between sides A and C. The more polar residues were situated towards the center of the tetramer where a pore was formed with the suitable geometry for the coordination of a zinc (II) ion.

1.4 Peptide design and synthesis

In general, proteins are necessarily complex in order to support their many functions that give rise to the many diverse living organisms that exist. Despite these intricacies, scientists are determined to better understand the relationship between a protein's structure and mechanism of action. The development of techniques like structural genomics and computational modeling have helped to expedite the process of structural elucidation.[25] The mechanism of protein function has been determined by these same techniques and many others, including solid phase peptide synthesis. Solid phase peptide synthesis (SPPS), developed by Robert Bruce Merrifield, has provided a method for rapidly synthesizing small physical portions of a protein in question. SPPS is useful for building small 6-40 residue peptides using theoretically any imaginable sequence of available amino acids. The polymerization occurs via an orchestrated exchange of terminal amine deprotection and amide bond formation (**Scheme 1.1)**. SPPS is limited by several factors, including but not limited to: amino acid deletions and duplications, diminishing synthetic efficiency, the availability of building blocks, and cost. The most common type of automated peptide synthesizers rely on so-called "Fmoc chemistry," in which the N atoms of the individual amino acid building blocks have been protected with 9-fluorenylmethoxycarbonyl (fmoc) groups (Scheme 1.1).

Scheme 1.1, Fmoc-Solid Phase Peptide Synthesis: A total representation of the sequence of steps that leads to the coupling of sequential amino acids in Fmoc-based solid phase peptide synthesis. (1) A polystyrene bead or resin with a methylbenzhydrylamine (MBHA) functional group is available for the coupling of the first amino acid. Note that the amino acids are protected on the backbone amino group in order to avoid unwanted multiple couplings of the same residue. (2) The first amino acid is activated on the free carboxylic acid to provide a better electrophile for amide bond formation. In this case *N,N,N′,N′*-Tetramethyl-*O*-(1*H*-benzotriazol-1-yl)uronium hexafluorophosphate (HBTU) is shown. (3) The first amide bond was formed and now the fmoc protecting group must be removed for coupling of the next residue. (4) The use of a secondary amine (piperidine is shown) is used to absorb the most acidic proton and initiate the cleavage of the fmoc protecting group. (5) The loss of the proton at the 9 position on fmoc causes the protecting group to kick off as an alkene. (6) The remaining carbamate on the amino acid falls apart as a free amine through the loss of carbon dioxide. (7) The next amino acid is activated on the carboxylic acid with HBTU for amide bond formation. (8) The coupling is complete and the cycle continues for the next residue.

Scheme 1.1, Fmoc-Solid Phase Peptide Synthesis: (continued.)

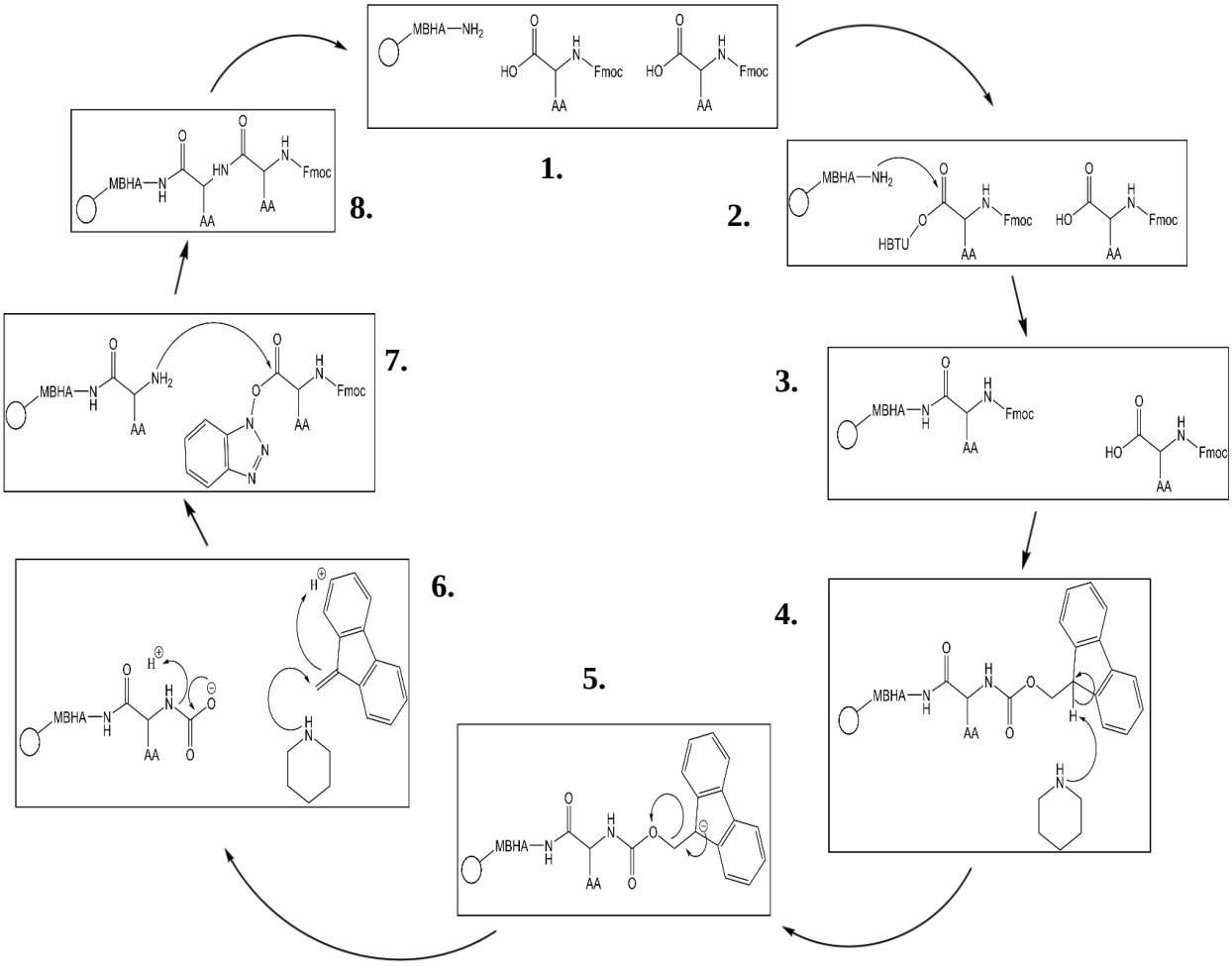

Another manner of studying proteins is to couple a fluorophore to the macromolecule. Small organic molecules that fluoresce can be used to do many things: allow an associated molecule to be tracked, the structural integrity of a molecule in vitro and in vivo can be elucidated, and the binding properties of a peptide can be quantitatively determined using fluorescence titrations.

1.5 Fluorescent Probes and Sensors

Fluorescence is a powerful technique for visualizing what occurs on the nearly invisible inner workings of a cellular microenvironment. A huge part of current biotechnology deals with development of fluorescent tags or markers for enzymes, bacteria, and cancerous tissue.[26,27,28] The incorporation of fluorescent markers into synthetic peptides using SPPS has allowed researchers to track the whereabouts and final destination of small proteins in living organisms.[29,30] Enzymatic mechanisms have also been elucidated using responsive fluorescent markers.[31]

The use of fluorescent probes has revolutionized the way scientists test the structural integrity of small peptides and proteins. The amino acids phenylalanine, tyrosine, and tryptophan all have intrinsic absorptive and fluorescent spectroscopic properties.[32] It is common for the unknown concentration of pure peptide in solution to be determined through an absorbance value along with the use of the Beer's law equation and a standard molar absorptivity. The molar absorptivity for tyrosine, phenylalanine, and tryptophan can all be found as standard values in specific solutions.[32] A group at the University of Pennsylvania synthesized

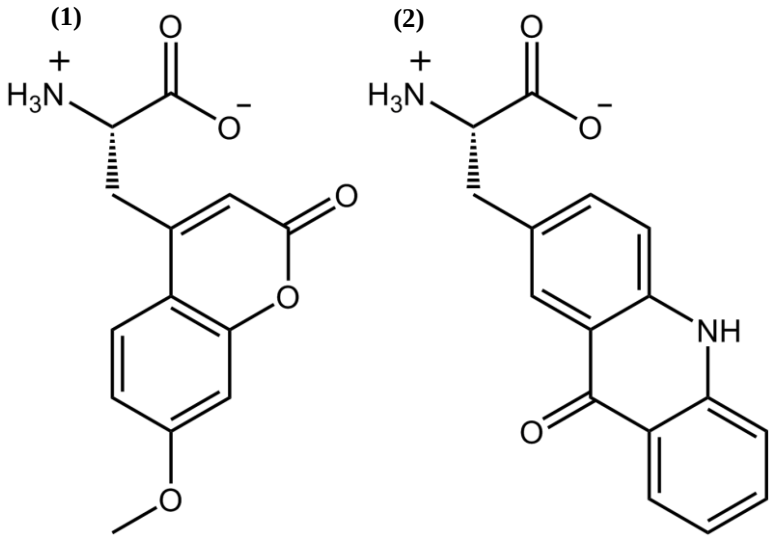

Figure 1.8: (1) 7-methoxycoumarin-4-ylalanine (λ_{ex}=325 nm, λ_{em}=393 nm) and (2) acridon-2-ylalanine (λ_{ex}=386 nm, λ_{em}=446 nm); all in phosphate buffer.

a set of fluorescent amino acids, **1.1** and **2.2** (Figure 1.8), that are quenched when in spatial association with an amino acid whose oxo-amide backbone has been replaced with a thioamide.[29] This means the group was able to engineer a series of small peptides in which the spatial significance to the novel chromophore of adjacent amino acids, modified to have a thioamide backbone, could be indirectly measured using fluorescence spectroscopy. The group used villin, a tissue specific actin binding protein that has been thoroughly characterized,[33,34] to provide evidence of a proof of concept model through temperature denaturation experiments. When the peptide was completely folded the fluorescent residue and thioamide residue were close together effectively quenching the fluorophore, and when the protein denatured, the emission signal increased.

The Martin group at the University of Utrecht in the Netherlands also synthesized a fluorescent amino acid, L-(7-hydroxycoumarin-4-yl)ethylglycine, **1.3**, and through protection of the α-N with 9-fluorenylmethyloxycarbonyl the product could be used on an automated solid phase peptide synthesizer, Figure 1.9.[30] They produced three different analogues of Leu-Enkephalin, a commonly used model peptide due to size and ease of preparation via SPPS. After successfully providing a model for a proof-of-concept with the production of the fluorescent Leu-Enkephalin derivatives the group moved on to produce a fluorescent analogues of the HIV-tat$_{48-60}$ peptide. It is well established that this peptide has significant implications in the ability of the HIV virus to infect

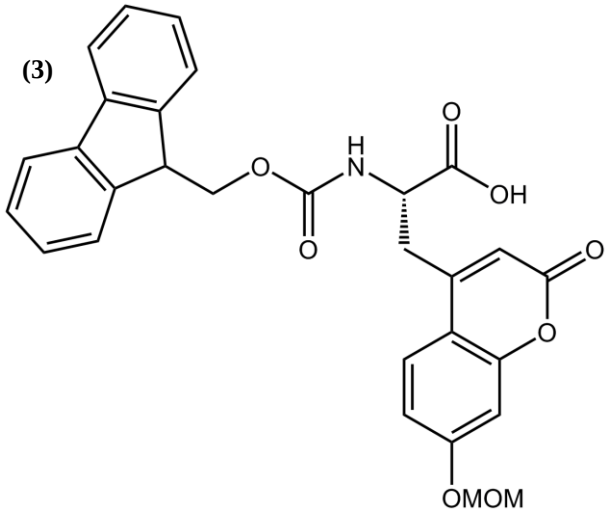

Figure 1.9: (**1.3**) *N*-Fmoc-L-(7-hydroxycoumarin-4-yl) ethylglycine (7-HC)

cells. The truncated, arginine rich region of the peptide, residues 48-60, is capable of crossing membranes and thus can be used to deliver molecular cargo into cells. The Martin group was successful in producing HIV-tat$_{48-60}$ with the fluorescent amino acid both at the C-terminus and in the middle of the peptide. Confocal microscopy was used on HeLa cells that were incubated with the fluorescent HIV-tat derivatives. The cells showed evidence of significant peptide uptake even with the addition of the larger unnatural amino acid.

Quenching or spectral shifts are properties of a fluorophore that can be measured and quantified into meaningful data.[35] These properties are most often manipulated via solvent polarities or the presence of ions.[36] The emission spectrum of a fluorescent compound will change with respect to its surroundings. For example, the fluorescence of 2-anilinonaphthalene will change significantly with a change from pure cyclohexane to a 0.2% concentration of ethanol in cyclohexane,[37] and at 3.0% or greater ethanol the emission spectrum changes very little. This high sensitivity is what makes fluorophores so useful for determining the conditions of previously inaccessible microenvironments, and one microenvironment in particular that seems to always be of great interest is the cellular membrane. The compound 1-pyrenehexadecanoic acid has been used since 1987 to determine the extent of water penetration into the hydrocarbon region of lipid bilayers.[37] This works because when the fluorophore is found in the nonpolar, hydrocarbon region of the bilayer it exhibits one type of emission spectrum, and when water penetrates into the nonpolar region the microenvironment of 1-pyrenehexadecanoic acid changes, and thus causes a change in the emission spectrum.

Compound **1.4**, developed by Brooks et. al. uses a combination of urea and amide hydrogen bond donors in a cyclic design to form a pocket for anion binding.[38] The group performs multiple experiments to test the solvent effects on the ability for anion binding. The association constants of **1.4** are analyzed using ^{1}H-NMR and the proton shifts that occur when those protons are shared between their respective nitrogen and the anion. Table 1.1 gives a collective representation of the association constants the group calculated. These results provide information about a few things. Compound **1.4** is much better at binding to carboxylate anions than it is to the other inorganic anions. The results also show how effective a small change in the amount of hydrogen bonding solvent present in the solvent can affect the ability for probe + anion complex to form. If a probe or sensor is based around the ability to form hydrogen bonds, then solvation effects are a significant matter that should be accounted for in an experiment.

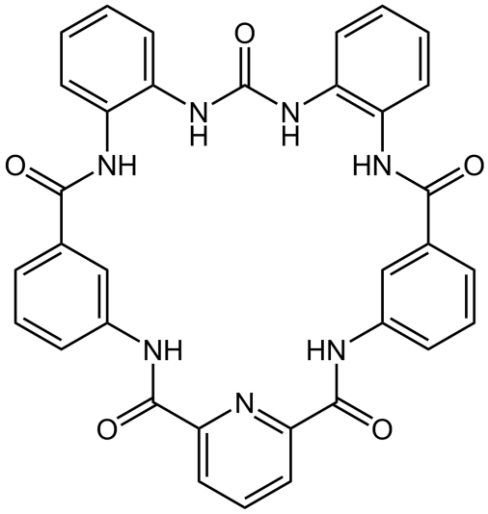

Figure 1.10: (**1.4**) A urea and multi-amide anion binder synthesized by Brooks et. al.

Table 1.1: The table provides the association constants for compound **1.4** with several anions using ^{1}H-NMR in DMSO-d_6 solutions containing different amounts of water. Generally, as the concentration of water increases the stability for the isolated anion is increased and does not bind as well.

	Association Constants (M^{-1})	
Anion (tetrabutylammonium salts)	DMSO-d_6-0.5% water	DMSO-d_6-5.0% water
Cl^-	194	42
Br^-	10	-
HSO_4^-	115	-
$H_2PO_4^-$	142	51
NO_3^-	<10	-
$CH_3CO_2^-$	16500	5170
$C_6H_5CO_2^-$	6430	1830

The design of small organic and supramolecular structures with the ability to sense anions is a constantly evolving area of supramolecular chemistry. The chelation abilities and anion sensing of these fluorophores are facilitated through the common motifs: amides, ureas, thioureas, pyrroles, indoles, and triazoles.[7,10,18,38-40] It is believed that this occurs through hydrogen bonding between the anion and the most electropositive hydrogen within each of these functional groups. An example of the

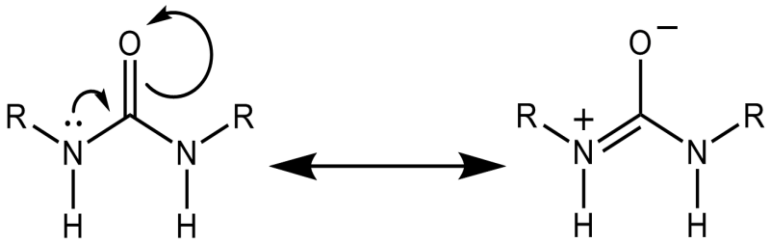

Figure 1.11: A representation of the resonance found in a single urea functional group and how this leads to a relatively acidic proton and efficient hydrogen bond donor.

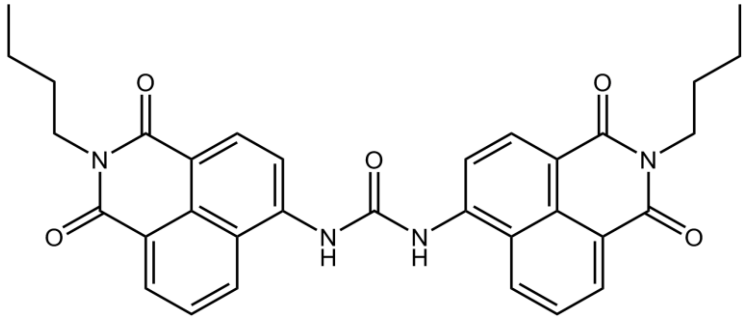

Figure 1.12: (**1.5**) *N*,*N*-dinaphthalimido urea

hydrogen bonding ability in a urea is given in Figure 1.11.

Fluorescent compounds are commonly used for the sensing of chloride, dihydrogen phosphate, fluoride, acetate, and bicarbonate. These particular anions are of great interest due to their relevance with medicine, food, biological systems and environmental remediation.[12] The most commonly used moiety for the production of neutral anion receptors is the urea functional group.[1,7,18,35,38,40-42] The Fabbrizzi group at the University of Pavia, Italy have expanded on the production of ureido-dimers, some of which have resulted in interesting colorimetric tests with fluoride through deprotonation.[35] In DMSO, addition of 1-5 equivalents of fluoride would deprotonate compound **1.5** (Figure 1.12) at one of the ureido N-H's, producing a vivid red color, and upon addition of greater than 10 equivalents the solution would take on a dark blue color. Their di-aryl urea groups also showed promise as colorimetric indicators for hydroxide, acetate, and dihydrogen phosphate. It was discovered that the association constant for dihydrogen phosphate and compound **1.6** (Figure 1.13) was 6.3 x 10^4.[42] Other association constants with phosphate are represented in Table 1.2.

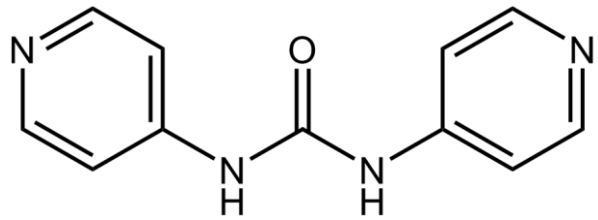

Figure 1.13: (**1.6**) *N,N*-dipyridino urea

Table 1.2: Reference table of several $H_2PO_4^-$ receptors and their K_{assoc} values.

Reference	DMSO-0.5% H_20	ACN	CH_2Cl_2 (DCM)
(38)	142		
(40) # 2	$>10^4$		
(40) # 4	523		
(41)		2344	
(42)		6.3 x 10^4	
(18) # 3			1.2 x 10^4
(18) # 4			3.7 x 10^5

1.6 Conclusion

Synthetic peptides represent a flexible platform for tissue and pathology-directed pharmacological design. As those peptides become more and more complex, the ability to accurately examine, manipulate, and functionalize designer peptides will be a flourishing area of research. The following chapters describe efforts to combine peptide scaffolds with fluorescent labels, allowing membrane incorporation and ion-transport function to be conveniently monitored. Synthesizing a library of fluorescent, anion responsive, protected amino acids that can be successfully incorporated into a peptide sequence via SPPS opens the door for use in multiple biotechnological fields.

CHAPTER 2: SYNTHESIS OF ANION SENSING FMOC-PROTECTED AMINO ACIDS

2.1 Results and Discussion

2.1.1 Introduction

This chapter describes the preparation and spectroscopic behavior of fluorescent non-natural amino acids that are environmentally sensitive, capable of binding specific anions, and can be successfully incorporated into designer synthetic peptides. The non-natural amino acids **2.1** and **2.2** (Figure 2.1) were successfully synthesized from commercially available (*S*)-4-(((9*H*-fluoren-9-yl)methoxy)carbonylamino)-5-*tert*-butoxy-5-oxopentanoic acid (Fmoc-Glu-OtBu) and (*S*)-3-(((9*H*-fluoren-9-yl)methoxy)carbonylamino)-4-*tert*-butoxy-4-oxobutanoic acid (Fmoc-Asp-OtBu). The fluorescent products **2.1** and **2.2** were evaluated for their response to titration with various biologically relevant anions and their ability to be inserted into peptides using standard solid phase synthesis protocols.

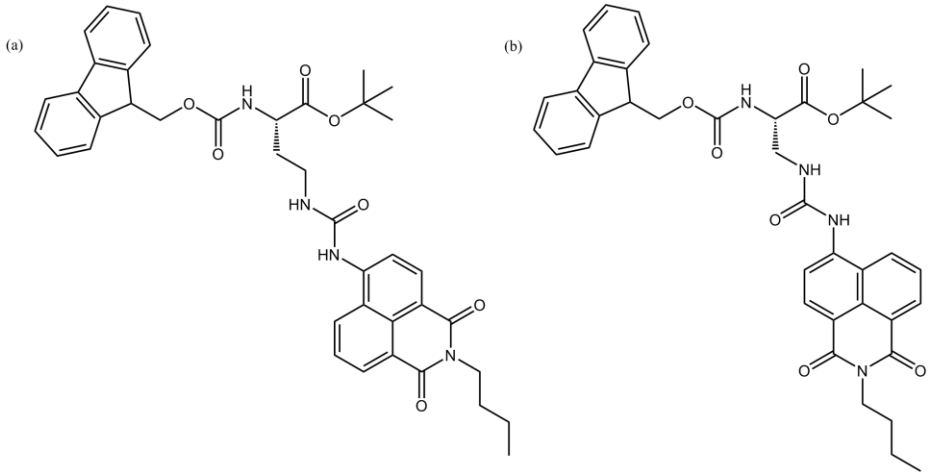

Figure 2.1: (a)(compound 2.1) (*S*)-*tert*-butyl 2-(((9*H*-fluoren-9-yl)methoxy)carbonylamino)-4-(3-(2-butyl-1,3-dioxo-2,3-dihydro-1*H*-benzo[*de*]isoquinolin-6-yl)ureido)butanoate **(b)(compound 2.2)** (*S*)-*tert*-butyl 2-(((9*H*-fluoren-9-yl)methoxy)carbonylamino)-3-(3-(2-butyl-1,3-dioxo-2,3-dihydro-1*H*-benzo[*de*]isoquinolin-6-yl)ureido)propanoate

2.1.2 Design and Synthesis

The non-natural amino acids **2.1** and **2.2** were chosen because they feature a urea group, which is a potential anion-recognition site, and a naphthalimide fluorophore, which has been shown to be bright and sensitive to its local micro-environment.[43,44] We recognized that reaction of a 4-aminonaphthalimide with an isocyanate (-N=C=O) would produce a urea with a directly-attached fluorescent reporter unit.

Synthesis of the requisite naphthalimide fluorophore was accomplished in a manner first developed by Triboni et. al. (Scheme 2.1).[46] Commercially available 4-nitro-1,8-naphthalic anhydride was mixed in a 250 ml Erlenmeyer flask along with 150 mL of distilled water and about 7 equivalents of n-butylamine. The reaction mixture was sonicated using a 50-60 mHz bath for 90 minutes or until all of the floating solid anhydride had suspended below the water surface. The mixture was then filtered through a fine frit glass funnel giving a 95% yield of crude solid after thoroughly drying on a high vacuum line to ensure removal of all remaining water. The solid *N*-butyl-4-nitro-1,8-naphthalimide was then placed in a Parr reaction bottle along with 200 mL anhydrous ethanol and 5 mole percent of 10% palladium on carbon catalyst. The reaction bottle was inserted into a hydrogenation apparatus, charged with 30 psi of hydrogen gas, and then shaken for 90 minutes or until all of the fluorophore had gone into solution. The amino-containing product is soluble in ethanol while the nitro compound is largely insoluble in ethanol. The catalyst was filtered off through two sheets of filter paper, and the filtrate evaporated to remove the organic solvent. The solid was then dissolved into a mixture of dichloromethane and methanol (9:1) and purified on a silica column via flash chromatography. The green band, easily identifiable with use of a 365 nm light bar, was collected and evaporated. Hydrogenation routinely gave a 65% overall yield for the production of 4-amino-*N*-butyl-1,8-naphthalimide, **2.3**.

Scheme 2.1: Synthesis of *N*-butyl-4-aminonaphthalimide fluorophore.

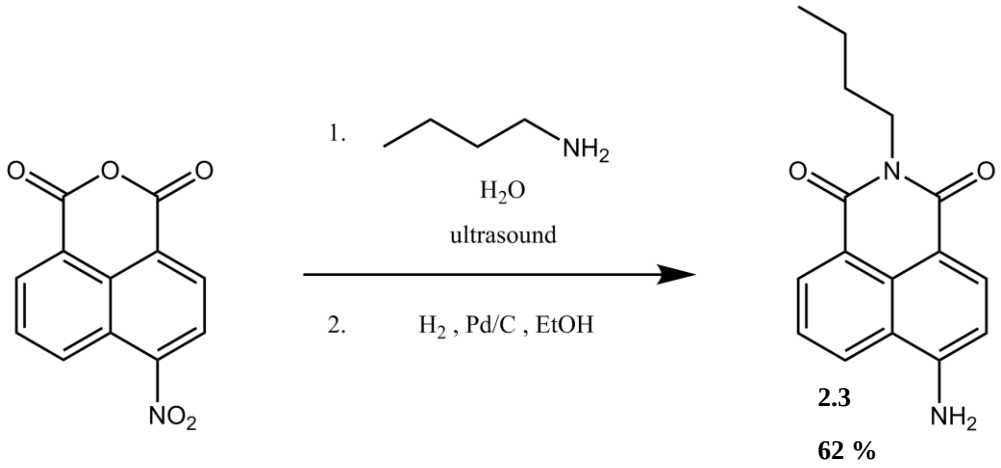

The fluorescent amino acids **2.1** and **2.2** were synthesized from glutamic and aspartic acids that are available commercially with *N*- and *O*-protecting groups already in place (as Fmoc and *t*-butyl, respectively). A purchased Fmoc-(AA)-OtBu was first dissolved in tetrahydrofuran (THF) along with one equivalent of *N*-methylmorpholine and the flask chilled in an ice-salt bath (Scheme 2.2). Once the contents had reached -15 ˚C, one equivalent of ethyl chloroformate was slowly introduced into the mixture. After stirring for 20 minutes, 1.5 equivalents of aqueous sodium azide was added as a solution in a minimal amount of water. The mixture was stirred in the ice for 30 minutes and then allowed to warm. Once the reaction mixture reached room temperature the organic solvent was removed *in vacuo* and the solid residue was dissolved in dichloromethane. The organic phase was washed three times each with 5% hydrochloric acid, 5% aqueous sodium bicarbonate, and water. The dichloromethane was dried with anhydrous sodium sulfate and then removed by rotary evaporation to yield an off-white foamy solid in ~90 % yield.

The next step was to convert the acid azide into an isocyanate via the Curtis rearrangement.[45] This was done by heating the acid azide to reflux in dry toluene. The acid

azide was first placed in a round-bottomed flask with the minimum amount of toluene needed to achieve dissolution, and 2.0 equivalents of **2.3**. The amino fluorophore was introduced before heating commenced to ensure that it would be present to trap any isocyanate as it formed *in situ*. After the reaction mixture had stirred for 48 hours at reflux the toluene was removed via rotary evaporation to yield a viscous, brown liquid. The crude product was dissolved in dichloromethane and methanol (19:1, v/v) and loaded onto a silica gel column for purification via flash chromatography. (The product is most easily identifiable as the first fluorescent blue band under 365 nm light. The green band that elutes later is the naphthalimide fluorophore that did not couple to an isocyanate; it can be collected for recycling and for calculation of yield "based on recovered starting material" (BRSM)). The collected blue band was evaporated to remove solvent and then dissolved in acetonitrile and water (3:1) for purification by HPLC. The product peak was collected and lyophilized for use in fluorescence studies and peptide synthesis. Analytical samples of compounds **2.1** and **2.2** can also be purified without the use of an HPLC through recrystallization with acetonitrile as the solvent.

Before the newly synthesized amino acids could be used for solid phase peptide synthesis, the *t*-butyl protecting groups had to be removed to open the carboxylic acid to amide bond formation. However, the *t*-butyl protecting groups were retained throughout the fluorescence studies in order to model an amino acid structure with the carboxyl group restricted as in a peptide; also, carboxylate is an anion of interest and the retention of the *t*-butyl ester was necessary to avoid interfering with anion binding results. It is important to note that peptide sequences containing aspartic or glutamic acids may hinder an accurate measurement with **2.1** and **2.2**. To convert the *t*-butyl ester into a carboxylic acid compounds **2.1** and **2.2** are dissolved into a cocktail of 70% trifluoroacetic acid, 20% methylene chloride, 5% triethylsilane, and 5%

anisole (all by volume). The mixture was allowed to cleave for 3 hours, with stirring under nitrogen, before the solvent was removed *in vacuo*. Finally, the carboxylic acids **2.4** and **2.5** were purified via HPLC or through trituration of the residue with anhydrous ethanol. The solid remaining in the flask after trituration was pure product, as judged by TLC.

Scheme 2.2: Synthesis of fmoc-protected, fluorescent naphthalimido-urea containing amino acids 2.1 and 2.2.

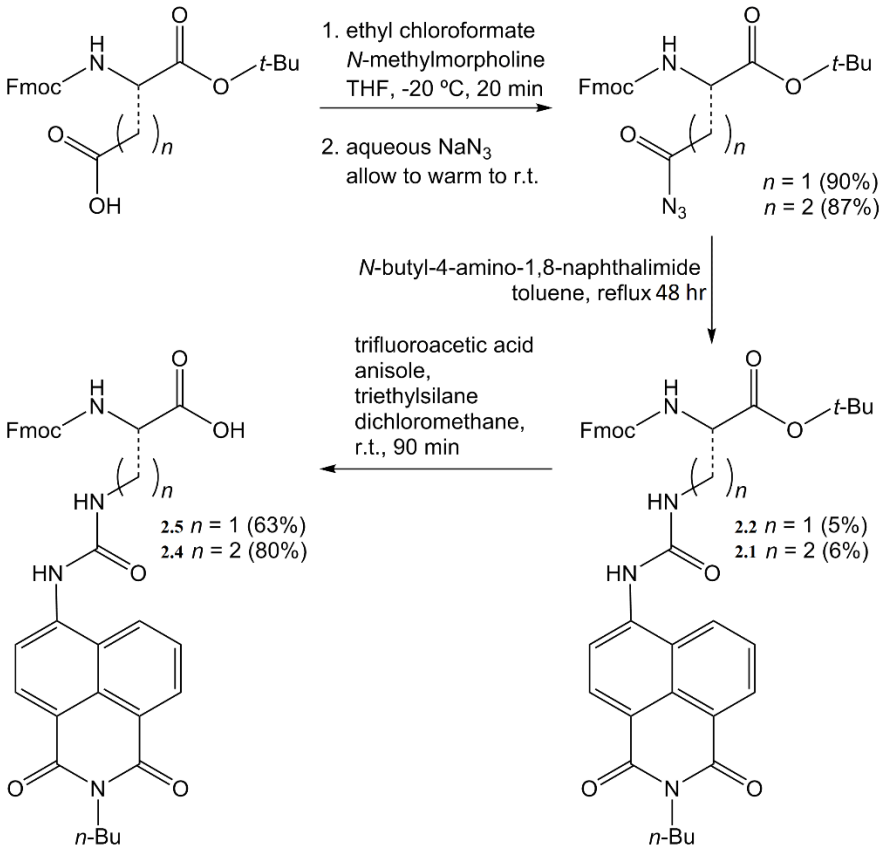

2.1.3 UV/vis and Fluorescence Results

The spectrophotometric properties of fluorophore **2.2** were analyzed to get benchmark values before fluorescence titrations with anion guests could be performed. Compound **2.2** was dissolved in three solvents: dichloromethane, acetonitrile, and H_2O-DMSO (50:1), and its electronic absorption maximum, extinction coefficient, and emission wavelength were determined (Table 1). Compound **2.1** was used to obtain fluorescence quantum yields in 1-octanol and acetonitrile (Table 2).

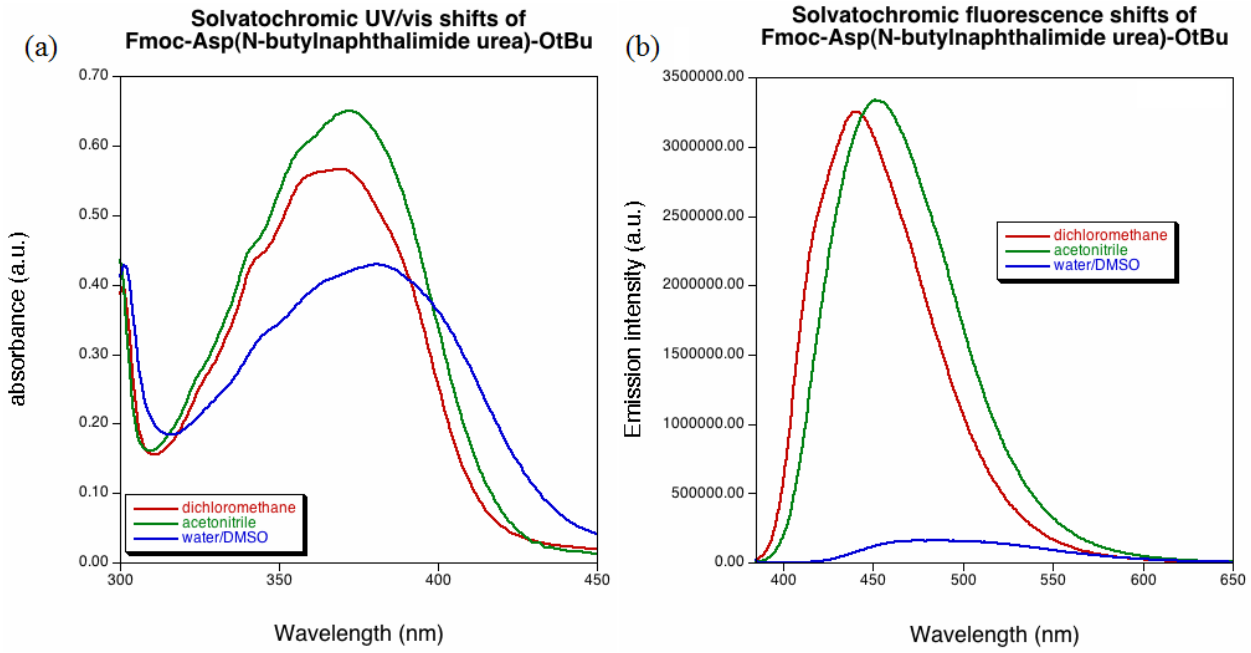

Figure 2.2: (a) UV/vis spectra of **2.2** (6.23×10^{-5} M) in three solvents with a range of polarities: dichloromethane (red λ_{max}= 370 nm), acetonitrile (green λ_{max}= 372 nm), water:DMSO (50:1) (blue λ_{max}= 381 nm). (b) Comparison of the change in fluorescence emission when **2.2** (8.90×10^{-6} M) was dissolved in the three solvents dichloromethane (red λ_{em}= 441 nm), acetonitrile (green λ_{em}= 451 nm), water:DMSO (50:1) (blue λ_{em}= 482 nm) and excited at the λ_{max} when dissolved in the respective solvent.

Table 2.1: UV/vis properties of **2.2** in three solvents of varying dielectric constants: dichloromethane (9.08), acetonitrile (36.64), water-DMSO (78.54).[a] ε = molar absorptivity

SOLVENT	Absorbance (nm)	ε (M^{-1} cm^{-1})	emission (nm)
CH_2CL_2	370	9250	441
CH_3CN	372	10600	451
H_2O-DMSO (50:1)	381	6800	482

[a] The dielectric constant is that of pure water.

Table 2.2: Fluorescence properties of **2.1** in 1-octanol and acetonitrile. Φ = quantum yield

SOLVENT	Absorbance (nm)	Φ	emission (nm)
1-OCTANOL	390	0.48	468
CH_3CN	390	0.54	463

Compound **2.1** was initially dissolved in 1-octanol to perform fluorescence titration experiments. The sample cuvette was inserted into a fluorometer with excitation wavelength set to 390 nm. An emission scan from 400 – 650 nm was acquired, with the maximum found to be 468 nm. A solution containing Cl^- as potential anionic guest (from tetrabutylammonium chloride; 66.7 mg/50 mL 1-octanol), was introduced into the cuvette at known aliquots and the fluorescence scans were repeated. Upon initial observation there was no appreciable quenching of the fluorescence during this experiment. A more basic anion, HCO_3^-, was tested (from tetraethylammonium bicarbonate; 21.4 mg/50 mL), and again little to no response was observed. As per good scientific technique, an additional solvent was chosen to repeat the experiment. Fluorophore **2.1** was dissolved in acetonitrile and the fluorescence was recorded. The excitation

wavelength remained at 390 nm and the emission maximum was measured to be 463 nm with a base width from 400 to 650 nm. When the anion chloride was first introduced a small increase in fluorescence intensity was noted along with a red-shift in the emission wavelength to 470 nm. Upon addition of 8 equivalents of chloride the fluorescence began to quench (Figure **2.3**). After addition of a significant excess of chloride the fluorescence intensity had only quenched by a net 2.0 percent. The descending slope of the curve appeared to be linear and was fitted to a Stern-Volmer quenching curve. This provided an association constant, K_{SV} of 70 M^{-1}. Stern-Volmer curves are used to fit an association value to a host + guest complex that quenches the fluorescence based on the presence of other material in a solution. Stern-Volmer quenching is also known as collisional quenching because an excited fluorophore will release energy through other avenues than fluorescence, such as colliding with material in the solution. As the presence of other stuff in a solution increases the fluorescence is further quenched.

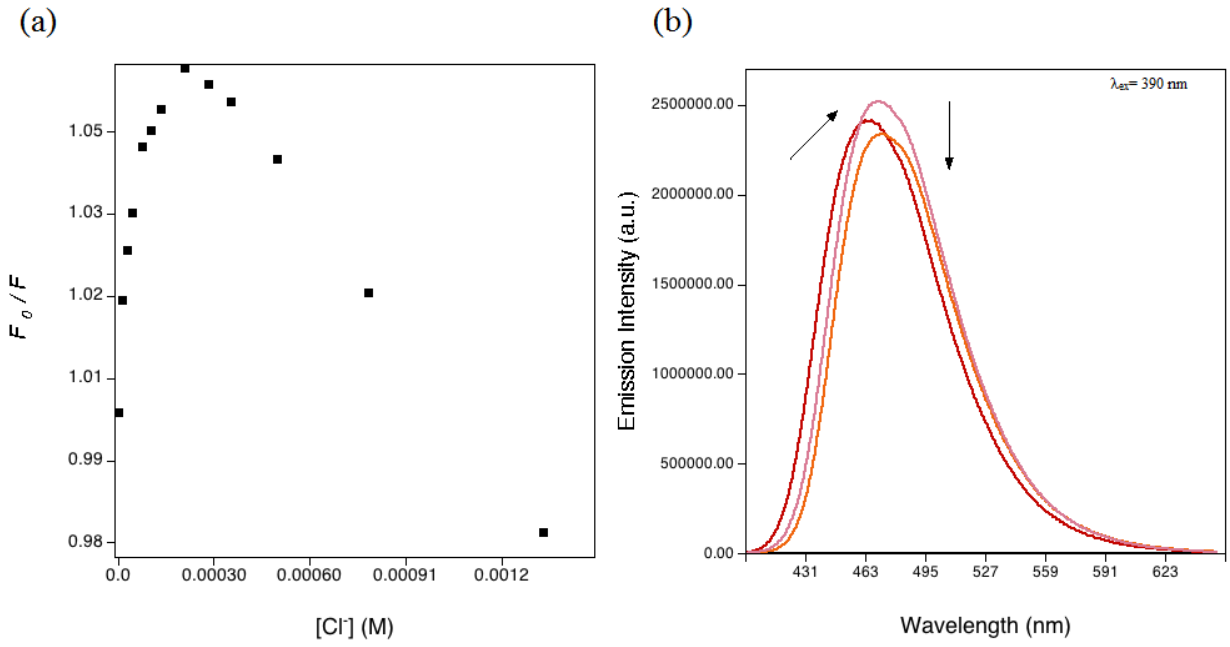

Figure 2.3: a) Fluorescence quenching curve of compound **2.1** from titration with tetrabutylammonium chloride hydrate in acetonitrile, and b) representative fluorescence spectra.

The next anion tested was $H_2PO_4^-$ (from tetrabutylammonium dihydrogenphosphate). The first aliquot of dihydrogenphosphate, while containing much less than 1 equivalent of the ion, quenched about 30% of the original integrated fluorescence (F_0) of compound **2.1**. Plots of F/F_0 vs $[H_2PO_4^-]_{total}$ were hyperbolic in shape, and ultimately about 90 % of the original fluorescence was quenched (Figure **2.4**).

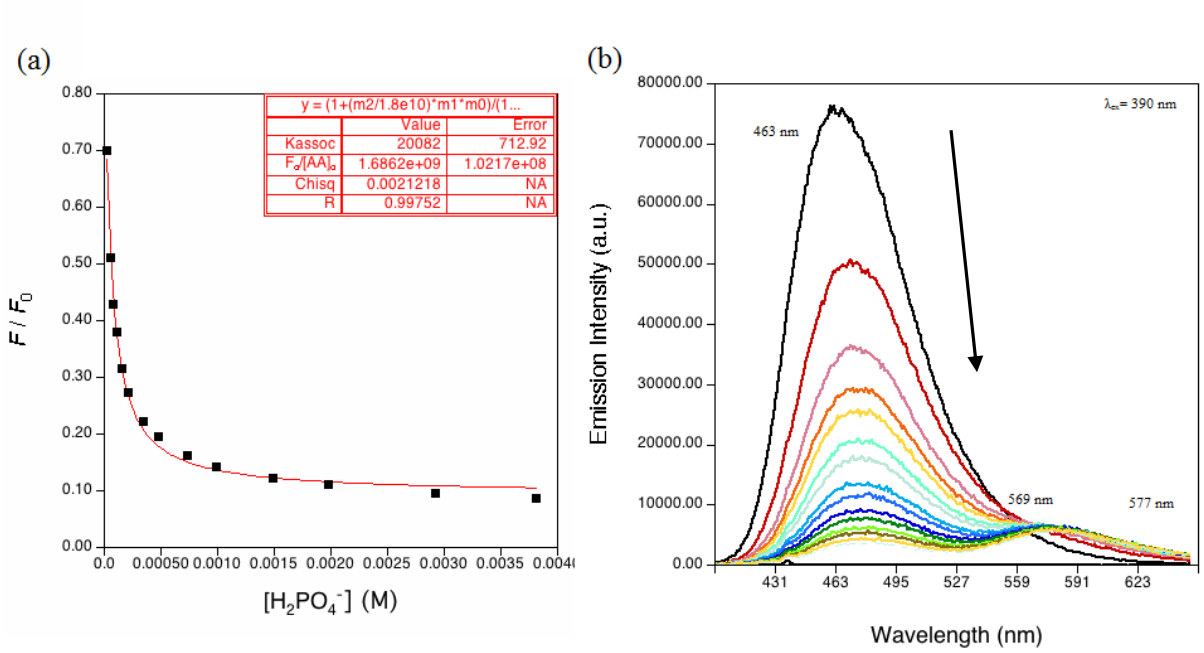

Figure 2.4: a) Fluorescence quenching curve of compound **2.1** from titration with tetrabutylammonium phosphate monobasic in acetonitrile and b) fluorescence spectra.

When graphs of F/F_0 vs. $[anion]_{total}$ have an "L"-shape, this is indicative of the fluorophore binding to the anionic species.[46] The λ_{em} of the fluorophore shifted from 463 nm to 476 nm. This red shift of the fluorescence arises from weakening of the urea N–H bond(s) as they interact with an anion. The weakening of this bond allows electron density on N to increase, and the aromatic fluorophore to become more electron-rich. This electron richness brings the HOMO-LUMO molecular orbital energy levels closer together, resulting in less energy being emitted when the excited state fluorophore lowers to the ground state. The lower energy emitted as fluorescence is directly related to a longer wavelength or red-shift in the fluorescence emission.

Another anionic species, bicarbonate, was tested next. The addition of increasing amounts of bicarbonate produced a fluorescence quenching curve with a sigmoidal shape, Figure 2.5. This suggests that at this specific concentration the host fluorophore had begun to form

oligomers through what is known as urea stacking (another result from the resonance ability of urea). The initial slow decrease in the fluorescence was because the bicarbonate must first break apart the oligomers before it can bind to urea. When the concentration was lowered the quenching curve took on a typical hyperbolic 1:1 binding curve (seen in Figure 2.6). The addition of more bicarbonate stopped having a significant effect after 80% of the fluorescence intensity had been quenched.

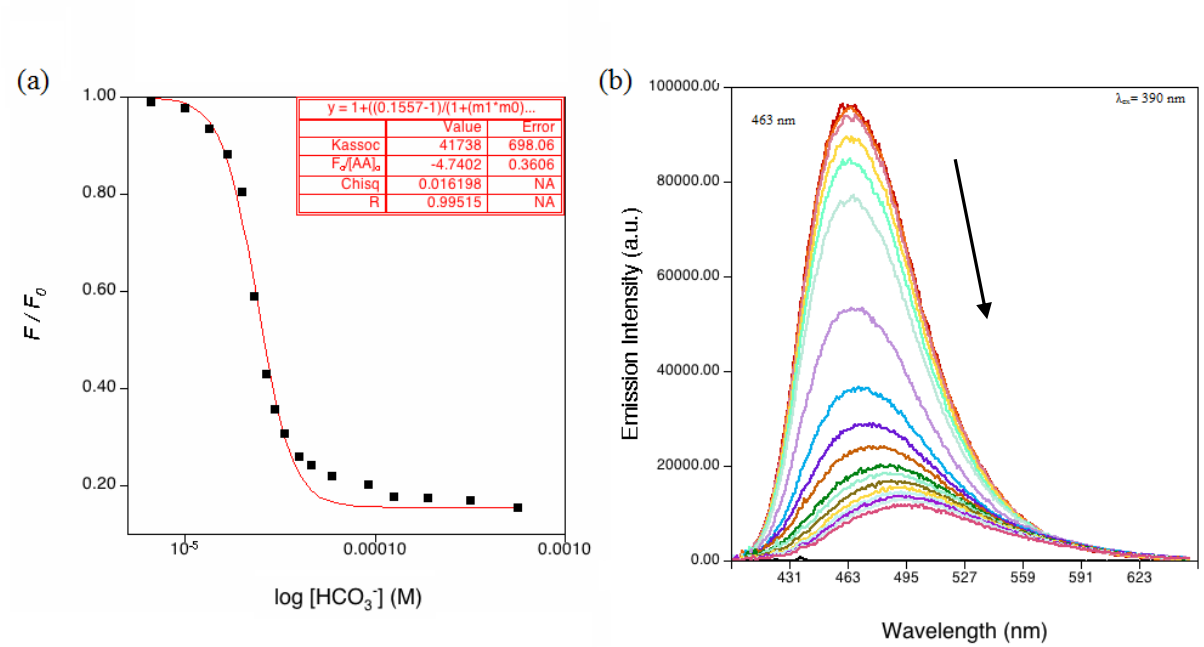

Figure 2.5: a) Fluorescence quenching curve of compound **2.1** from titration with tetraethylammonium bicarbonate in acetonitrile and b) the fluorescence spectra.

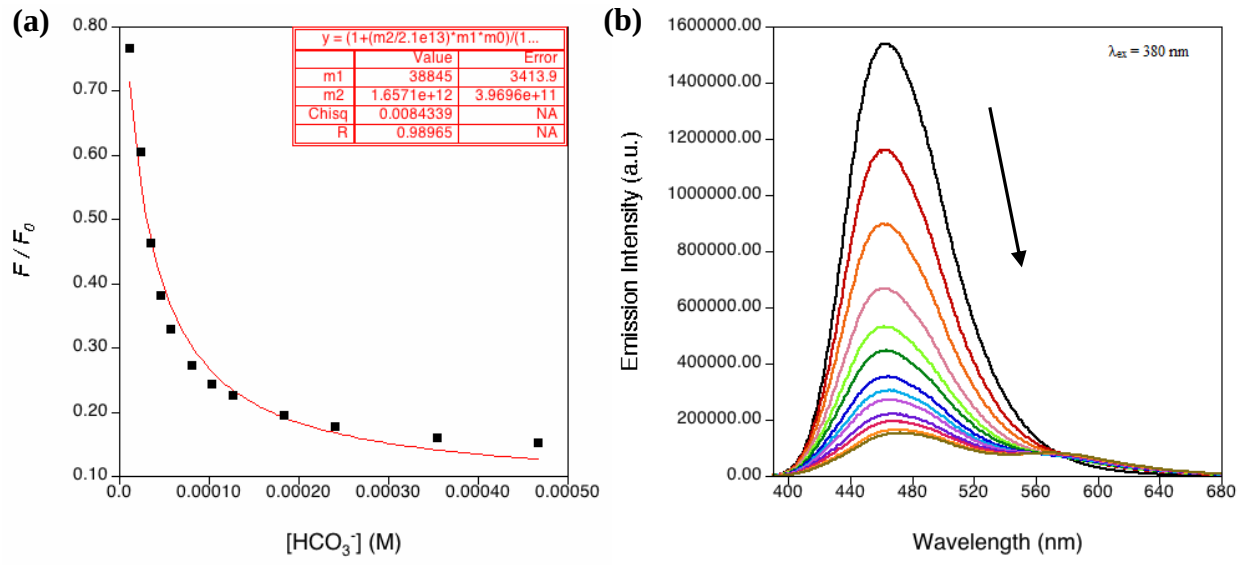

Figure 2.6: a) Fluorescence quenching curve of compound **2.1** from titration with tetraethylammonium bicarbonate in acetonitrile at a lower concentration than the host solution used in Figure 2.5 and b) the fluorescence spectra.

The λ_{em} of the fluorophore shifted from 463 nm to 494 nm. This significant red shift in the maximum wavelength of the fluorescence is evidence of the removal of the hydrogen from the aromatic nitrogen in the urea group. The removal of a hydrogen results in a full negative charge on the aromatic nitrogen.[35] Again, the negative charge gives a more electron rich fluorophore and thus a lower HOMO-LUMO energy gap.

Finally, the anion nitrate was titrated into a solution of compound **2.1**. Upon addition of a large excess of tetrabutylammonium nitrate the quenching appeared to be linear. This is known as collisional quenching and is best represented with a Stern-Volmer plot, K_{SV} was found to be $69 \pm 3\ M^{-1}$.

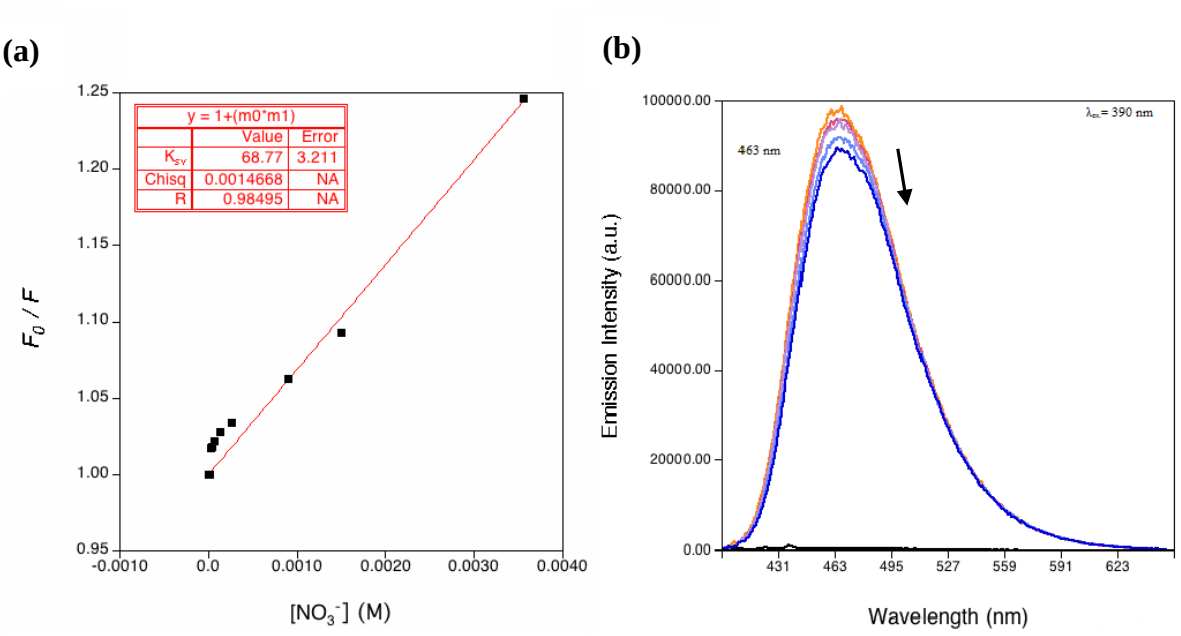

Figure 2.7: a) Fluorescence quenching curve of compound **2.1** from titration with tetrabutylammonium nitrate in acetonitrile and b) the fluorescence spectra.

The association constants, K_{assoc}, for compound **2.1** and $H_2PO_4^-$ were derived from the fluorescence titrations by fitting a line to the graph of the ratio of integrated fluorescence (F) to initial integrated fluorescence (F_0) vs the concentration of the anion; for **2.1** + bicarbonate K_{assoc} was found through fitting a line to the graph of F/F_0 vs. log[HCO_3^-]. The K_{assoc} for compound **2.1** with phosphate and bicarbonate were found to be 20151 ± 915 M^{-1} and 39881 ± 1475 M^{-1}, respectively.

Fluorescence titrations were repeated for compound **2.2** using dihydrogenphosphate, chloride, and bicarbonate. Some interesting trends developed from using compound **2.2** versus **2.1**. Notably, compound **2.2** appeared to bind to the anions much more tightly than compound **2.1**. After graphing the fluorescence quenching and fitting a curve to the data, K_{assoc} could be calculated. For **2.2** + H_2PO_4 the association constant was found to be $2.6 \times 10^4 \pm 1.2 \times 10^3$ M^{-1}.

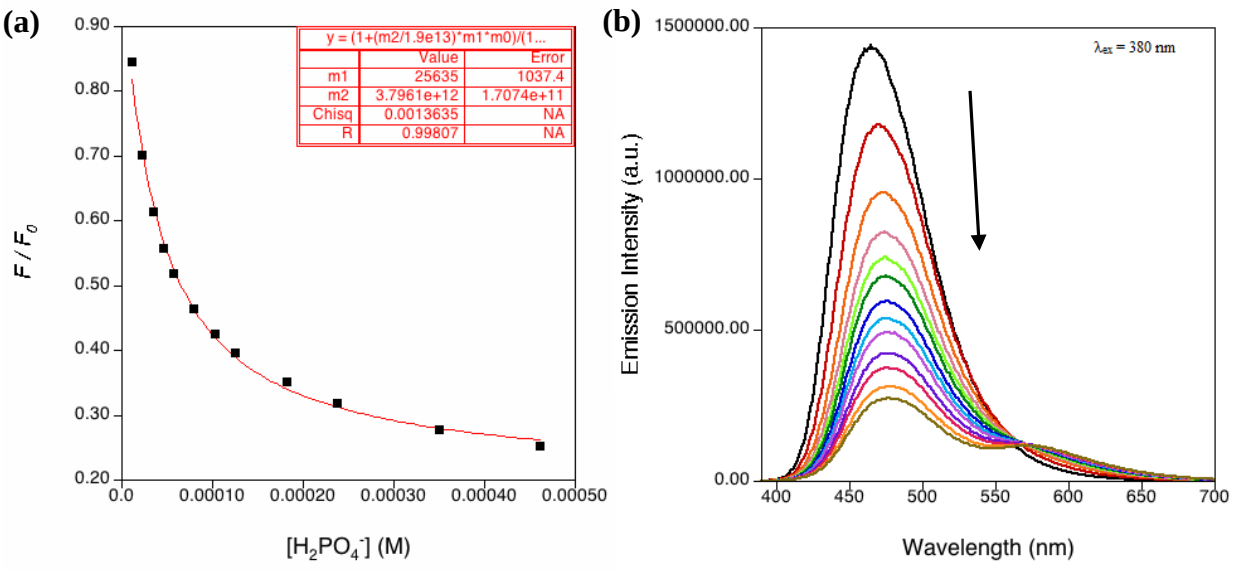

Figure 2.8: a) Fluorescence quenching curve of compound **2.2** from titration with tetrabutylammonium phosphate monobasic in acetonitrile and b) the fluorescence spectra.

The fluorescence response from titration with bicarbonate gave an L-shape. This further supports the theory that a higher concentration of the fluorescent amino acids may in fact cause urea stacking since titrations with compound **2.2** were performed at lower concentrations of host. However, titrations on compound **2.2** were performed multiple times and each time the calculated association constant was different than the last. The K_{assoc} was found to range from 6.2 × 10^4 to 2.8 × 10^5 M^{-1}. While the data results achieved were unreliable it does suggest that the association constant for **2.2** and HCO_3^- is >1.0 × 10^5 M^{-1}. Fluorescence titrations were also performed on **2.2** using tetrabutylammonium chloride. Again, the titration caused the fluorescence to increase slightly (also causing a slight red shift in the emission band) before causing the fluorescence to quench a net 30 %. This was only achieved after greater than a 2000-fold excess of guest had been added. Again, the descending portion of the curve appeared to have a linear relationship and when a Stern-Volmer quenching curve was fitted to this data it gave a K_{SV} = 70 M^{-1} (Figure 2.9).

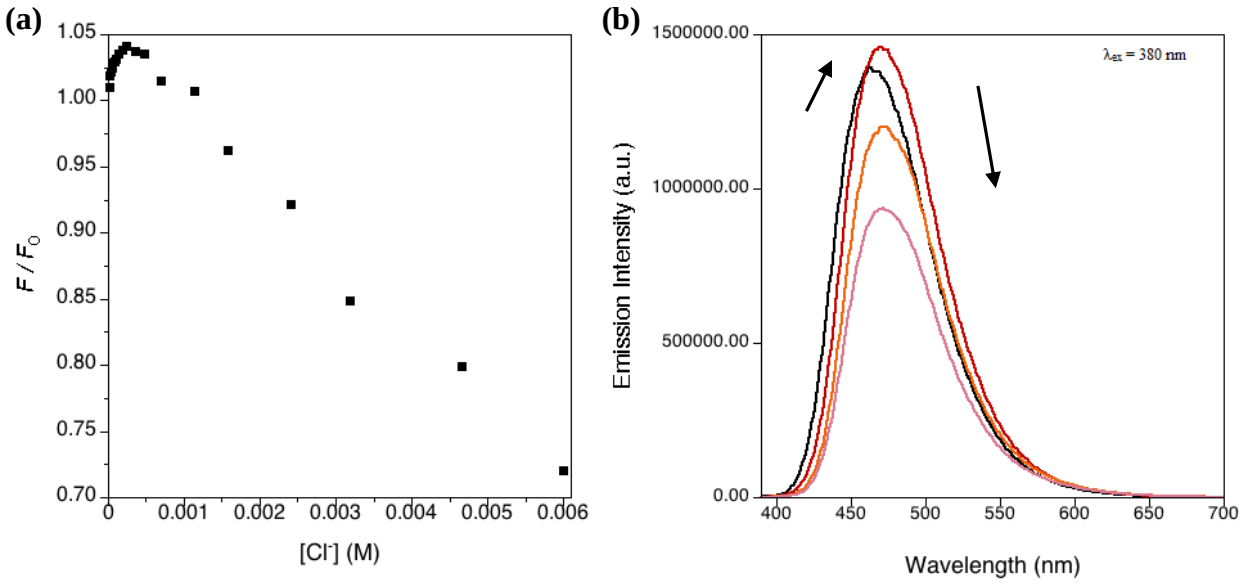

Figure 2.9: a) Fluorescence quenching curve of compound **2.2** from titration with tetrabutylammonium chloride in acetonitrile and b) the fluorescence spectra.

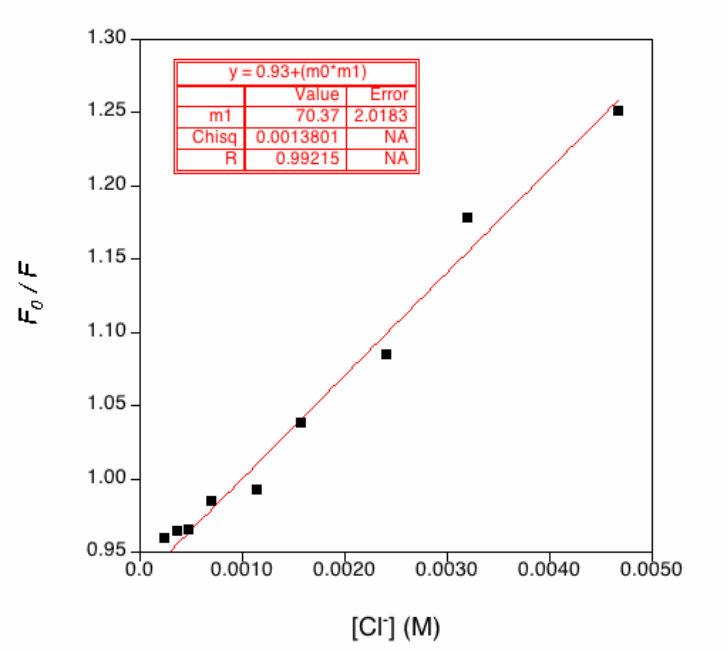

Figure 2.10: Stern-Volmer quenching curve of compound **2.2** from titration with tetrabutylammonium chloride in acetonitrile.

Particularly for the Glu derivative **2.1**, when certain anions were introduced a change in the visible color of the solution was observed. While $H_2PO_4^-$ would cause the solutions to change from colorless to a light/dark yellow, HCO_3^- (and other relatively basic species, when in acetonitrile, like F^- and CH_3COO^-) would cause the solution to change to a dark orange or red. It was hypothesized that the dark orange or red was a result from deprotonation of the fluorophore[35] at the most acidic proton, the aryl N-*H* urea proton. To test this hypothesis with Asp derivative **2.2**, a solution in acetonitrile (6.0×10^{-6} M) was prepared in a cuvette and increasing amounts of anion were added. The UV/vis spectrum of the compound was taken to look for a shift in the absorbance of visible light. No deprotonation could be detected by UV/vis when 55 equivalents of tetraethylammonium bicarbonate were present. Only after a large excess of solid tetraethylammonium bicarbonate was added to the cuvette was the λ_{max} observed to shift (to 388 nm) while a new, lower-energy peak appeared (at 467 nm). When the same sample was inserted in a fluorometer and excited at 388 nm the fluorescence emission band was seen at 463 nm as in Figure 2.11. When the system was excited at 467 nm, an emission band was observed at 569 nm with an intensity about 10% of the 463 nm feature. The same series of experiments were performed using tetrabutylammonium dihydrogenphosphate in a fresh cuvette of the same solution of fluorophore **2.2**. By UV/vis, after addition of a large amount of anion the λ_{max} shifted from 369 nm to 376 nm and another peak became apparent at 475 nm. Results of fluorescence measurements are shown in Figure 2.12. These qualitative tests prompted a qualitative experiment to see how the fluorophores would behave when treated with a series of anions; this could open a door for use as a fast colorimetric indicator for selected biologically and environmentally relevant anions.

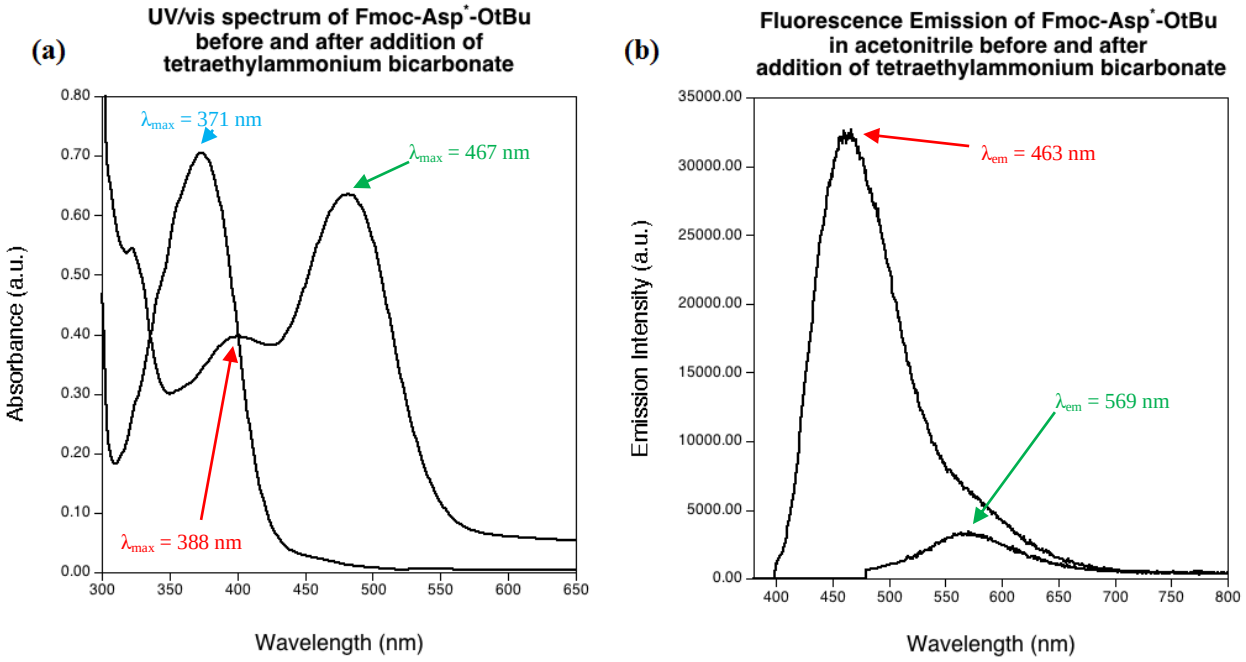

Figure 2.11: (a) UV/vis spectra of Fmoc-Asp*-OtBu (**2.2**) in acetonitrile before (371 nm) and after (388 nm and 467 nm) the addition of a large excess of solid tetraethylammonium bicarbonate. (b) Emission spectra of Fmoc-Asp*-OtBu excited at 388 nm (red annotation) and 467 nm (green annotation).

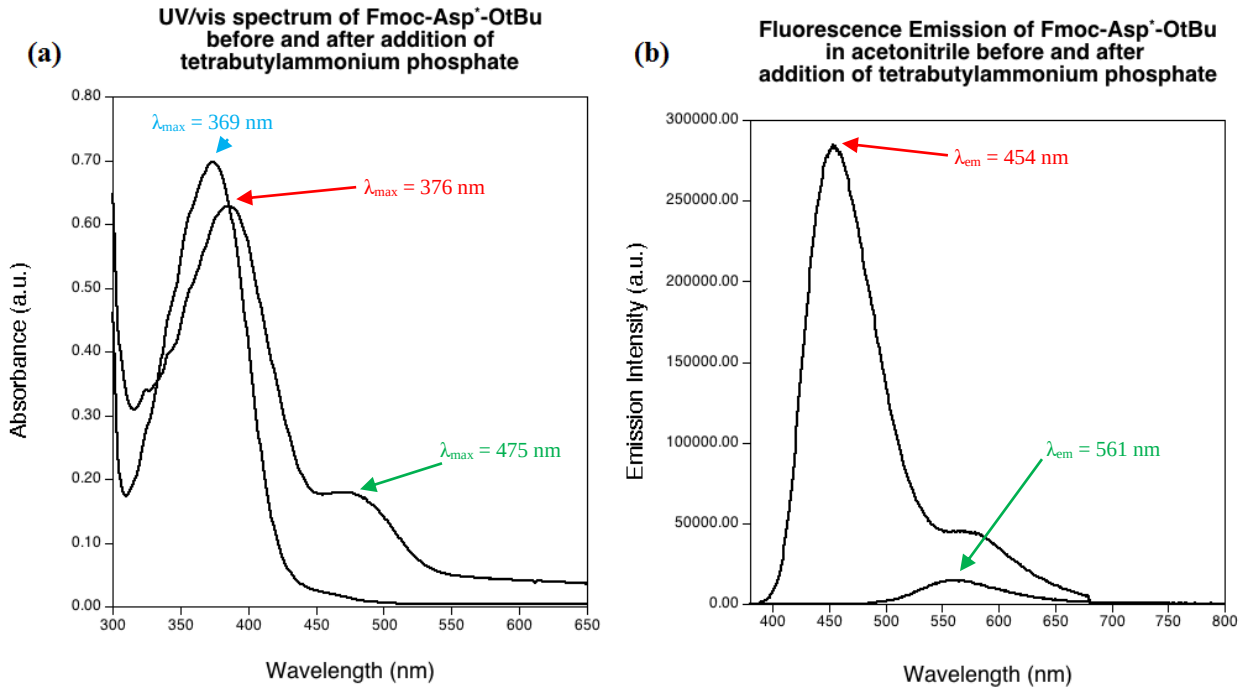

Figure 2.12: (a) UV/vis spectra of Fmoc-Asp*-OtBu (**2.2**) in acetonitrile before (369 nm) and after (376 nm and 475 nm) addition of a large excess of solid tetrabutylammonium dihydrogenphosphate. (b) Emission spectra of Fmoc-Asp*-OtBu when excited at 376 nm (red annotation) and 475 nm (green annotation).

A colorimetric experiment was performed using compound **2.1** to observe qualitative changes in the visible color and fluorescence when a variety of anions were added to the solution. The anions tested were: chloride, tosylate, nitrate, dihydrogen phosphate, fluoride, azide, acetate, and bicarbonate. The anions are listed in order of increasing basicity in aqueous solution. It is important to note that this test was performed in acetonitrile and the relative basicity of these anions is likely different than that in water due to a change in the stability of the conjugate base. Concerning the color changes seen in Figures 2.13, the response by the fluorophore does not track predictably with increasing pK_b.

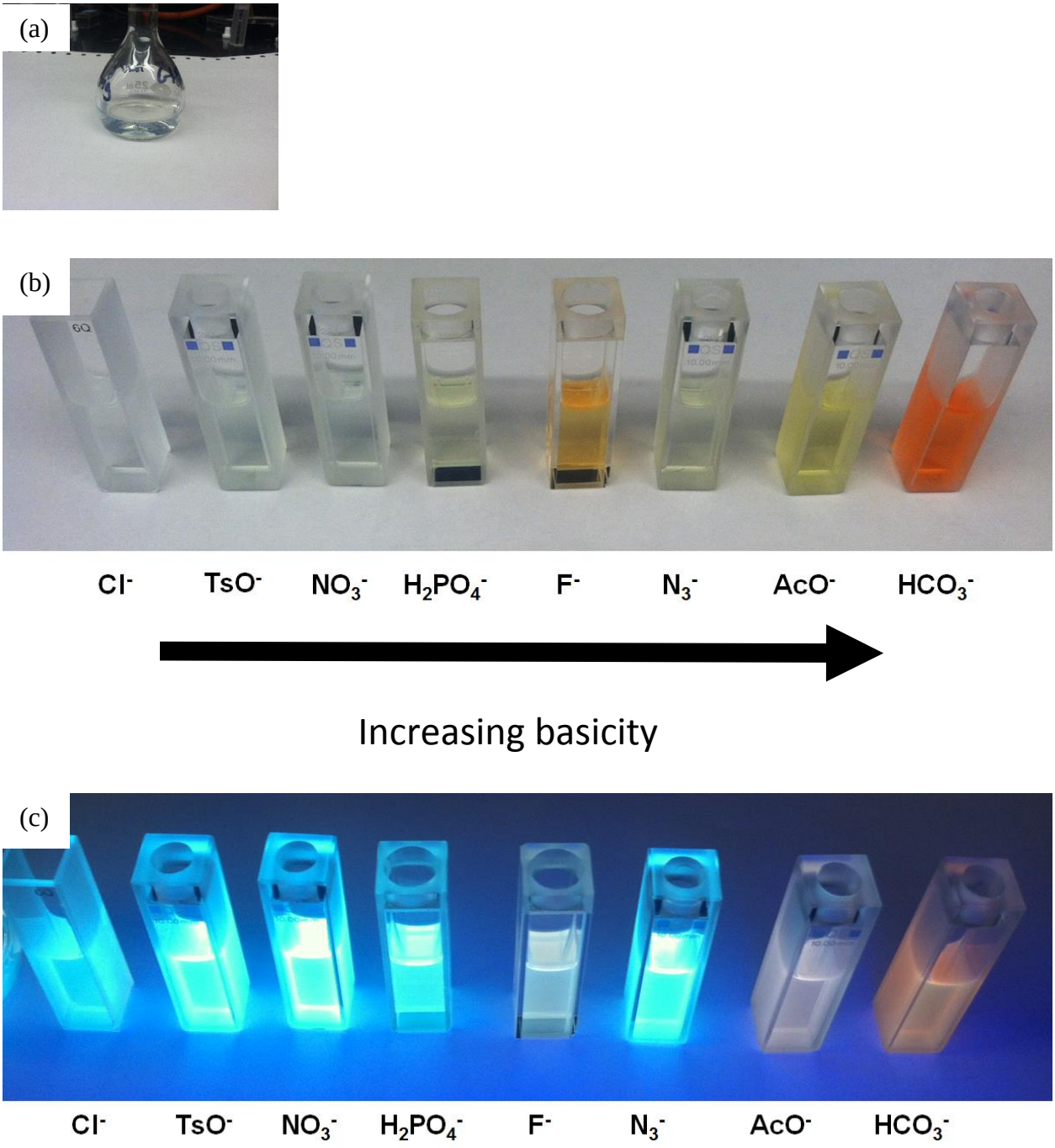

Figure 2.13: (a & b) Change in the visible color of acetonitrile solutions of **2.1** after the addition of one equivalent of respective anion. The cuvettes are organized in order of increasing aqueous pK_b of the added anion. (c) The fluorescence response from a solution containing compound **2.1** and one equivalent of the respective anion. Little change was observed with further addition of 2 and 3 equivalents of analyte.

Table 2.3: Relative p*K*b values of the anions added to the cuvettes in Figure 2.13.

ANION	pK_B IN H_2O	pK_A IN ACETONITRILE
CHLORIDE	21	5.1
TOLSYLATE	16.8	5.6
NITRATE	15.4	5.2
DIHYDROGENPHOSPHATE	11.9	-
FLUORIDE	10.8	-
AZIDE	9.4	-
ACETATE	9.2	-9.5
BICARBONATE	7.7	-

2.1.4 ^{1}H-NMR Titration

Proton NMR was used to monitor chemical shifts of compound **2.1** in DMSO-d_6 (6.9 mM) while a solution of tetrabutylammonium dihydrogenphosphate (47 mM) was added. A significant downfield shift in the urea proton peaks was observed over the course of 9 additions of phosphate. The most fascinating aspect is that the peaks for the urea protons did not begin to shift until more than 1 equivalent of anion had been added to the solution. The shift in the proton peaks is represented in Figure 2.15. It was hypothesized that intramolecular hydrogen bonding occurs which initially limits the ability for the urea receptor to bind to phosphate. Also, it has been shown that when urea containing molecules are in high concentrations intermolecular urea stacking may occur and initially limit the ability for hydrogen bonding.[18] While the evidence suggests that the phosphate is not binding to the urea moiety before one equivalent is reached, the anion may still able to associate with **2.1** elsewhere on the molecule, but most likely may need to dissociate oligomers formed when the fluorophore is in solution at high concentrations.

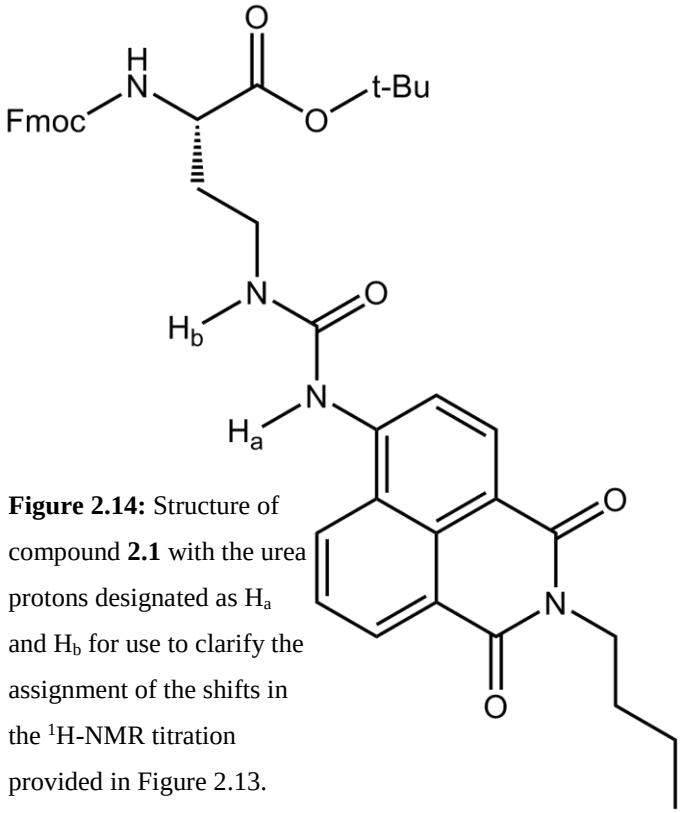

Figure 2.14: Structure of compound **2.1** with the urea protons designated as H_a and H_b for use to clarify the assignment of the shifts in the ^{1}H-NMR titration provided in Figure 2.13.

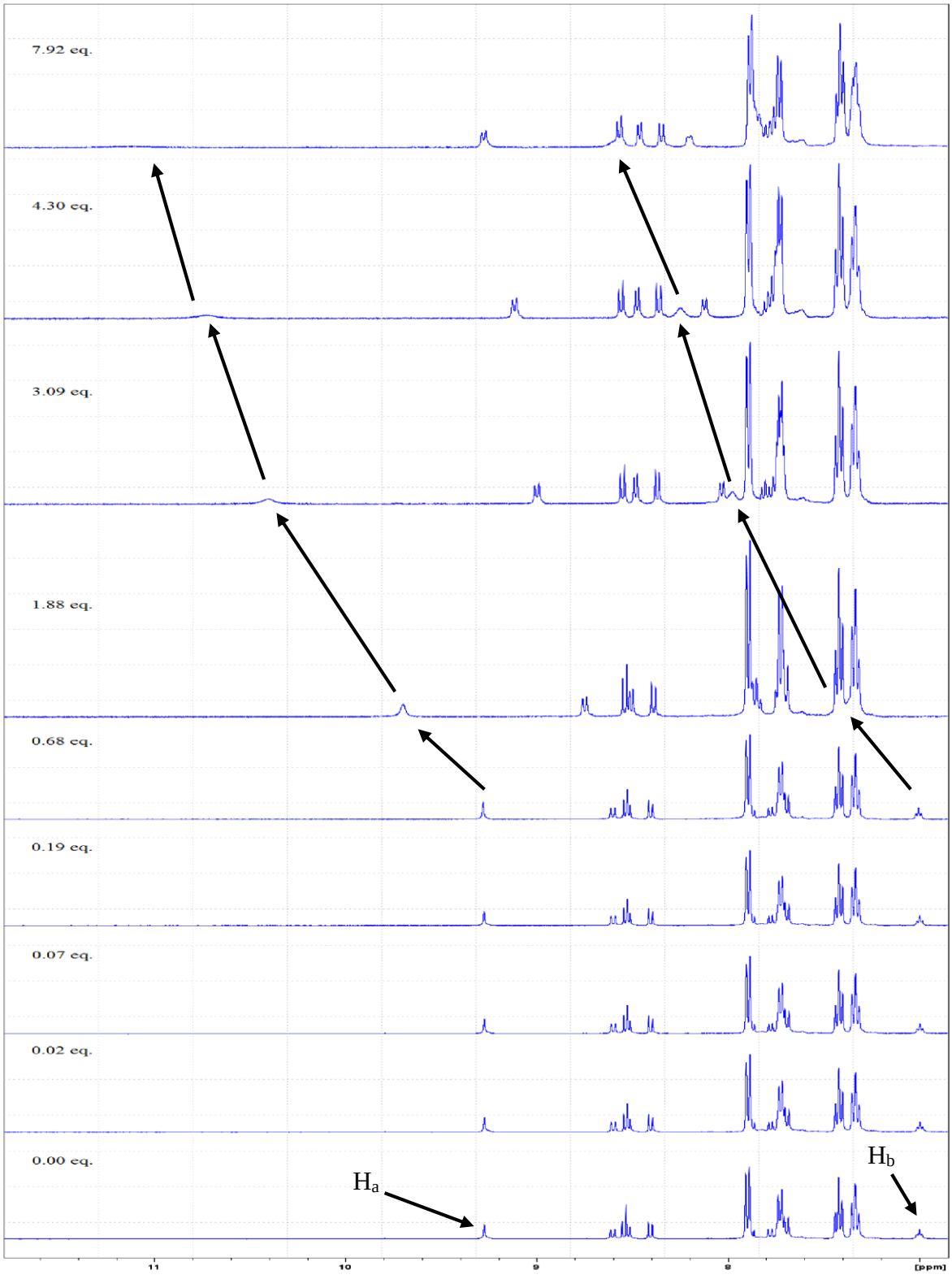

Figure 2.15: Representation of the proton shifts of H_a and H_b during titration of **2.1** with dihydrogenphosphate in DMSO-d_6.

A ^{1}H-NMR titration was performed on compound **2.2** as well. The titration was performed in DMSO-d_6 at 3.6 mM **2.2** with tetrabutylammonium dihydrogenphosphate at a concentration of 5.2×10^{-2} M^{-1}. The urea N-*H* peaks for compound **2.2** began to move at the first addition of phosphate anion. Two plots representing the ppm shift of the urea aryl N-*H* proton vs [$H_2PO_4^-$] added are presented in Figure 2.16. A plot of the ppm shift for the urea alkyl *N*-*H* proton vs [Cl^-] added is also represented in Figure 2.17. The use of aryl vs. alkyl was chosen based on which proton was seen to give the largest shift in ppm. Plotting of this specific data would provide the most accurate association constant. Using the plotting program WinEQNMR the association constants for compound **2.2** + $H_2PO_4^-$ and **2.2** + Cl^- were found to be 1300 ± 77 M^{-1} and 19 ± 5 M^{-1}, respectively.[47]

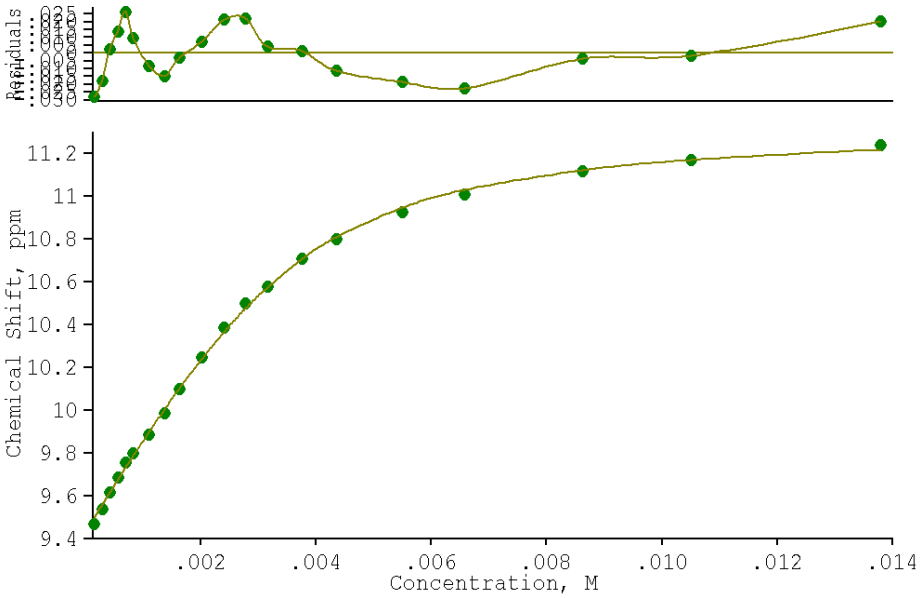

Figure 2.16: Graphical representation of the ppm shift in the aryl N-*H* urea proton during NMR titration of **2.2** with tetrabutylammonium dihydrogenphosphate. The WinEQNMR program was used to fit an NMR binding curve to the data. K_{assoc} = 1300 ± 77 M^{-1}. The small graph at the top is simply a representation of how well the relative data point falls on the fitted curve. The closer the value is to zero the closer it is to the fitted line. This provides support that the WinEQNMR program supplied a proper fit.

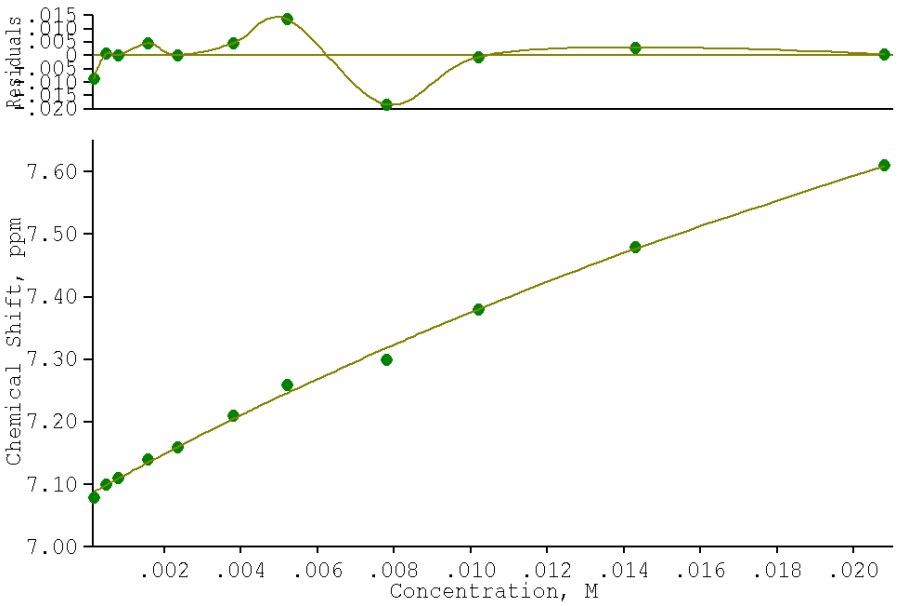

Figure 2.17: Graphical representation of the ppm shift in the alkyl N-*H* urea proton during NMR titration of **2.1** with tetrabutylammonium chloride hydrate. The WinEQNMR program was used to fit an NMR binding curve to the data. K_{assoc} = 19 ± 5 M^{-1}. The small graph at the top is simply a representation of how well the relative data point falls on the fitted curve. The closer the value is to zero the closer it is to the fitted line. This provides support that the WinEQNMR program supplied a proper fit.

2.1.5 Discussion

When chloride and bicarbonate were introduced into solutions of compound **2.1** in 1-octanol, no fluorescence quenching occurred. The design of compound **2.1** and **2.2** was chosen because hydrogen bonding between the anions and the urea group was expected to cause a change to the immediately bonded fluorophore. Since 1-octanol has the ability to hydrogen bond, it was probably interfering with the ability of the anion to come into contact with the urea.[48] The

1-octanol was replaced with a solvent without H-bond donor ability, acetonitrile. Upon addition of the analyte ions, changes in fluorescence were observed. All subsequent fluorescence titrations were performed in this solvent. Titrations were repeated three times each and the peak areas under the curve were collected to give a value directly proportional to the total number of photons emitted by the excited fluorophore. Graphs were made to display the change in the area under the curves (F/F_0) versus the [anion]. A few examples of these curves are represented in Figures 2.3-2.8 and the rest are provided in Appendix A.

For Glu derivative **2.1**, addition of chloride initially brings about a small (6%) increase in the fluorescence intensity (Figure 2.5). This behavior is consistent with a process that replaces relatively strong urea H-bonds (within the host molecule itself) with relatively weaker ones (to Cl^-). The NMR behavior of **2.1**, in which no shifting of the N-*H* resonances was observed until >1 equiv of anion was present, can thus be rationalized: intramolecular N*H*•••O interactions in **2.1** are retained until sufficient anion is present to drive "unfolding" of the host. The same result is witnessed in **2.2** plus Cl^-, about a 4% increase in the fluorescence intensity before what appears to be a linear quenching of the fluorescence. For both amino acids, when the linear portion of the quenching curve is matched to a Stern-Volmer equation an association constant of 70 M^{-1} is obtained. With the addition of tetrabutylammonium nitrate a linear decrease in the fluorescence was observed. Although the trigonal planar nitrate ion would seem to have an optimal shape for binding to the urea, as the conjugate base of a strong acid, it does not have the basicity needed to form a hydrogen bond with the urea protons and elicit a response. The linear behavior was fitted to give a Stern-Volmer quenching constant K_{SV} of 69 ± 3 M^{-1}. This is significant because Stern-Volmer or collisional quenching should remain the same no matter

what species is introduced into the solution. For both **2.1** and **2.2**, chloride and nitrate give a collisional quenching response.

Upon addition of small aliquots of $H_2PO_4^-$ solution there is an immediate 30% decrease in the fluorescence of **2.1**, followed by continued quenching until saturation is observed. The hyperbolic curve obtained from this response is evidence of phosphate-urea binding (Figure 2.4). The average association constant, K_{assoc}, from the three titrations was found to be 20151 ± 915 M^{-1} and the K_{assoc} for **2.2** was found to be 25600 ± 1200 M^{-1}. These values are comparable to those found for compounds **2.6** and **2.7**, which report binding constants to dihydrogenphosphate in acetonitrile of 2300 and 63000 M^{-1}, respectively.[22,23] The predicted orientation of the bound phosphate with **2.1** and **2.2** will be discussed in a later section.

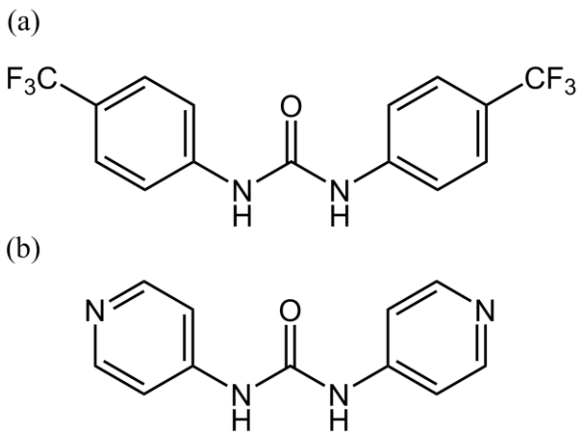

Figure 2.18: Structures of (a) compound **2.6** and (b) compound **2.7**.

For bicarbonate ion, there was initially very little change in the fluorescence peak area, but as more bicarbonate was added to the solution the effect of the analyte became more pronounced. Once the integrated intensity of **2.1** had been quenched by about 80%, the addition of more bicarbonate caused no further change. The quenching curve took on a sigmoidal shape. After further consideration it was suspected that the sigmoidal shape was a result of the host molecule forming intermolecular oligomers through urea stacking. Before bicarbonate could bind to the urea and cause quenching the bicarbonate must break apart the intermolecular

stacking. A more dilute solution of host fluorophore yielded a hyperbolic, L-shaped curve as seen in Figure 2.6.

Despite the small structural difference between amino acids **2.1** and **2.2**, the latter binds to phosphate and bicarbonate much more robustly than the former. After further calculation the **2.2** + $H_2PO_4^-$ complex had a K_{assoc} value slightly greater than **2.1** + $H_2PO_4^-$. The differences continued to present themselves after titration of **2.2** with bicarbonate. When the titration data was plotted and fitted to a curve it took on a hyperbolic shape, that provided an association constant that was unable to accurately be measured; at least $>1.0 \times 10^5$ M^{-1}.

The proton on the nitrogen of the urea closest to the aromatic ring is the most acidic in the molecule, and previous work has shown that basic anions are able to deprotonate ureas in polar aprotic solvents. In our case, the appearance of a dramatic orange color may have potential in colorimetric indication of pH. It may also be possible to use this to bracket the p*K*a range of the urea protons in a non-aqueous solvent like acetonitrile.

2.1.6 Computer Modeling

DFT optimizations were performed on compounds **2.1** and **2.2** in a solvent dielectric corresponding to acetonitrile. It is important to note that the Fmoc group was truncated to a methyl unit for simplification. The calculated association energies (ΔE_{assoc}) for phosphate binding to compounds **2.1** and **2.2** were found to be -31.1 and -36.8 kcal/mol, respectively. These results follow the trend in K_{assoc} values for **2.1** (2.1×10^4 M^{-1}) and **2.2** (2.5×10^4 M^{-1}) obtained through fluorescence titrations. The computational results predict that Glu derivative **2.1** (Figure 2.19 (b)) forms only a pair of H-bonds at one phosphate oxygen. The bond distances were calculated to be 2.01 Å to the alkyl N-*H* and 1.93 Å to the aryl N-*H*. For compound **2.2** (Figure 2.19 (a)) it is predicted that phosphate has a multi-point interaction through hydrogen bonding. Again, one oxygen from the phosphate is shared between the two urea protons (1.96 Å to the aryl N-*H* and 2.03 Å to the alkyl N-*H*), but also another phospho-oxygen is associated with the N-*H* from the backbone carbamate (1.99 Å to the amide N-*H*). One of the phosphate hydroxyls is predicted to hydrogen bond with the carbonyl oxygen found at the backbone *t*-butyl-ester (1.95 Å to the ester C=*O*). These unique results suggest that the Asp derivative produces a enzymatic-like pocket for the association with

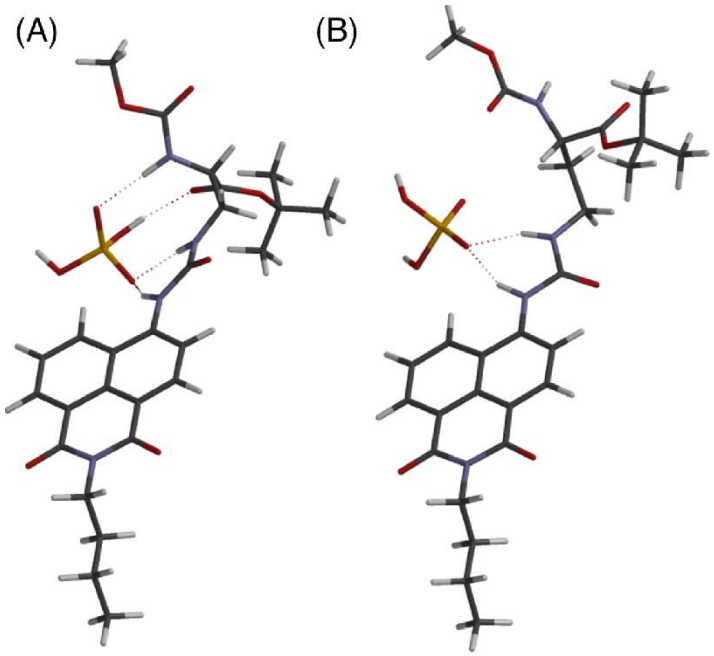

Figure 2.19: COSMO-DFT molecular structures in acetonitrile of **(a) 2.2** and **(b) 2.1** with a dihydrogenphosphate anion. black = C, blue = N, red = O, orange = P, white = H.

phosphate; while the glu derivative merely associates through direct, head-to-head association with the two ureido-protons and a single P=*O*. Simply put, the Asp derivative has the ability bind through more coordination sights and is expected to have a stronger binding ability. The computer models also agree with the ^{1}H-NMR titration of compounds **2.1** and **2.2** with phosphate, which produces a shift in the alkyl urea protons of 1.58 ppm and 1.67 ppm and aryl urea protons of 1.85 ppm and 1.82 ppm, respectively (note that ^{1}H-NMR titration of **2.1** was terminated after addition of 7.9 equivalents of anion, and the ^{1}H-NMR titration of **2.2** was terminated after the addition of 3.8 equivalents of anion).

The optimization for the binding of **2.1** to bicarbonate is not shown, however it produced an image similar to Figure 2.19(b), with exception that two separate oxygen atoms from the bicarbonate each associated with one of the ureido-protons through hydrogen bonding; 1.92 Å to the aryl N-*H* and 1.93 Å to the alkyl N-*H* . The relative association energies for **2.1** + $H_2PO_4^-$ and **2.1** + HCO_3^- were provided through computer modeling and the trend in the association energies agrees with the results found through fluorescence titration. When **2.1** was titrated with tetrabutylammonium dihydrogenphosphate a fit line matched to the quenching curve provided a K_{assoc} of 2.0×10^4 M^{-1}, and when **2.1** was titrated with tetraethylammonium bicarbonate the K_{assoc} was calculated to be 4.0×10^4 M^{-1}. Although the difference in the energies was relatively small, the equilibrium constants found from the fluorescence titrations match the trend that would be predicted from the calculated association energies.

2.1.7 Peptide Results and Discussion

Once the *tert*-butyl protecting groups were removed from the amino acids, they were used as reactants in solid-phase peptide synthesis to ensure that the products would behave in a

manner similar to commercially available Fmoc protected amino acids. Compound **2.4** was inserted into "Glu-peptide" YKKE*IAHALFSA-$CONH_2$ (**2.6**) and compound **2.5** was inserted into "Asp-peptide" YKKEIAHALD*SA-$CONH_2$ (**2.7**). These 12-mers were prepared by classic Merrifield solid phase peptide synthesis on Rink amide resin, at a 0.058 mM scale. The sequence chosen for the peptides was derived from the first 12 residues of a helical peptide named "Rocker" synthesized by the DeGrado group, *YYKEIAHALFSALFALSELYIAVRY*.[24] The "Rocker" peptide was found to spontaneously form a transmembrane alpha helix that transports zinc ions, and thus provided an ideal scaffold for the development of an anion transporting peptide. The original "Rocker" peptide was first truncated to the first 12 residues in order to provide an example for successful incorporation of the novel amino acid, as well as to test the ability for the new peptide to enter the interior of a lipid bilayer. The first change made to the original sequence was the exchange of the tyrosine (Y) at the second position for a lysine (K) residue to help increase water solubility. The second change made for the "Glu-peptide" was the exchange of the glutamic acid (E) for **2.4**, as for "Asp-peptide the second change was the exchange of an aromatic phenylalanine (F) to compound **2.5**.

Liposomes are used as a model to represent the lipid bilayer that acts as the barrier between what is outside of and inside a cell. Liposomes are made up of a spherical collection of individual lipid molecules that form two layers each with their polar head groups facing the aqueous solvent while the hydrocarbon tails aggregate inwards to form a relatively large non-polar layer. The liposomes used for the experiments performed here are made from the phospholipid 1-Palmitoyl-2-oleoylphosphatidylcholine or POPC. As shown in Figure 2.2(b) the fluorescence intensity and wavelength of compounds **2.1** and **2.2** can change significantly when compared in an organic solvent versus an aqueous solvent. This solvatochromism can be used to

determine if a fluorophore is capable of integrating with the non-polar region of a lipid bilayer in a buffer solution. The "Asp-peptide" was designed to give a peptide that would spontaneously insert into a lipid bilayer. The change in emission wavelength due to a change in surrounding polarity will provide evidence as to where the molecule is located. Likewise, the change in fluorescence intensity will be measured as various anions are titrated into the solution. If the "Asp-peptide" sits in the lipid bilayer as predicted any change in the fluorescence indicative of anion binding will be due to an anion localizing into the interior of the bilayer.

The "Glu-peptide" was purified by HPLC as confirmed by mass spectroscopy and ^{1}H-NMR (see appendix B). While attempting to form liposomes with the "Glu-peptide" the model membranes failed to form and the small amount of purified peptide was lost.

The "Asp-peptide" was formed using compound **2.5**. Although there was a 68 % crude yield of peptide collected after it was cleaved from the resin only <1 mg of the recovered peptide consisted of the complete sequence and had successfully incorporated the new synthetic amino acid. With such a small amount of peptide recovered from HPLC an ^{1}H-NMR was not able to be obtained; however, mass spectroscopy (MS) coupled with an HPLC spectra of a lone large peak absorbing light at 375 nm provided enough evidence to support the purity of the desired peptide (see appendix B).

The "Asp-peptide" was first dissolved into DMSO which was then used to test for insertion into liposomal cell models. Upon addition of 2 µl of the peptide to a Tris-NO_3 buffer solution the fluorescence was found to have a λ_{em}= 490 nm, (Figure 2.20(a)) which is consistent with the λ_{em} of compound **2.2** in H_2O:DMSO (50:1). Next the peptide solution was added to a 2.9 mM liposomal solution. Upon addition of 2 µl the λ_{em} was found to be 487 nm (Figure 2.18

(c)). The max emission is not indicative of the fluorophore being present in a non-polar environment, Figure 2.2 (b) above and Figure 2.20 (b).

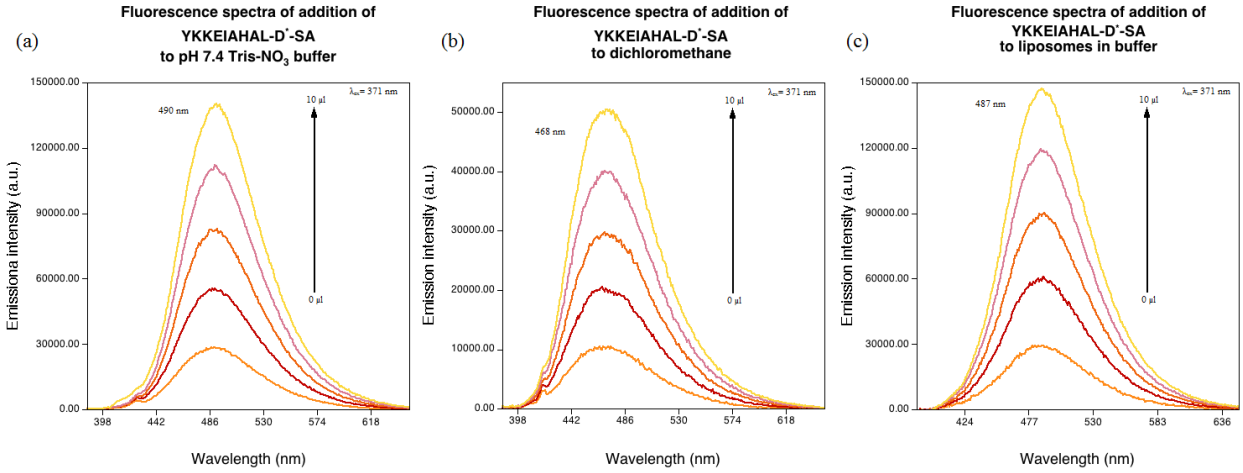

Figure 2.20: Comparative fluorescence spectra of the addition of the "Asp-peptide" to (a) Tris-NO_3 buffer, pH 7.4 (b) dichloromethane (c) a buffered solution of 0.1 µm liposomes (3.0×10^{-3} M)

2.1.8 Conclusion

The rising interest in designer peptides, peptido-pharmaceutical agents, and the use of selective fluorescent markers has created a need for derivatized Fmoc-protected amino acids. Previous studies have shown the utility for fluorescent amino acids that can be used in the elucidation of protein structure,[29] fluorescent tagging of cells,[30] and solvatochromic and pH sensitivity.[53] Compounds **2.1** and **2.2** were successfully synthesized to give fluorescent amino acids with an emission band significantly red-shifted from that of the naturally occurring residues tryptophan, tyrosine, and phenylalanine. Amino acids **2.1** and **2.2** are selectively sensitive to anions containing a carboxylate group and those that have tetrahedral geometry. **2.1**

and **2.2** were both successfully incorporated into a *de novo* peptide through the use of standard solid phase synthesis protocols without limiting residue deprotection or chain lengthening reactions later in the sequence. The novel side chains were capable of surviving treatment with cocktails containing in excess of 95% trifluoroacetic acid (TFA) when the peptides are cleaved from the resin. Future experiments will include further incorporation of amino acids **2.1** and **2.2** into larger, more robust peptides with the hope that a transmembrane helix will be produced that has the ability to discriminately transport anions.

2.2 Experimental Section

2.2.1 Fluorescence Titrations

Fluorescence emission characterization was performed on a PTI QM-4CW system. The naphthalimide amino acids were dissolved in spectroscopic grade acetonitrile at a concentration in between 1.0×10^{-7} M and 1.0×10^{-6} M. At these concentrations, compounds **2.1** and **2.2** were easily soluble in the acetonitrile and did not require any heating or sonication. An absorption spectrum was taken to insure that the absorbance was between 0.05 and 0.10. This was considered a safe range to achieve a significant signal to noise ratio but stay below the threshold that would create interfiltering affects. The titrations were performed on 3.00 mL of sample that was measured using a volumetric pipette into a 1 cm path length quartz cuvette. The wavelength used for sample excitation was the predetermined λ_{max} from the absorbance spectra previously collected. The anions chosen were chloride, bicarbonate, phosphate, and nitrate due to their significance in biological systems. The anions were prepared in spectrophotometric grade acetonitrile in concentrations of 9.0×10^{-5} M to 1.0×10^{-4} M. The anion solutions were added to

the cuvette in small aliquots using a 10.00 µL glass syringe and allowed to stir for 1 minute before a fluorescence spectrum was taken. After a fluorescence titration was completed the area of each emission peak was recorded, *F*, and F_0 is for the initial peak integration before the introduction of any anion guest.

The binding constant K_{assoc} was calculated for the exponential data by plotting the F / F_0 vs. [anion] and using Equation 2.1.

$$F/F_0 = \left(1 + \left(k_{complex}/k_{fluoro}\right)K_{assoc}[anion]\right)/(1 + K_{assoc}[anion]) \qquad \textbf{\textit{eq. 2.1}}$$

Where the values $k_{complex}$ and K_{assoc} were allowed to vary freely, and the constant k_{fluoro} is equal to $F_0/[fluoro]_0$.[46,49,50] Where $[fluoro]_0$ is the initial concentration of the fluorophore host before and anion guest had been added to the solution.

As for the sigmoidal plot given by the complex of **2.1** +bicarbonate the K_{assoc} was calculated from plotting the F / F_0 vs. log[anion] and using Equation 2.2.

$$F/F_0 = 1 + \left(\left((F_{max}/F_0) - 1\right)/(1 + (K_{assoc}[anion]_{total})^p)\right) \qquad \textbf{\textit{eq. 2.2}}$$

Where F_{max} is the integrated intensity at the highest anion concentration, and p is a slope parmeter. Both K_{assoc} and p are allowed to vary freely.[49,50]

The collisional quenching constant K_{SV} was calculated from the best fit line by plotting the F_0 / F vs. [anion] and using Equation 2.3.[51,50]

$$F_0/F = 1 + K_{SV}[anion]_{total} \qquad \textbf{\textit{eq. 2.3}}$$

All of the fluorescence titrations were at least repeated twice except for the nitrate fluorescence titration with compound **2.1** due to a lack of available pure product.

2.2.2 Extinction coefficients

The extinction coefficient was recorded for product **2.2** and the results can be found in Table 1. The amino acid was dissolved into spectrophotometric grade dichloromethane, acetonitrile, and H_2O:DMSO (50:1) at a concentration of approximately 6.2×10^{-5} M. Using a volumetric pipette 3.00 mL of sample is transferred to a 1.00 cm quartz cuvette and the absorption spectra is obtained using an Agilent Technologies Cary 8454 spectrophotometer. Using the Beer's Law equation: $A = \varepsilon C l$ the extinction coefficient ε (M^{-1} cm^{-1}) can be calculated with an experimental absorbance (A) and known concentration (C).

2.2.3 Quantum Yields

The quantum yield of compound **2.1** was measured in spectrophotometric grade 1-octanol and acetonitrile, the results can be found in Table **2.2**. The UV/vis spectra of compound **2.1** (~5.0×10^{-6} M) was taken to insure that the absorbance was between 0.06 and 0.10. Each sample was degassed with nitrogen gas for at least 60 seconds before being capped and inserted in the fluorometer. The samples were excited at the previously determined λ_{max} in order to take an emission scan. The area under the emission band was recorded (F). This process was then repeated for a standard fluorophore (7-amino-4-methylcoumarin) which has a known quantum yield in acetonitrile, $\Phi = 0.63$. To determine the unknown quantum yield of **2.1** in 1-octanol and acetonitrile all of the data was plugged into Equation 2.4.

$$\Phi_{unk} = \frac{A_{std}}{A_{unk}} \cdot \frac{F_{unk}}{F_{std}} \cdot \left(\frac{\eta_{unk}}{\eta_{std}}\right)^2 \cdot \Phi_{std} \qquad \textit{eq. 2.4}$$

2.2.4 Liposomes

Liposomes were prepared with 1-Palmitoyl-2-oleoylphosphatidylcholine or POPC and cholesterol at a ratio of 7:3, lipid to cholesterol. The lipids and cholesterol were first dissolved into a 50/50 mixture of dichloromethane and cyclohexane (~ 10 mL) by gently swirling. Once the lipids were fully dissolved the solvent was removed *in vacuo*. The dry lipids were then hydrated with a 0.10 M aqueous Tris-HNO_3 buffer at pH 7.4. The mixture was magnetically stirred for 1 hour. To obtain unilamellar vesicles the liposomes were treated to 3 freeze-thaw cycles using liquid nitrogen and room temperature water. The unilamellar vesicles were then extruded through a 0.1 µm polycarbonate membrane to achieve liposomes of uniform size. The mixture typically takes on an iridescent blue color as confirmation for the formation of liposomes.

2.2.5 ^{1}H-NMR Titration

All of the ^{1}H-NMR spectra were collected on a Bruker AVANCE400 spectrometer, 400 MHz. Compound **2.1** was dissolved into 0.75 mL of DMSO-d_6 (7.0×10^{-4} M) and compound **2.2** was dissolved into 1.50 mL of DMSO-d_6 (3.6×10^{-4} M). The analyte tetrabutylammonium phosphate monobasic is also dissolved into 0.75 mL of DMSO-d_6 (5.0×10^{-2} M for titration of compound **2.1** and 5.2×10^{-2} M for titration of compound **2.2**). Compound **2.2** was split into two tubes each containing 0.75 mL and was also titrated with tetrabutylammonium chloride hydrate (6.1×10^{-2} M). An initial spectra was taken of just the plain fluorophore without any anion added. The ppm shifts of the N-*H* proton peaks of the ureido group were recorded. Upon addition

of each aliquot of anion the NMR tube was capped and inverted 20 times to ensure complete mixing of the solution. This process was repeated until the concentration of the anion in the solution was about eight or four times the concentration of the host fluorophore **2.1** and **2.2**, respectively. The results of the titration can be seen as Figures 2.15, 2.16, and 2.17.

Association constants were calculated by using the non-linear fitting program WinEQNMR.[47]

2.2.6 Computational Modeling Studies

Computational modeling calculations were performed with the numerical DFT program DMol3,[52,53] where double-numerical plus polarization basis functions with 20.0 Bohr radial cutoffs were employed to form the wave function. The Becke-Tsuneda-Hirao gradient-corrected exchange-correlation functional [54,55] was employed in the Hamiltonian operator. All calculations were performed in the presence of a COSMO (Conductor-like Screening Model) approximation to the solvent field with a 36.6 dielectric constant that is appropriate for acetonitrile.[56,57,58]

2.2.7 Synthesis and Characterization

(*S*)-*tert*-butyl 2-(((9*H*-fluoren-9-yl)methoxy)carbonylamino)-3-(3-(2-butyl-1,3-dioxo-2,3-dihydro-1*H*-benzo[*de*]isoquinolin-6-yl)ureido)propanoate (Compound **2.2**, Scheme 2.3) Under N_2, a mixture of Fmoc-Asp-OtBu (1.05 mmole) and *N*-methylmorpholine (0.116 mL, 1.05 mmole) in dry THF (5 mL) was chilled to -20^o C and stirred for 5 minutes. Ethyl chloroformate (0.102 mL, 1.08 mmole) was slowly added to the solution and allowed to stir for an additional 20

minutes. After 20 minutes, a solution of sodium azide (0.111 g, 1.7 mmole) dissolved in 0.75 mL of water was added to the reaction and the mixture was warmed to room temperature while stirring for 1 hr. Upon completion the solvent was removed by rotary evaporation and the residue was dissolved into methylene chloride (20 mL). The organic phase was washed three times each with 5% HCl, 5% aq. $NaHCO_3$, and water, and dried with anhydrous sodium sulfate. Rotary evaporation removed the methylene chloride and the resulting off-white foamy solid was left on high vacuum overnight. The solid acid azide (0.41 g, 0.95 mmole) was dissolved into freshly distilled toluene (20 mL) along with 4-amino-*N*-butylnaphthalimide (0.3 g, 1.1 mmole). The reaction mixture is heated to reflux for 14 hrs. The toluene is removed by rotary evaporation and the resulting dark orange-brown residue is dissolved into dichloromethane:methanol (9:1). The mixture purified via flash chromatography on regular-phase silica gel where the produce can be collected as the blue fluorescent band (365 nm light bar). The product is further purified via reverse phase HPLC. The product was lyophilized into a dark yellow powder (6%). Mp = 210-212 ^oC; ^1H-NMR (DMSO-d_6, δH ppm, TMS): δ 9.32 (s, 1H), 8.50 (d, 1H), 8.44 (d, 1H), 8.39 (d, 1H), 8.33 (d, 1H), 7.91 (t, 1H), 7.86 (d, 2H), 7.81 (d, 2H), 7.39 (t, 2H), 7.33 (t, 2H), 7.00 (t,1H), 6.16 (broad, 1H), 4.80 (dd, 1H), 4.47 (m, 2H), 4.29 (m, 2H), 4.16 (t, 2H), 3.64 (m, 1H), 1.55 (m, 2H), 1.34 (s, 9H), 1.29 (m, 2H), 0.86 (t, 3H); ^{13}C NMR (DMSO-d_6) δ 163.81, 155.03, 142.69, 141.20, 132.47, 131.48, 128.73, 128.41, 127.52, 126.46. 125.96, 123.37, 122.88, 120.68, 69.20, 47.10, 30.13, 28.10, 20.28, 14.20; ESI-mass: *m/z* (positive ion mode) calcd for ($M+H^+$) 677.2970, found 677.2990. R_f (19:1, DCM:MeOH) = 0.79.

(*S*)-*tert*-butyl 2-(((9*H*-fluoren-9-yl)methoxy)carbonylamino)-4-(3-(2-butyl-1,3-dioxo-2,3-dihydro-1*H*-benzo[*de*]isoquinolin-6-yl)ureido)butanoate (Compound **2.1**, Scheme 2.3) This compound was prepared in a similar manner as compound 2a except that Fmoc-Glu-OtBu was substituted in as the starting material instead of Fmoc-Asp-OtBu. The resulting lyophilized product was a pale green color (5%). Mp = 126 – 127 ^{o}C; ^{1}H-NMR (DMSO-d_6, δH ppm, TMS): δ 9.27 (s, 1H), 8.60 (d, 1H), 8.54 (d, 1H), 8.52 (d, 1H), 8.40 (d, 1H), 7.89 (d, 2H), 7.77 (d, 1H), 7.72 (d, 2H), 7.41 (t, 2H), 7.33 (t, 2H), 6.99 (t, 1H), 5.91 (broad, 1H), 4.22 - 4.34 (m, 3H), 4.04 (t, 1H), 3.91 (m, 1H), 3.28 (m, 1H), 3.04 (dm, 2H), 1.68/1.94 (dm, 2H), 1.78 (m, 2H), 1.61 (m, 2H), 1.39 (s, 9H), 0.93 (t, 3H); ^{13}C NMR (DMSO-d_6) δ 172.02, 156.59, 144.26, 141.19, 128.12, 127.55, 125.74, 120.60, 81.22, 81.00, 66.10, 52.85, 47.11, 28.10, 20.28, 14.21; ESI-mass: *m/z* (positive ion mode) calcd for ($M+H^+$) 691.3126, found 691.3112. R_f (19:1, DCM:MeOH) = 0.82.

2-(((9*H*-fluoren-9-yl)methoxy)carbonylamino)-3-(3-(2-butyl-1,3-dioxo-2,3-dihydro-1*H*-benzo[*de*]isoquinolin-6-yl)ureido)propanoic acid (Compound **2.5**, Scheme 2.3) To convert the *tert*-butyl ester into a carboxylic acid the dark yellow solid 2a is dissolved into a cocktail of 50% trifluoroacetic acid, 40% methylene chloride, 5% triethylsilane, and 5% anisole (v/v). The mixture is allowed to cleave for 90 minutes, with occasional shaking, before the solvent is removed *in vacuo*. The resulting solid is purified via reverse phase HPLC and lyophilized to give a light yellow powder. (63%). Mp = 177 – 178 ^{o}C; ^{1}H-NMR (DMSO-d_6, δH ppm, TMS): 9.33 (s, 1H), 8.53 (d, 1H), 8.47 (d, 1H), 8.44 (d, 1H), 8.33 (d, 1H), 7.81 (d, 2H), 7.78 (d, 1H), 7.73 (d, 1H), 7.65 (dd, 2H), 7.33 (t, 2H), 7.23 (t, 2H), 7.04 (t, 1H), 4.24 (d, 2H), 4.13 – 4.17 (m, 3H), 3.97 (t, 2H), 3.67 (m, 1H), 1.54 (m, 2H), 1.28 (m, 2H), 0.86 (t, 3H); ^{13}C NMR (DMSO-d_6) δ 172.68, 164.02, 163.44,156.75, 155,11, 144.20, 142.74, 141.20, 132,94, 131.20, 128.98, 128.10, 127.54,

126.45, 125.69, 122.89, 122.41, 120.57, 66.29, 54.73, 47.08, 30.19, 20.28, 14.20; ESI-mass: *m/z* (positive ion mode) calcd for ($M+H^+$) 621.2344, found 621.2364.

2-(((9*H*-fluoren-9-yl)methoxy)carbonylamino)-4-(3-(2-butyl-1,3-dioxo-2,3-dihydro-1*H*-benzo[*de*]isoquinolin-6-yl)ureido)butanoic acid (Compound **2.4**, Scheme 2.3) This compound was prepared in a similar manner as compound 3a except that 2b was substituted in as the starting material instead of 2a. The resulting lyophilized product was a pale green color (80%). Mp = 144 – 146 ^{o}C; ^{1}H-NMR (DMSO-d_6, δH ppm, TMS): δ 12.71 (s, 1H), 9.29 (s, 1H), 8.60 (d, 1H), 8.54 (d, 1H), 8.52 (d, 1H), 8.40 (d, 1H), 7.89 (d, 2H), 7.75 (t, 1H), 7.73 (d, 2H), 7.42 (t, 2H), 7.33 (t, 2H), 7.02 (t, 1H), 6.52 (s, 1H), 4.31 (d, 2H), 4.25 (m, 1H), 4.08 (m, 1H), 4.04 (t, 2H), 3.2 (m, 2H, obscured by water), 1.91 (dm, 2H), 1.61 (m, 2H), 1.35 (m, 2H), 0.93 (t, 3H); ESI-mass: *m/z* (positive ion mode) calcd for ($M+H^+$) 635.2500, found 635.2568.

CHAPTER 3: OTHER FLUORESCENT *N*-FMOC-PROTECTED AMINO ACIDS

3.1 Results and Discussion

3.1.1 Diphenylacetylenes

Before settling on the ureido-naphthalimide compounds that make up the bulk of this thesis, several other Fmoc-protected structures were considered. Initially a diphenylacetylene moiety was pursued as a possible anion-responsive group. Previous work in the Allen laboratory with compounds like Figure 1.6 (see Chapter 1) showed that diphenylacetylenes can be prepared in high yield, and are sensitive to their local solvent environment. Target **3.1**, adapted from the compound in Figure 1.6, was pursued first. The synthetic route to produce compound **3.1** began with the formation of the urea group through the coupling of *N*-Fmoc-protected lysine and 4-bromophenyl isocyanate (see Scheme 3.1). The bromine found at the para-position from the urea could then be used to perform a Sonogashira palladium-catalyzed coupling reaction to a phenylacetylene unit.[18,60] In principle, the functional groups associated with the phenylacetylene could be changed to produce a vast library for testing how the anion binding ability of the amino acid would change (see Scheme 3.1). The coupling between the bromophenyl and phenylacetylene was found to be unsuccessful. The reaction was attempted under a battery of reaction conditions, changing the reaction solvent, bases, the reaction temperature, and the time.

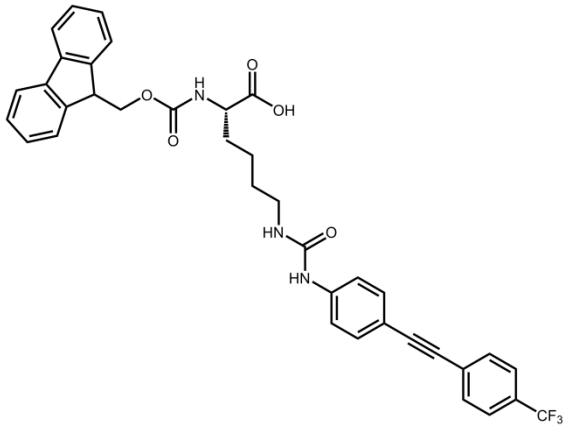

Figure 3.1: Fmoc-protected diarylacetylene amino acid derivative **3.1.**

Scheme 3.1: Synthesis of diarylacetylene fluorescent fmoc-protected amino acids.

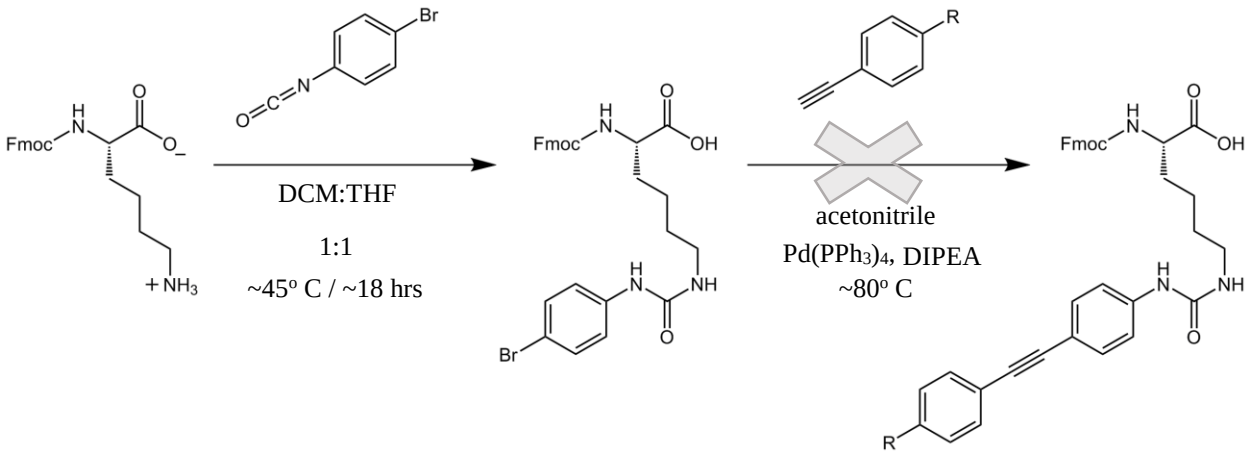

A Negishi coupling reaction which uses zinc chloride as a precursor catalyst for the insertion of palladium at the activated phenyl position was attempted next.[61] The yield was not sufficient to justify the extensive purification, which would not have provided enough material for solid phase peptide synthesis (SPPS). Suzuki coupling reaction conditions were then attempted.[62] Instead of a phenylacetylene unit the reaction called for an aromatic boronic acid, which led to the aromatic rings being directly attached. The loss of an acetylene spacer in the product was potentially problematic, however. The acetylene extends electronic conjugation in the product, which is typically required for generation of long-wavelength absorption/emission. The absence of the acetylene unit could be overlooked if the respective boronic acid unit was a larger aromatic group that would provide a rigid and extended conjugated system. A pyrene 1-boronic acid was chosen to couple to the bromophenyl unit (see Scheme 3.2).

Scheme 3.2: Synthesis of Suzuki coupled diaryl-urea fluorescent fmoc-protected amino acids.

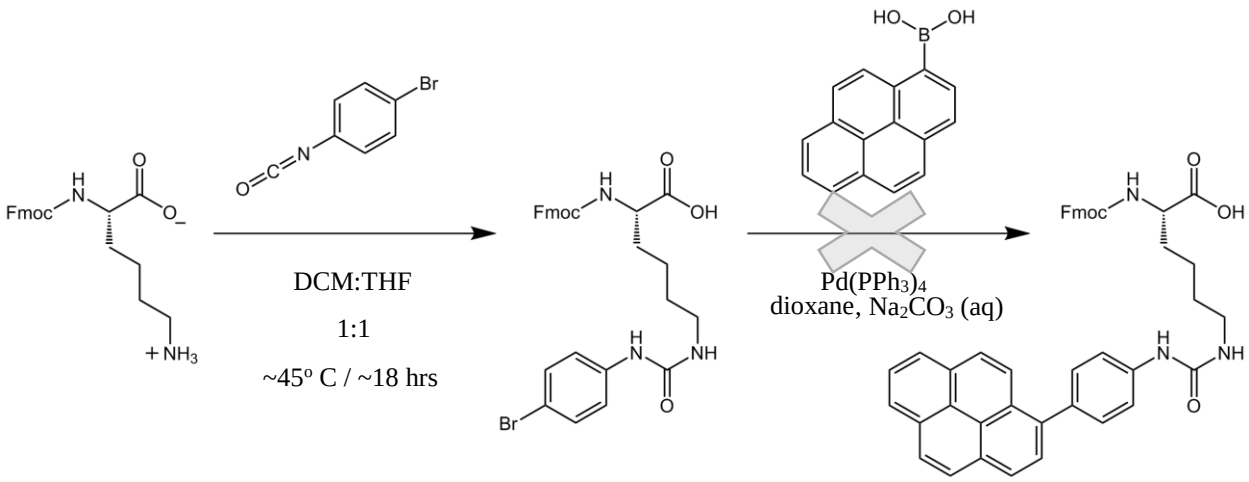

After several attempts at the Suzuki coupling the reaction was deemed a failure. Due to constraints on time and other resources the production of a non-natural amino acid in this manner was abandoned.

3.1.2 Triazoles

The synthesis of new triazole-based derivatives was found to be easily obtainable through the use of azido amino acids and acetylene units. Although the synthesis was a success the desired action of anion binding and sensitivity was absent. Compounds **3.2-3.7** found in Scheme 3.3 were all produced from commercially available materials: either Fmoc-Asn-OH, Fmoc-Gln-OH, or Fmoc-Lys-OH. The triazole moiety was chosen because it was discovered that triazoles are one of the many functional groups that are often found in anion binding molecular sensors.[10,63] Triazoles are also easily synthesized via the coupling of an azide with an acetylene through a Huisgen 1,3-dipolar cycloaddition.[ref] The reaction has been termed more colloquially

as a ‘Click Reaction’ because it could be used to join two pieces of a molecule into a larger structure; similar to the clicking together of two toy Lego blocks to form a single larger, multicolored block. The formation of a triazole through a click reaction has been shown as an effective tool for the introduction of a variety of functional group through interchangeable parts; even on superstructures like fullerenes, porphyrin, calices, and liposomes.[64,65,66] The aromatic, anion-binding triazole provides a perfect jumping-off point for the production of a library of non-natural fluorescent amino acid derivatives.

The synthesis of compounds **3.2-3.5** began with the conversion of the side-chain amide group on asparagine and glutamine into a primary amine through a Hofmann rearrangement.[67] Compounds **3.6** and **3.7** were derived from Fmoc-Lys-OH, which already has a primary amine as the side-chain. Compounds **3.2-3.7** were then converted into azides through the transfer of a diazo unit from imidazole-1-sulfonyl azide hydrochloride via a copper(II) catalyzed reaction.[68] The resulting azides were then coupled with two different aryl acetylene units, 1-ethynyl-2,4-difluorobenzene and 2-ethynyl-6-methoxynaphthalene, using the 1,3-dipolar cycloaddition conditions used by Cau et. al.[69] The full synthesis is provided as Scheme 3.1 and the product designation is given in Table 3.1.

Scheme 3.3: Synthesis of fmoc-protected, fluorescent aryl-triazole containing amino acids 3.2-3.7.

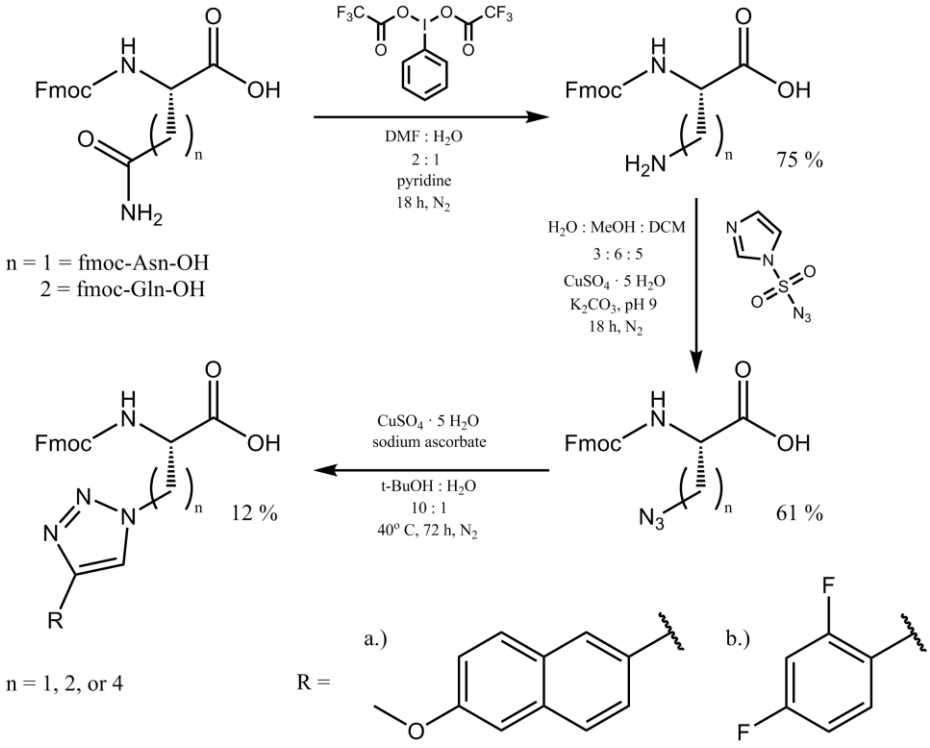

Table 3.1: Compound number and name of the final products in Scheme 3.1.

Compound #/ name	R =	n =
3.2/ Ala(MNT)	a	1
3.3/ Ala(DFB)	b	1
3.4/ Aha(MNT)	a	2
3.5/ Aha(DFB)	b	2
3.6/ Lys(MNT)	a	4
3.7/ Lys(DFB)	b	4

Once the non-natural amino acids were synthesized, the spectrophotometric properties were evaluated to determine if incorporation into peptides should go forward. Thus, compound **3.7** was dissolved in dichloromethane and dimethyl sulfoxide (99:1) and a UV/vis spectrum was acquired. The compound was found to have a λ_{max} at 276 nm and this was the wavelength used to excite the molecule for fluorescence studies. Titrations with both chloride and acetate showed the fluorescence behavior to be consistent with collisional quenching, best represented by a Stern-Volmer plot (Figures 3.2 and 3.3). The Stern-Volmer constants for compound **3.7** with tetrabutylammonium chloride and acetate were 7.4 M^{-1} or 83 M^{-1}, respectively.

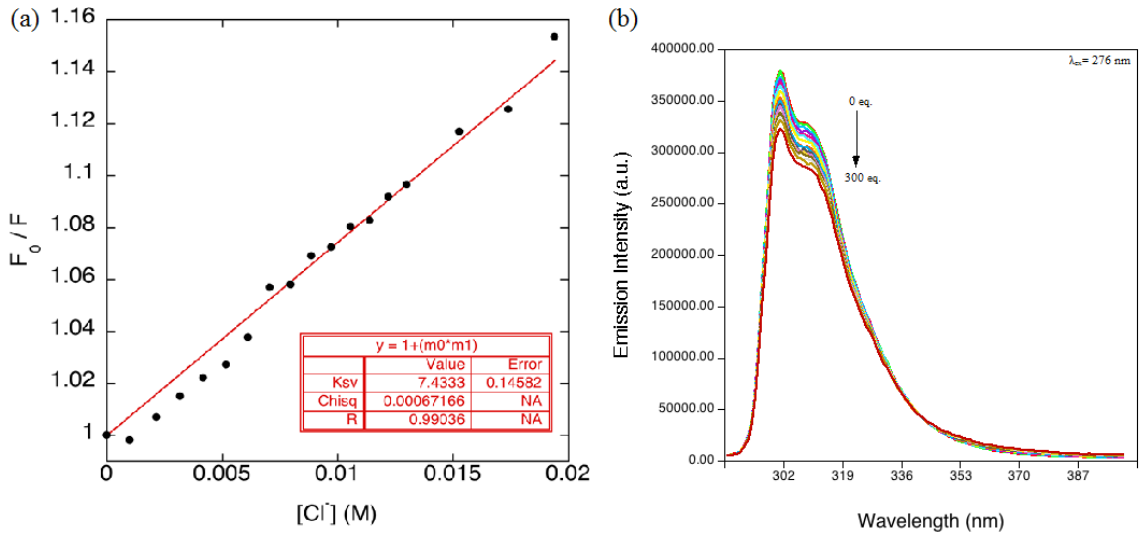

Figure 3.2: a) Fluorescence quenching of compound **3.7** measured via titration with tetrabutylammonium chloride in CH_2Cl_2:DMSO (99:1) and b) corresponding fluorescence spectra.

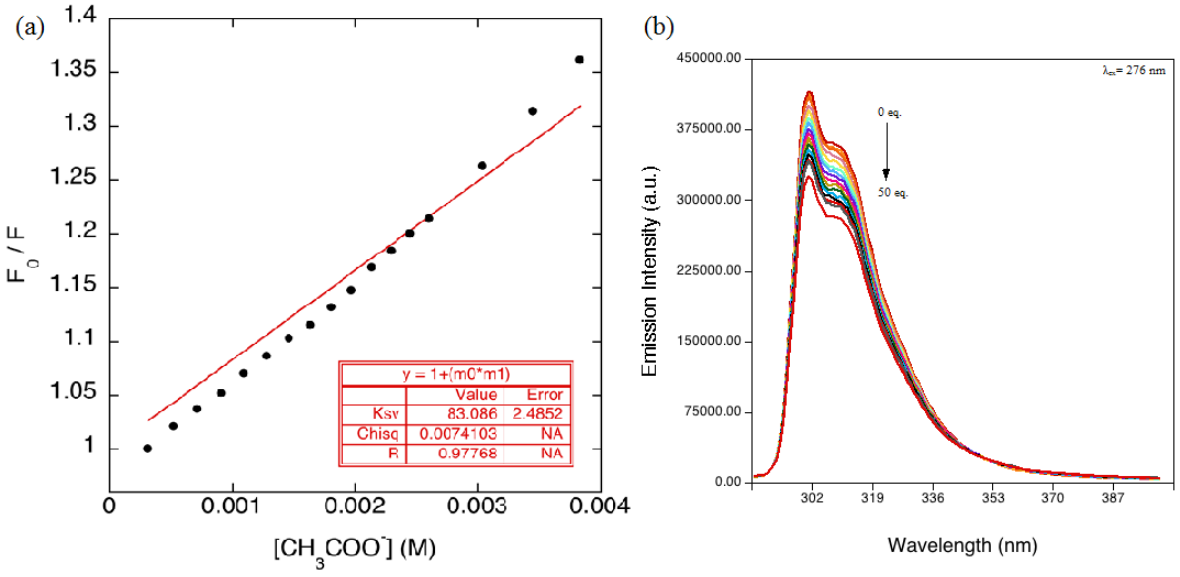

Figure 3.3: a) Fluorescence quenching of compound **3.7** measured via titration with tetrabutylammonium acetate in CH_2Cl_2:DMSO (99:1) and b) corresponding fluorescence spectra.

Compound **3.2** was also subjected to a fluorescence titration experiment. The electronic absorption maximum was determined to be 300 nm; the molecule was excited at this wavelength during titration with tetrabutylammonium chloride. Again, the results followed a collisional quenching pattern (Figure 3.4).

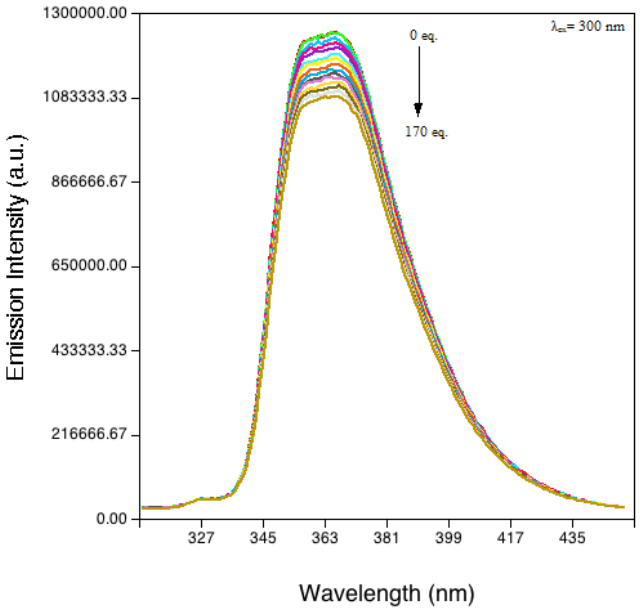

Figure 3.4: Fluorescence spectra of compound **3.2** during titration with tetrabutylammonium chloride in CH_2Cl_2:DMSO (99:1).

Compound **3.2** was also successfully incorporated into the eight residue peptide Ac-Ala-Ala-Ala-Ala-Ala(MNT)-Ala-Arg-Arg-NH_2. This short peptide was synthesized to provide evidence that the non-natural amino acid would behave like normal Fmoc-amino acids during standard solid phase synthesis protocols. It was shown that the derivatization of the amino acid side-chain did not affect its solubility in *N*,*N*-dimethylformamide, it could survive interactions with piperidine and *N*,*N*-diisopropylethylamine, it did not significantly hinder the coupling of any residue in the sequence, and it could survive treatment with trifluoroacetic acid, the main ingredient used to cleave the finished peptide off of the solid resin.

3.1.3 Conclusions

Compounds **3.2-3.7** must be excited in the UV region (276 or 300 nm) in order to record a fluorescence measurement, meaning they are not well-suited to biological applications where many intrinsic chromophores might interfere. From the results previously discussed, the compounds were also poor receptors for the biologically relevant anions that were the greatest concern for this research. Although, **3.1** was not successfully synthesized, the use of a urea moiety was reconsidered as the most beneficial anion binding receptor and thus would lead to the most desirable results. A pre-established fluorophore with a red-shifted excitation wavelength from that of native amino acids would be needed in order to assure that a finished synthetic peptide could eventually be used in a biological system as an analytical tool.[29,32]

3.2 Experimental Section

3.2.1 Fluorescence Titrations

Fluorescence emission characterization was performed on a PTI QM-4CW system. The triazole derivatized amino acids were dissolved into spectrophotometric grade dichloromethane and dimethylsulfoxide (99:1) at a concentration in between 8.0×10^{-6} and 1.0×10^{-5} M. The amino acids would not go directly into dichloromethane and must be first dissolved into DMSO. An absorption spectrum was taken of compounds 3.2 and 3.7 were taken to reassure that the absorbance was between 0.05 and 0.10 a.u. This was considered a safe range to achieve a significant signal to noise ratio with creating interfiltering affects. The titrations were performed on 3.00 mL of sample that was measured using a volumetric pipette. The measurements were taken in a 1 cm path length quartz cuvette. The wavelength used for sample excitation was

determined from the maximum absorbance found through UV/vis experiments. The anions that were used were chloride and acetate, obtained through dissolving the tetrabutylammonium salts of each in spectroscopic DCM and DMSO (99:1). The anion solutions were dissolved in concentrations ranging from 5×10^{-4} to 1×10^{-3} M. The anion solutions were added to the cuvette in small aliquots using a 10.00 µL glass syringe and allowed to stir for 1 minute before a fluorescence spectrum was taken. After a fluorescence titration was completed the area of each emission peak was recorded. The collisional quenching constant K_{SV} was calculated from the best fit line by plotting the F_0 / F vs. [anion] and using Equation 3.1.[51,50]

$$F_0/F = 1 + K_{SV}[anion]_{total} \qquad \textbf{\textit{eq. 3.1}}$$

3.2.2 Synthesis and Characterization

(*S*)-2-(((9*H*-fluoren-9-yl)methoxy)carbonylamino)-3-(4-(6-methoxynaphthalen-2-yl)-1*H*-1,2,3-triazol-1-yl)propanoic acid (compound **3.2**, Ala(MNT)) Under N_2 Fmoc-Asn-OH (1.6 mmol) is added to a solution of 8 mL *N*,*N*-dimethylformamide and 4 mL water along with [bis(trifluoroacetoxy)iodo]benzene (2.4 mmole). After stirring for ~15 mins pyridine (6.0 mmol) was added and the mixture was allowed to stir vigorously overnight at room tempereature. The following morning the solvent was removed through rotary evaporation and the remaining viscous residue was dissolved into 10 mL or 6.6 % HCl (v/v). The solution was washed three times with 20 mL of diethyl ether and then the aqueous phase was adjusted to a pH of 6 using 2 M sodium hydroxide. Upon addition of the sodium hydroxide a beige precipitate formed. The solid was collected via suction filtration and washed with cold water, cold ethanol, and cold

diethyl ether. The solid was collected and dried under reduced pressure overnight. (51-75 % yield)

Under nitrogen the solid Fmoc-Dap-OH (0.82 mmole) was dissolved in a solution containing 2.5 mole percent (5.0 mg) of copper (II) sulfate pentahydrate and imidazole-1-sulfonyl azide hydrochloride (2.6 mmole) in a biphasic mixture of water (4 mL), methanol (7 mL), and methylene chloride (6 mL). The solution is adjusted to a pH of 9 through the addition of three mL of saturated potassium carbonate solution. The reaction mixture is allowed to stir vigorously overnight at room temperature. The following morning the reaction mixture is diluted with eight additional milliliters of methylene chloride. The aqueous phase is isolated and the organic phase is extracted twice with 15 mL of saturated sodium bicarbonate solution. The combined aqueous phases were washed twice with 15 mL of diethyl ether and then acidified to a pH of 2 with concentrated hydrochloric acid. Upon addition of the hydrochloric acid a white precipitate began to form. The aqueous mixture was extracted with three sets of 20 mL of diethyl ether. The ether is dried with magnesium sulfate and then removed *in vacuo* to give a viscous yellow oil that was allowed to dry on high vacuum overnight. (31-61 % yield)

The viscous oil, Fmoc-Ala(N_3)-OH (0.26 mmole) was dissolved into a solution of *tert*-butanol and water (9:1) along with a 3.0 mole percent of copper (II) sulfate pentahydrate, an 11.0 mole percent of sodium ascorbate, and 1 equivalent of 2-ethynyl-6-methoxynaphthalene. The solution was heated to 55^{o} C and stirred overnight. No product was visible by TLC using a 50:49:1 methylene chloride, ethyl acetate solution, and formic acid. The mixture was monitored over the course of five days before a new spot developed by TLC. The solvent was removed by reduced pressure and the crude residue was subjected to flash silica gel column chromatography (50:49:1, DCM:EtOAc:formic acid). The spot with an R_f value of 0.32 was collected and the

solvent removed by rotary evaporation and left to dry on high vacuum overnight leaving a thin yellow film. (7-22 % yield) ^{1}H-NMR (DMSO-d_6, δH ppm, TMS): δ 8.28 (s, 1H), 7.94 (d,1H), 7.87 (m, 5H), 7.64 (m, 3H), 7.37, (m, 2H), 7.35 (s, 1H), 7.26 (m, 2H), 7.19 (d, 1H), 4.87 (dd, 1H), 4.72 (dd, 1H), 4.59 (m, 1H), 4.24 (m, 1H), 4.22 (m, 2H), 3.98 (s, 3H); ^{13}C NMR (DMSO-d_6) δ 171.15, 157.93, 156.35, 146.86, 144.13, 141.12, 134.35, 129.99, 129.99, 128.08, 127.84, 127.53, 126.39, 125.67, 125.62, 124.55, 123.88, 122.36, 120.55, 119.60, 106.50, 66.33, 55.70, 46.97, 25.95; ESI-mass: *m/z* (positive ion mode) calcd for ($M+H^+$) 535.1981, found 535.1541.

(*S*)-2-(((9*H*-fluoren-9-yl)methoxy)carbonylamino)-3-(4-(2,4-difluorophenyl)-1*H*-1,2,3-triazol-1-yl)propanoic acid (compound **3.3**, Ala(DFB)) This compound was prepared in a similar manner as compound **3.2** except that 1-ethynyl-2,4-difluorobenzene was substituted in as a reagent instead of 2-ethynyl-6-methoxynaphthalene. ESI-mass: *m/z* (positive ion mode) calcd for ($M+H^+$) 491.1531, found 491.1401.

(*S*)-2-(((9*H*-fluoren-9-yl)methoxy)carbonylamino)-4-(4-(6-methoxynaphthalen-2-yl)-1*H*-1,2,3-triazol-1-yl)butanoic acid (compound **3.4**, Aha(MNT)) This compound was prepared in a similar manner as compound **3.2** except that instead of starting with Fmoc-Asn-OH the amino acid Fmoc-Gln-OH was used to extend the side chain by one methylene unit.

(*S*)-2-(((9*H*-fluoren-9-yl)methoxy)carbonylamino)-4-(4-(2,4-difluorophenyl)-1*H*-1,2,3-triazol-1-yl)butanoic acid (compound **3.5**, Aha(DFB)) This compound was prepared in a similar manner as compound **3.4** except that 1-ethynyl-2,4-difluorobenzene was substituted in as a reagent instead of 2-ethynyl-6-methoxynaphthalene.

(*S*)-2-(((9*H*-fluoren-9-yl)methoxy)carbonylamino)-6-(4-(6-methoxynaphthalen-2-yl)-1*H*-1,2,3-triazol-1-yl)hexanoic acid (compound **3.6**, Lys(MNT)) This compound was prepared in a similar manner as compound **3.2** except that the initial conversion of a side-chain amide group into a primary amine was unnecessary because the starting material was Fmoc-Lys-OH which already contains an primary amino group on its side chain. ESI-mass: *m/z* (positive ion mode) calcd for ($M+H^+$) 577.2451, found 577.2029.

(*S*)-2-(((9*H*-fluoren-9-yl)methoxy)carbonylamino)-6-(4-(2,4-difluorophenyl)-1*H*-1,2,3-triazol-1-yl)hexanoic acid (compound **3.7**, Lys(DFB)) This compound was prepared in a similar manner as compound **3.6** except that 1-ethynyl-2,4-difluorobenzene was substituted in as reagent instead of 2-ethynyl-6-methoxynaphthalene. ESI-mass: *m/z* (positive ion mode) calcd for ($M+H^+$) 533.2000, found 533.1526.

REFERENCES

1. Andrews, Natalie J.; Haynes, Cally J. E.; Light, Mark E.; Moore, Stephen J.; Tong, Christine C.; Davis, Jeffrey T.; Harrell, William A.; Gale, Phillip A. Structurally Simple lipid bilayer transport agents for chloride and bicarbonate. *Chem. Sci.* **2011,** *2,* 256-260.
2. Lebecque, Patrick. The Prognosis of Cystic Fibrosis-A Clinician's Perspective. *In Cystic Fibrosis-Renewed Hopes Through Research;* Sriramulu, D., Ed.; InTech, **2012,** pp. 1-30.
3. Marco Lucarelli, Silvia Pierandrei, Sabina Maria Bruno and Roberto Strom. The Genetics of CFTR: Genotype-Phenotype Relationship, Diagnostic Challenge and Therapeutic Implications. *In Cystic Fibrosis-Renewed Hopes Through Research;* Sriramulu, D., Ed.; InTech, 2012. pp. 91-122.
4. Thibodeau, Patrick H.; Brautigam, Chad A.; Machius, Mischa; and Thomas, Philip J. Side chain and backbone contributions of Phe508 to CFTR folding. *Nat. Struct. & Mol. Biol.* **2005,** *12,* 10-16.
5. National Institutes of Health: National Heart, Lung, and Blood Institute: Health Information for the Public: Health Topics: Cystic Fibrosis. http://www.nhlbi.nih.gov/health/health-topics/topics/cf/signs.html (accessed April 4th, 2014).
6. Cystic Fibrosis Foundation. http://www.cff.org/treatments/Therapies/Kalydeco/ (accessed April 2, 2014).
7. Busschaert, N., Gale, P., Haynes, C., Light, M., Moore, S., Tong, C., Davis, J., Harrell, W. Tripodal transmembrane transporters for bicarbonate. *Chem. Commun.* **2010,** *46,* 6252-6254
8. Gale, Phillip A.; Sessler, Jonathan L.; Kral, Vladimir; and Lynch, Vincent. Calix[4]pyrroles: Old yet New Anion-Binding Agents. *J. Am. Chem. Soc.* **1996,** *118,* 5140-5141.
9. Sessler, Jonathan L.; Gross, Dustin E.; Cho Won-Seob; Lynch, Vincent M.; Schmidtchen, Franz P.; Bates, Gareth W.; Light, Mark E.; Gale, Phillip A. Calix[4]pyrrole as a Chloride Anion Receptor: Solvent and Countercation Effects. *J. Am. Chem. Soc.* **2006,** *128,* 12281-12288.

10. Fisher, M.; Gale, P.; Hiscock, J.; Hursthouse, M.; Light, M.; Schmidtchen, F.; Tong, C. 1,2,3-Triazole-strapped calix[4]pyrrole: a new membrane transporter for chloride. *Chem. Commun*. **2009,** *21*, 3017-3019.
11. Lee, Gon-Ann; Wang, Wen-Chieh; Shieh, Minghuey; Kuo, Ting-Shen. A novel synthesis of calix[4]thiophenes and calix[4]furans. *Chem. Commun.* **2010,** *46*, 5009-5011.
12. Deng, Gang; Dewa, Takehisa; and Regen, Steven L. A Synthetic Ionophore That Recognizes Negatively Charged Phospholipid Membranes. *J. Am. Chem. Soc.* **1996,** *118*, 8975-8976.
13. Otto, Sijbren; Osifchin, Manette; Regen, Steven L. Modular Control over the Selectivity of Self-Assembling and Membrane-Spanning Ion Conductors. *J. Am. Chem. Soc.* **1999,** *121*, 7276-7277.
14. Quesada, Jorge Sanchez-; Isler, Markus P.; Ghadiri, M. Reza. Modulating Ion Channel Properties of Transmembrane Peptide Nanotubes through Heteromeric Supramolecular Assemblies. *J. Am. Chem. Soc.* **2002,** *124*, 10004-10005.
15. Horne, Seth W.; Stout, C. David; Ghadiri, M. Reza. A Heterocyclic Peptide Nanotube. *J. Am. Chem. Soc.* **2003,** *125*, 9372-9376.
16. Khazanovich, Nina; Granja, Juan R.; McRee, Duncan E.; Milligan, Ronald A.; Ghadiri, M. Reza. Nanoscale Tubular Ensembles with Specified Internal Diameters. Design of a Self-Assembled Nanotube with a 13-Å Pore. *J. Am. Chem. Soc.* **1994,** *116*, 6011-6012.
17. Quesada, Jorge Sanchez-; Kim, Hui Sun; Ghadiri, M. Reza. A Synthetic Pore-Mediated Transmembrane Transport of Glutamic Acid. *Angew. Chem. Int. Ed.* **2001,** *40*, 2503-2506.
18. Jessen, Danielle. M.; Wercholuk, Ashley N.; Xiong, Ber; Sargent, Andrew L.; Allen, William E. Dimerization and Anion Binding of a Fluorescent Phospholipid Analogue. *J. of Org. Chem*. **2012,** *77*, 6615-6619.
19. Hodges, Robert S. and Kohn, Wayne D. De novo design of α-helical coiled coils and bundles: models for the development of protein-design principles. *Tibtech.* **1998,** *16*, 379-389.
20. Van Woerkom, W.J.; and Van Nispen, J.W. Difficult couplings in stepwise solid phase peptide synthesis: predictable or just a guess?. *Int. J. Peptide Protein Res.* **1991,** *38*, 103-113.

21. MacCallum, Justin L.; Bennett, W.F. Drew; Tieleman, D. Peter. Distribution of Amino Acids in a Lipid Bilayer from Computer Simulations. *Biophys. J.* **2008,** *94,* 3393-3404.
22. Bilgicer, Basar and Kumar, Krishna. De novo design of defined helical bundles in membrane environments. *PNAS.* **2004,** *101,* 15324-15329.
23. Anfinsen, Christian B. Principles that Govern the Folding of Protein Chains. *Science.* **1973,** *181,* 223-230.
24. Joh, Nathan H.; Wang, Tuo; Bhate, Manasi P.; Acharya, Rudresh; Wu, Yibing; Grabe, Michael; Hong, Mei; Grigoryan, Gevorg; DeGrado, William F. De novo design of a transmembrane Zn^{2+} -transporting four-helix bundle. *Science.* **2014,** *346,* 1520-1524.
25. Lukasz Slabinski; Lukasz Jaroszewski; Ana P.C. Rodrigues; Leszek Rychlewski; Ian A. Wilson; Scott A. Lesley; Adam Godzik,. The Challenge of protein structure determination-lessons from structural genomics. *Protein Science*. **2007,** *16,* 2472-2482.
26. Kobayashi, Hisataka; Ogawa, Mikako; Alford, Raphael; Choyke, Peter L. and Yasuteru Urano. New Strategies for Fluorescent Probe Design in Medical Diagnostic Imaging. *Chem. Rev.* **2010,** *110,* 2620-2640.
27. Yasuteru Urano; Daisuke Asanuma; Yukihiro Hama; Yoshinori Koyama; Tristan Barrett; Mako Kamiya; Tetsuo Nagano; Toshiaki Watanabe; Akira Hasegawa; Peter L Choyke; and Hisataka Kobayashi. Selective Molecular Imaging of Viable Cancer Cells with pH-activatable Fluorescence Probes. *Nat. Med.* **2009,** *15,* 104-109.
28. Taotao Zou; Ching Tung; Lum Stephen; Sin-Yin Chui; and Chi-Ming Che. Gold(III) Complexes Containing N-Heterocyclic Carbene Ligands: Thiol “Swith-on” Fluorescent Probes and Anti-Cancer Agents. *Angew. Chem.* **2013,** *125,* 3002-3005.
29. Goldberg, Jacob M.; Speight, Lee C.; Fegley, Mark W.; and Petersson, E. James. Minimalist Probes for Studying Protein Dynamics: Thioamide Quenching of Selectively Excitable Fluorescent Amino Acids. *J. Am. Chem. Soc.* **2012,** *134,* 6088-6091.
30. Koopmans, Timo, van Haren, Matthijs; van Ufford, Linda Q.; Beekman, Jeffrey M.; Martin, Natheniel I. A concise preparation of the fluorescent amino acid L-(7-hydroxycoumarin-4-yl)ethylglycine and extension of its utility in solid phase peptide synthesis. *Bioorg. Med. Chem.* **2013,** *21,* 553-559.

31. Goddard, Alan D. and Watts, Anthony. Contributions of Fluorescence Techniques to Understanding G Protein-Coupled Receptor Dimerisation. *Biophys. Rev.* **2012,** *4,* 291-298.
32. Pace, C. Nick; Vajdos, Felix; Fee, Lanette; Grimsley, Gerald; and Gray, Theronica. How to measure and predict the molar absorption coefficient of a protein. *Prot. Sci.* **1995,** *4,* 2411-2423.
33. Mcknight, C.J.; Doering, D.S.; Matsudaira, P.T.; Kim, P.S. A Thermostable 35-Residue Subdomain within Villin Headpiece. *J. Mol. Biol.* **1996,** *260,* 126-134.
34. Cellmer, Troy; Buscaglia, Marco; Henry, Eric R.; Hofrichter, James; and Eaton, William A. Making connections between Ultrafast protein folding kinetics and molecular dynamics simulations. *PNAS.* **2011,** *108,* 6103-6108.
35. Esteban-Gomez, David; Fabbrizzi, Luigi; and Licchelli, Maurizio. Why, on Interaction of Urea-Based Receptors with Fluoride, Beautiful Colors Develop. *J. Org. Chem.* **2005,** *70,* 5715-5720.
36. Kaschny, Peter and Goni, Felix M. The components of merocyanine-540 absorption spectra in aqueous, micellar and bilayer environments. *Eur. J. Biochem.* **1992,** *207,* 1085-1091.
37. Valeur, Bernard. *Molecular Fluorescence: Principles and Applications*.; Wiley-VCH: Weinheim, **2002,** 218-219, 224, 300.
38. Brooks, Simon J.; Gale, Phillip A.; Light, Mark E. Anion-binding modes in a macrocyclic amidurea. *Chem. Commun.* **2006,** 4344-4346.
39. Cap, L.; Jiang, R.; Zhu, Y.; Wang, X.; Li, Y.; Li, Y. Synthesis of 1,2,3-Triazole-4-carboxamide-Containing Foldamers for Sulfate Recognition. *Euro. J. Org. Chem*. **2014**.
40. Caltagirone, Claudia; Gale, Phillip A.; Hiscock, Jennifer R.; Brooks, Simon J.; Hursthouse, Michael B.; and Light, Mark E. 1,3-Diindolylureas: high affinity dihydrogen phosphate receptors. *Chem. Commun.* **2008,** 3007-3009.
41. Amendola, Valeria; Fabbrizzi, Luigi; Mosca, Lorenzo; and Schmidtchen, Franz-Peter. Urea-, Squaramide-, and Sulfonamide-Based Anion Receptors: A Thermodynamic Study. *Chem. Eur. J.* **2011,** *17,* 5972-5981.

42. Baggi, Giorgio; Boiocchi, Massimo; Fabbrizzi, Luigi; and Mosca, Lorenzo. Moderate and Advanced Intramolecular Proton Transfer in Urea-Anion Hydrogen-Bonded Complexes. *Chem. Eur. J.* **2011,** *17,* 9423-9439.
43. Loving, Galen and Imperiali, Barbara. A Versitile Amino Acid Analogue of the Solvatochromic Fluorophore 4-*N,N*-Dimethylamino-1,8-naphthalimide: A Powerful Tool for the Study of Dynamic Protein Interactions. *J. Am. Chem. Soc.* **2008,** *130,* 13630-13638.
44. Tian, Yanquing; Su, Fengyu; Weber, Warner; Nandakumar, Vivek; Shumway, Bradley R.; Jin, Yuguang; Zhou, Xiangeng; Holl, Mark R.; Johnson, Roger H. Meldrum, Deirdre R. A series of naphthalimide derivatives as intra and extracellular pH sensors. *Biomat.* **2010,** *31,* 7411-7422.
45. Suresh Babu, Vommina V.; Ananda, Kuppanna; Vasanthakumar, Ganga-Ramu. (Fluoren-9-ylmethoxy)carbonyl (Fmoc) amino acid azides: Synthesis, isolation, characterization, stability and application to synthesis of peptides. *J. Chem. Sol., Perkin Trans.* **2000,** *1,* 4328-4331.
46. Triboni, Eduardo R.; Filho, Pedro B.; de Souza Berlinck, Roberto Gomes; Politi, Mario J. Efficient Sonochemical Synthesis of 3- and 4-Electron Withdrawing Ring Substituted *N*-Alkyl-1,8-naphthalimides from the Related Anhydrides. *Syn. Comm.* **2004,** *34,* 1989-1999.
47. Hynes, M.J. EQNMR: A Computer Program for the Calculation of Stability Constants from Nuclear Magnetic Resonance Chemical Shift Data. *J. Chem. Soc., Dalton Trans.* **1993,** 311-312.
48. Causey, Corey P. and Allen, William E. Anion Binding by Fluorescent Biimidazole Diamides. *J. Org. Chem.* **2002,** *67,* 5963-5968.
49. Uppadine, L. H.; Drew, M. G. B.; Beer, P. D. Anion selectivity properties of ruthenium(II) tris(5,5'-diamide-2,2'-bipyridine) receptors dictated by solvent and amide substituent. *Chem. Commun.* **2001,** 291-292.
50. Connors, K. A. *Binding Constants;* Wiley: New York, 1987.
51. Jordan, Lisa M.; Boyle, Paul D.; Sargent, Andrew L.; Allen, William E. Binding of Carboxylic Acids by Fluorescent Pyridyl Ureas. *J. Org. Chem.* **2010,** *75,* 8450-8456.

52. Delley, B. An all-electron numerical method for solving the local density functional for polyatomic molecules. *J. Chem. Phys.* **1990,** *92,* 508-517.
53. Delley, B. From molecules to solids with the DMol^3 approach. *J. Chem. Phys.* **2000,** *113,* 7756-7764.
54. Becke, A.D. Correlation energy of an inhomogeneous electron gas: A coordinate-space model. *J. Chem. Phys.* **1988,** *88,* 1053-1062.
55. Tsuneda, Takao and Hirao, Kimihiko. A new spin-polarized Colle-Salvetti-type correlation energy functional. *Chem. Phys. Lett.* **1997,** *268,* 510-520.
56. Klamt, A. and Schuurmann, G. COSMO: A New Approach to Dielectric Screening in Solvents with Explicit Expressions for the Screening Energy and its Gradient. *J. Chem. Soc., Perkin Trans.* **1993,** *2,* 799-805.
57. Klamt, Andreas. Conductor-like Screening Model for Real Solvents: A New Approach to Quantitative Calculation of Solvation Phenomena. *J. Phys. Chem.* **1995,** *99,* 2224-2235.
58. Klamt, Andreas and Jonas, Volker. Treatment of the outlying charge in continuum solvation models. *J. Chem. Phys.* **1996,** *105,* 9972-9981.
59. McFarland, Sherri A. and Finney, Nathaniel S. Fluorescent Signaling Based on Control of Excited State Dynamics. Biarylacetylene Fluorescent Chemosensors. *J. Am. Chem. Soc.* **2002,** *124,* 1178-1179.
60. Sonogashira, Kenkichi; Tohda, Yasuo; Hagihara, Nobue. A Convenient Synthesis of Acetylenes: Catalytic Substitutions of Acetylenic Hydrogen with Bromoalkenes, Iodoarenes, and Bromopyridines. *Tet. Lett.* **1975,** *50,* 4467-4470.
61. **Huo**, Shouquan; Mroz, Robert, and Carroll, Jeffrey. Negishi coupling in the synthesis of advanced electronic, optical, electrochemical, and magnetic materials. *Org. Chem. Front,* **2015,** *2,* 416-445.
62. Miyaura, Norio and Suzuki, Akira. Palladium-Catalyzed Cross-Coupling Reactions of Organoboron Compounds. *Chem. Rev.* **1995,** *95,* 2457-2483.
63. Lee, Semin; Hua, Yuran; Park, Hyunsoo; Flood, Amar H. Intramolecular Hydrogen Bonds Preorganize an Aryl-triazole receptor into a Crescent for Chloride Binding. *Org. Lett.* **2010,** *12,* 2100-2102.
64. Fazio, Michael A.; Lee, Olivia P.; and Schuster, David I. First Triazole-Linked Porphyrin-Fullerene Dyads. *Org. Lett.* **2008,** *10,* 4979-4982.

65. Baskin, Jeremy M.; Prescher Jennifer A.; Laughlin, Scott T.; Agard, Nicholas J.; Chang, Pamela V.; Miller, Isaac A.; Lo, Anderson; Codelli, Julian A.; Bertozzi, Carolyn R. Copper-free click chemistry for dynamic *in vivo* imaging. *PNAS.* **2007,** *104,* 16793-16797.
66. Sletten, Ellen M. and Bertozzi, Carolyn R. Bioorthogonal Chemistry: Fishing for Selectivity in a Sea of Functionality. *Angew. Chem. Int. Ed.* **2009,** *48,* 6974-6998.
67. Lau, Y.H.; Spring, D.R. Efficient synthesis of Fmoc-protected azido amino acids. *Synlett* **2011,** *13,* 1917-1919.
68. Goddard-Borger, Ethan D. and Stick, Robert V. An Efficient, Inexpensive, and Shelf-Stable Diazotransfer Reagent: Imidazole-1-Sulfonyl Azide Hydrochloride. *Org. Lett.* **2007,** *9,* 3797-3800.
69. Cap, L.; Jiang, R.; Zhu, Y.; Wang, X.; Li, Y.; Li, Y. Synthesis of 1,2,3-triazole-4-carboxamide-containing foldamers for sulfate recognition. *Eur. J. Org. Chem.* **2014,** *13,* 2687-2693.

APPENDIX A: FLUORESCENE TITRATION SPECTRA AND CURVE FITS

2.1 + $H_2PO_4^-$

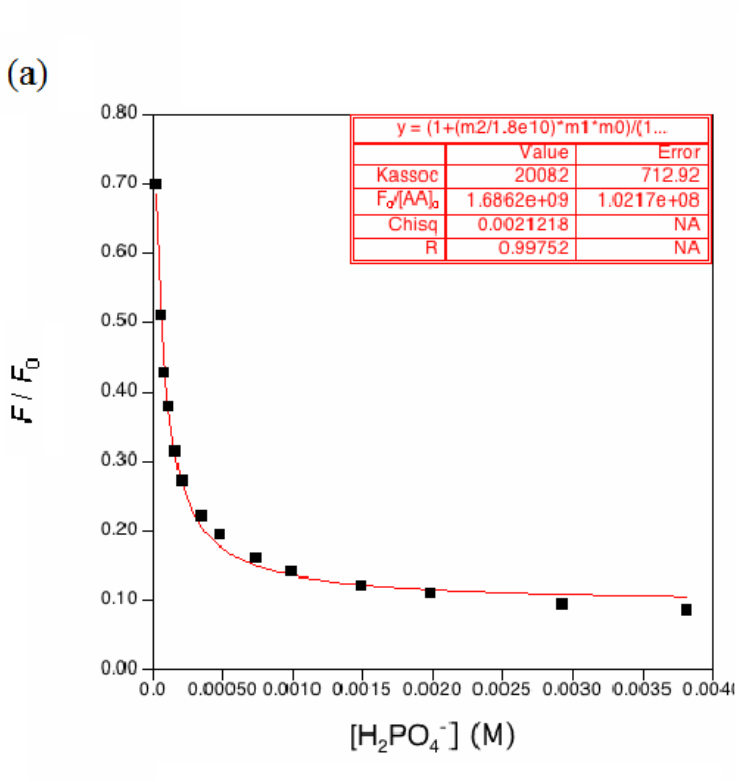

2.1 + $H_2PO_4^-$

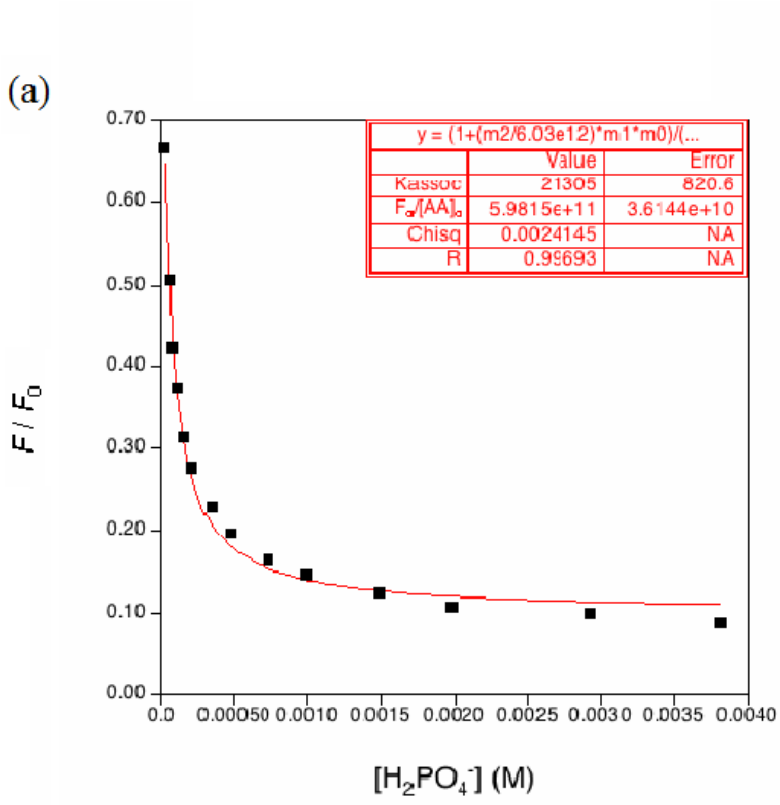
(a)
y = (1+(m2/6.03e12)*m1*m0)/(...
Value Error
Kassoc 21305 820.6
F0/[AA]0 5.9815e+11 3.6144e+10
Chisq 0.0024145 NA
R 0.99693 NA
F / F0
0.70
0.60
0.50
0.40
0.30
0.20
0.10
0.00
0.0 0.0005 0.0010 0.0015 0.0020 0.0025 0.0030 0.0035 0.0040
[H2PO4-] (M)

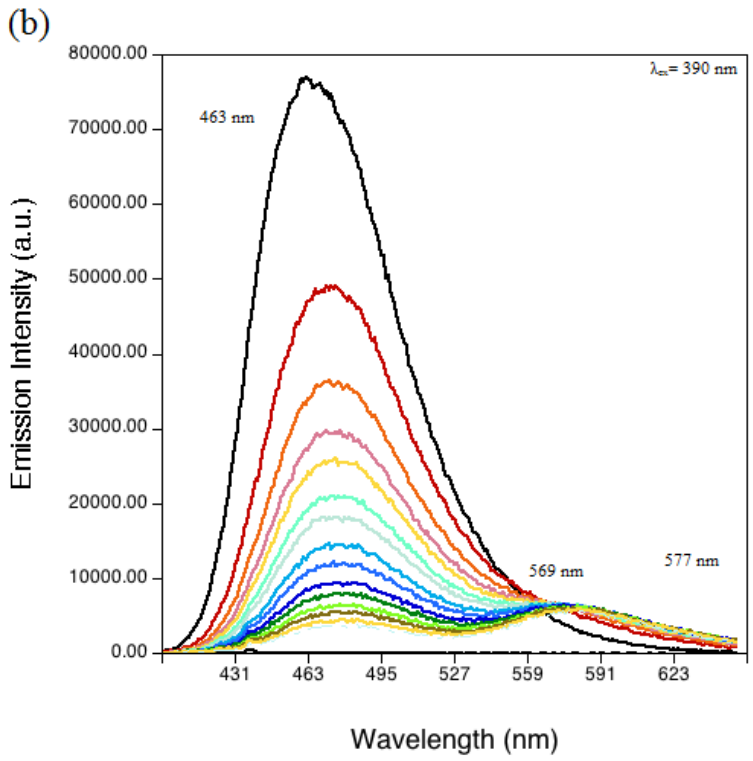
(b)
λex= 390 nm
463 nm
569 nm
577 nm
Emission Intensity (a.u.)
80000.00
70000.00
60000.00
50000.00
40000.00
30000.00
20000.00
10000.00
0.00
431 463 495 527 559 591 623
Wavelength (nm)

2.1 + $H_2PO_4^-$

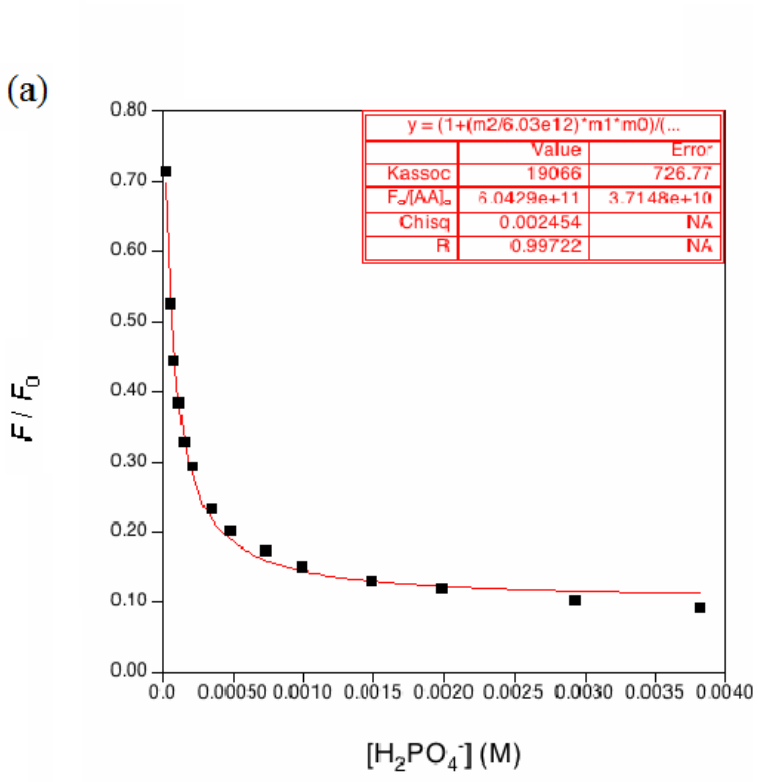
(a)
y = (1+(m2/6.03e12)*m1*m0)/(...
Value
Error
Kassoc
19066
726.77
F0[AA]0
6.0429e+11
3.7148e+10
Chisq
0.002454
NA
R
0.99722
NA
F / F0
[H2PO4-] (M)

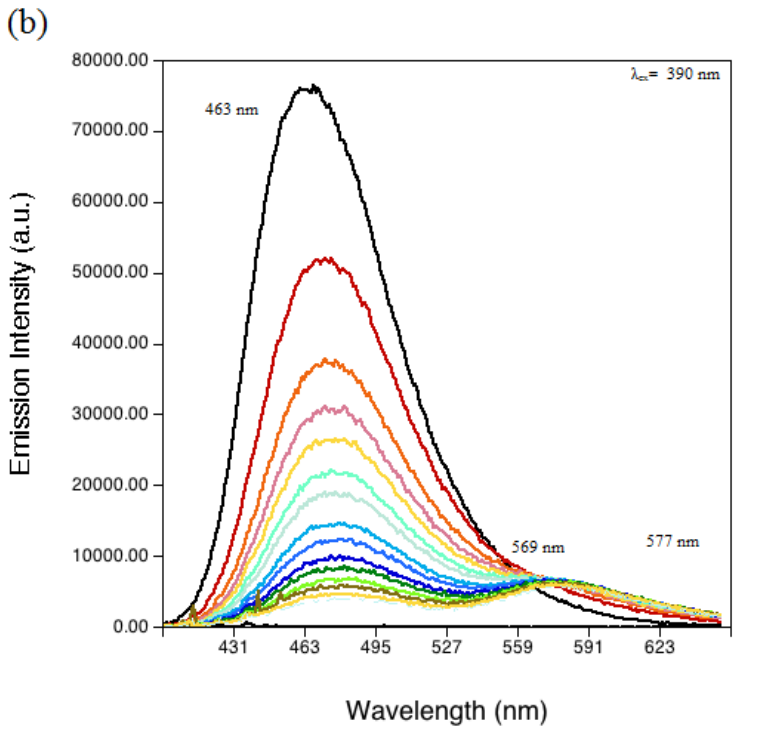
(b)
λex= 390 nm
463 nm
569 nm
577 nm
Emission Intensity (a.u.)
Wavelength (nm)

2.1 + HCO_3^-

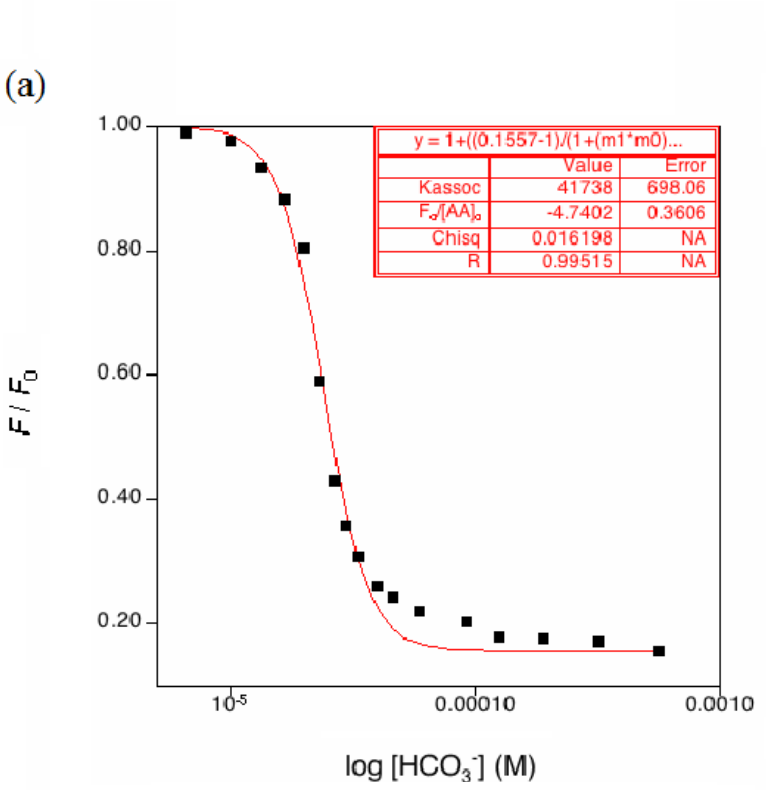
(a)
y = 1+((0.1557-1)/(1+(m1*m0)...
Value Error
Kassoc 41738 698.06
F0/[AA]0 -4.7402 0.3606
Chisq 0.016198 NA
R 0.99515 NA
1.00
0.80
0.60
0.40
0.20
F / F0
10-5
0.00010
0.0010
log [HCO3-] (M)

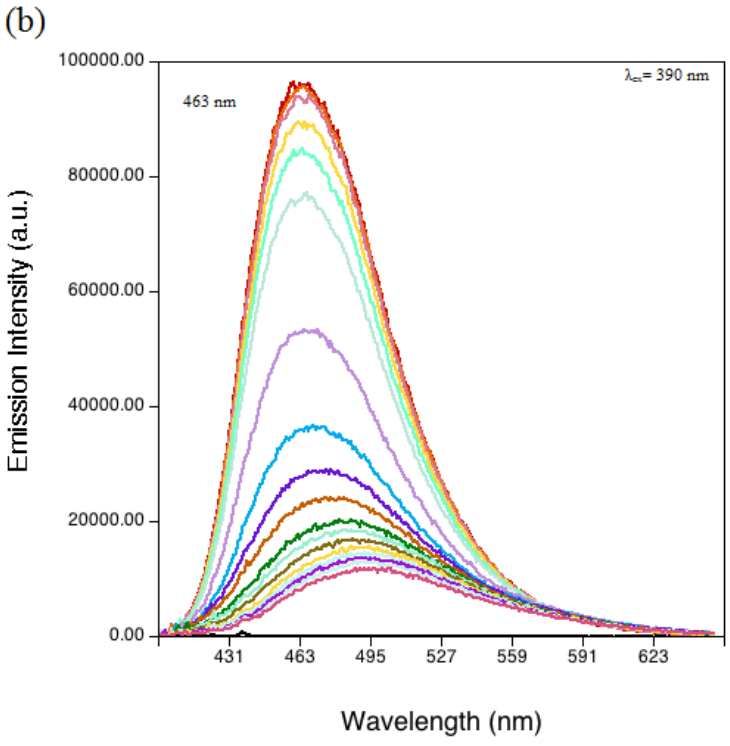
(b)
λex= 390 nm
463 nm
100000.00
80000.00
60000.00
40000.00
20000.00
0.00
Emission Intensity (a.u.)
431
463
495
527
559
591
623
Wavelength (nm)

2.1 + HCO_3^-

(a)

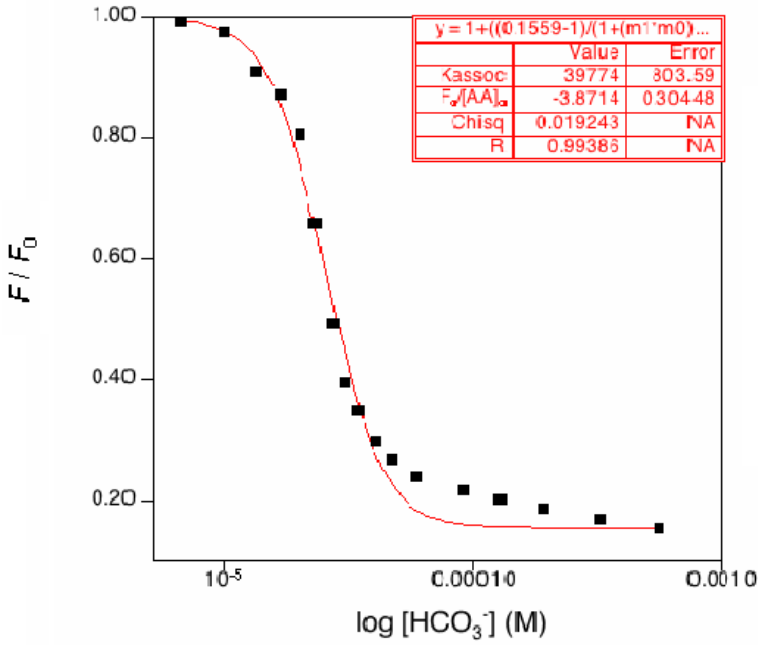
y = 1+((0.1559-1)/(1+(m1*m0)...
Value
Error
Kassoc
39774
803.59
Chisq
0.019243
NA
R
0.99385
NA
1.00
0.80
0.60
0.40
0.20
F / F0
10-5
0.00010
0.0010
log [HCO3-] (M)

(b)

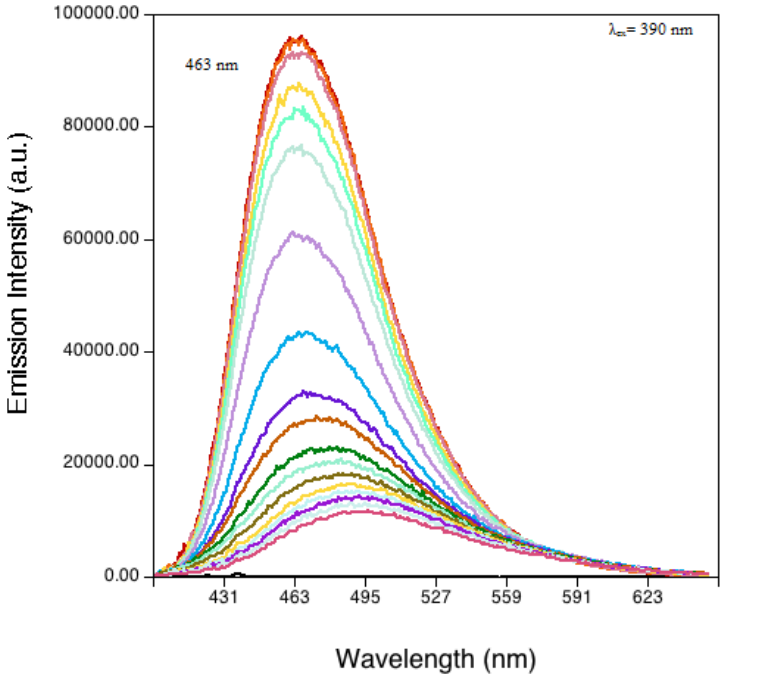
λex= 390 nm
463 nm
100000.00
80000.00
60000.00
40000.00
20000.00
0.00
Emission Intensity (a.u.)
431
463
495
527
559
591
623
Wavelength (nm)

2.1 + HCO_3^-

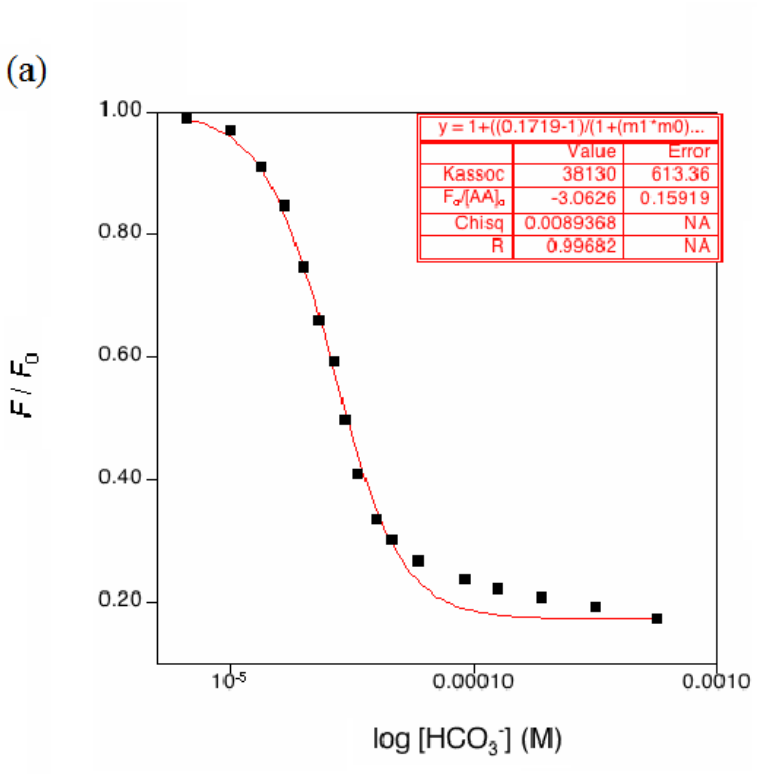
(a)
y = 1+((0.1719-1)/(1+(m1*m0)...
Value Error
Kassoc 38130 613.36
F∞/[AA]o -3.0626 0.15919
Chisq 0.0089368 NA
R 0.99682 NA
1.00
0.80
0.60
0.40
0.20
F / F0
10-5
0.00010
0.0010
log [HCO3-] (M)

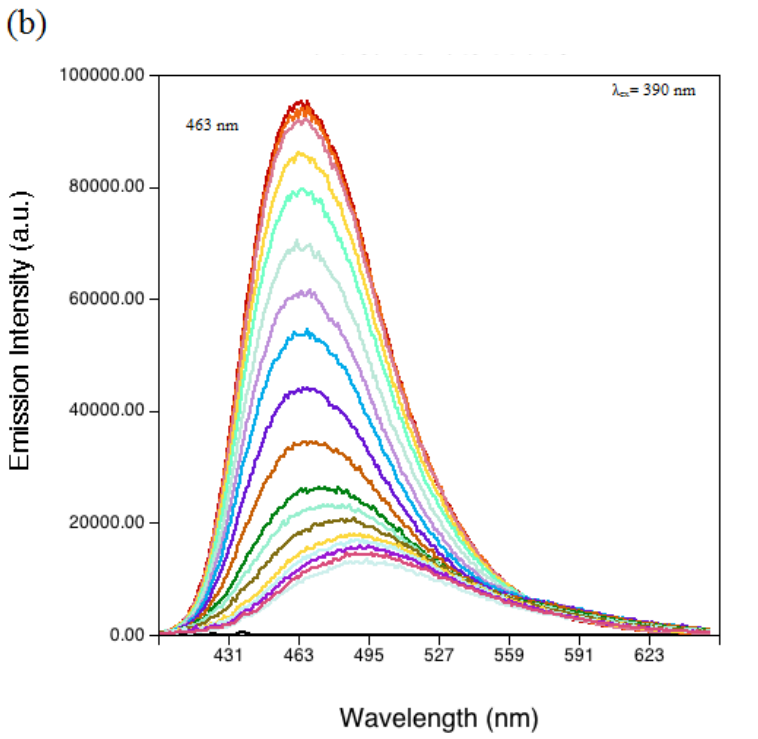
(b)
λex= 390 nm
463 nm
100000.00
80000.00
60000.00
40000.00
20000.00
0.00
Emission Intensity (a.u.)
431
463
495
527
559
591
623
Wavelength (nm)

2.1 + HCO_3^-

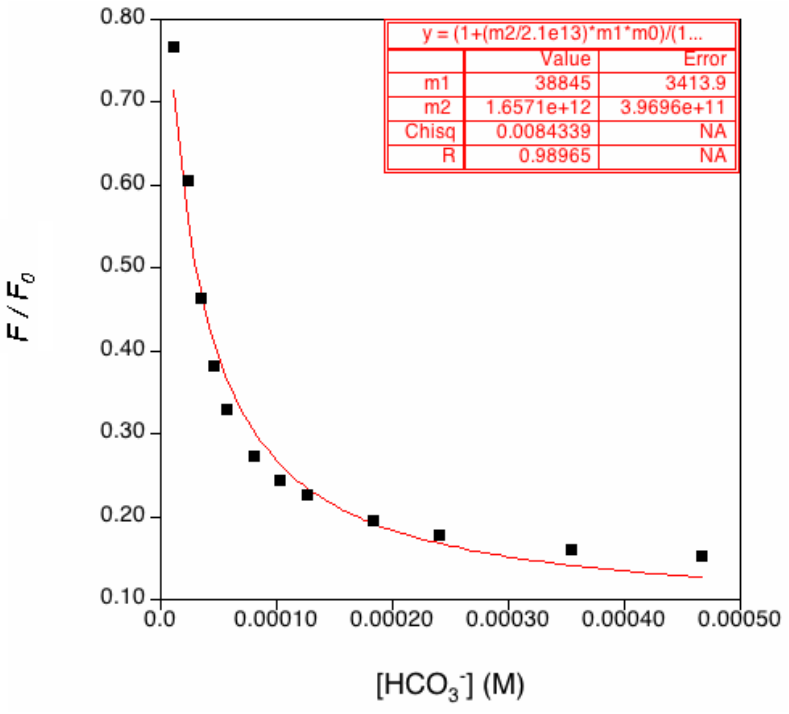

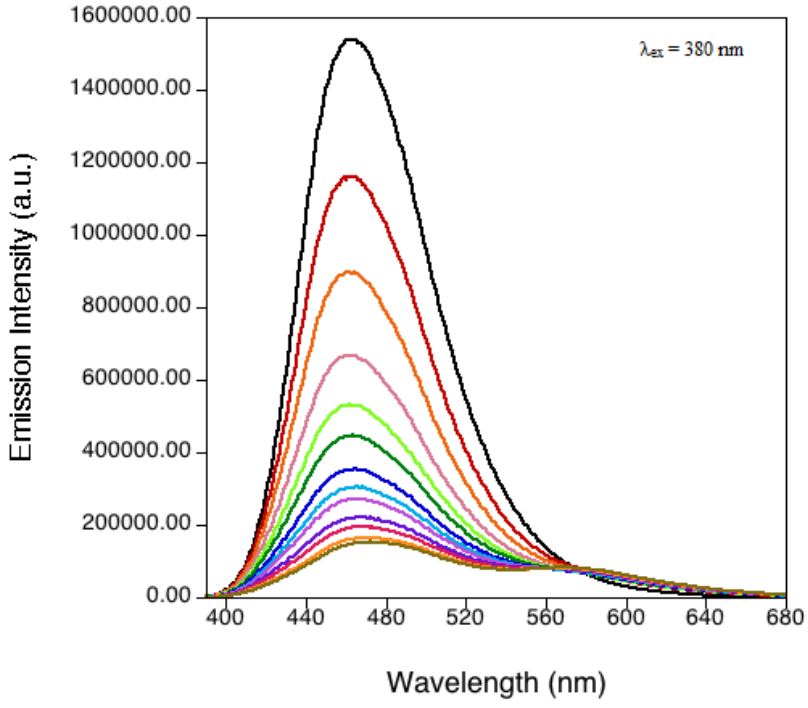

(A Fluorescence titration performed on a less concentrated host solution than used in the titrations that gave a sigmoidal shaped curve (Reference Figures 2.5 and 2.6))

2.1 + Cl^-

(a)

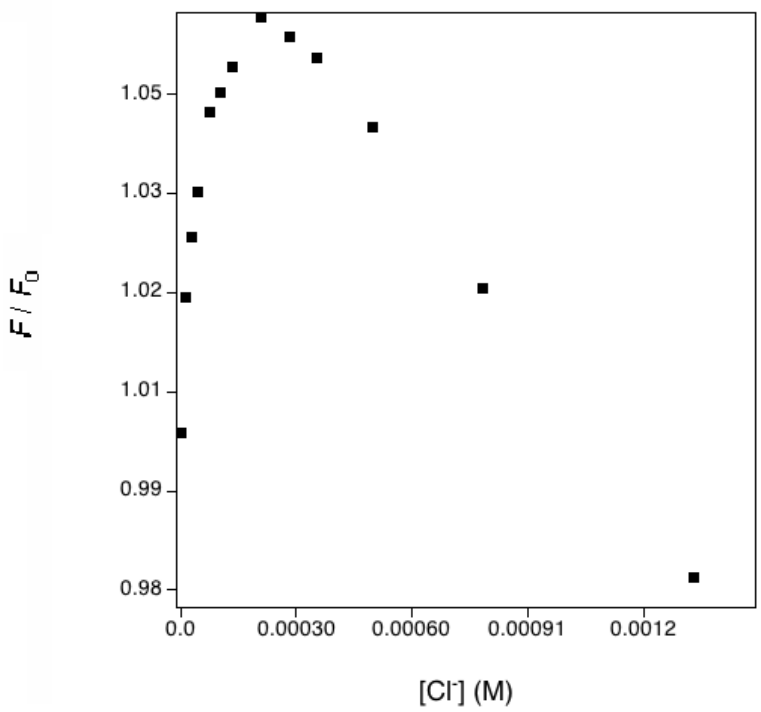
1.05
1.03
1.02
1.01
0.99
0.98
F / F0
0.0
0.00030
0.00060
0.00091
0.0012
[Cl-] (M)

(b)

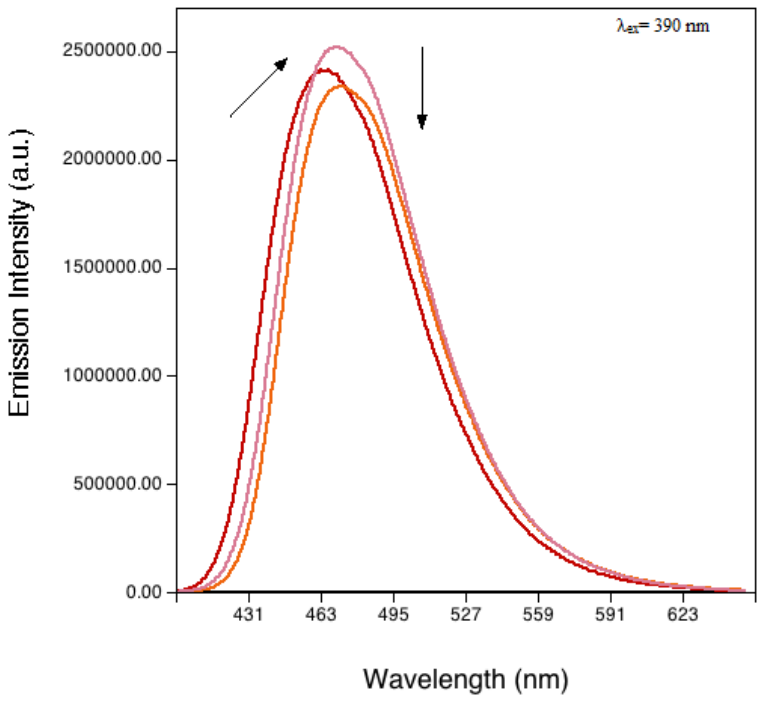
λex= 390 nm
2500000.00
2000000.00
1500000.00
1000000.00
500000.00
0.00
Emission Intensity (a.u.)
431
463
495
527
559
591
623
Wavelength (nm)

2.1 + NO_3^-

(a)

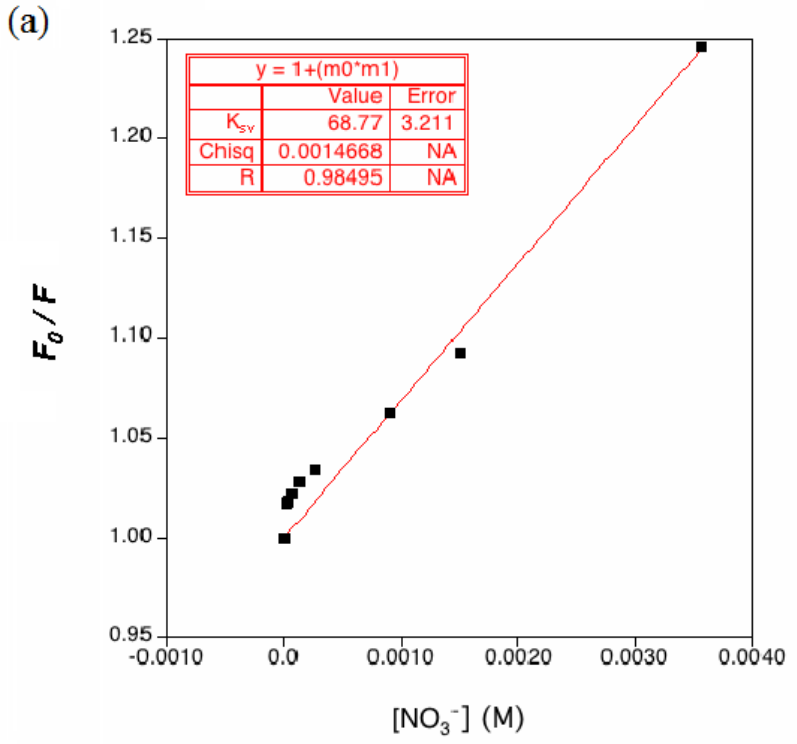
y = 1+(m0*m1)
Value Error
K_{SV} 68.77 3.211
Chisq 0.0014668 NA
R 0.98495 NA
F_0 / F
1.25
1.20
1.15
1.10
1.05
1.00
0.95
-0.0010
0.0
0.0010
0.0020
0.0030
0.0040
[NO_3^-] (M)

(b)

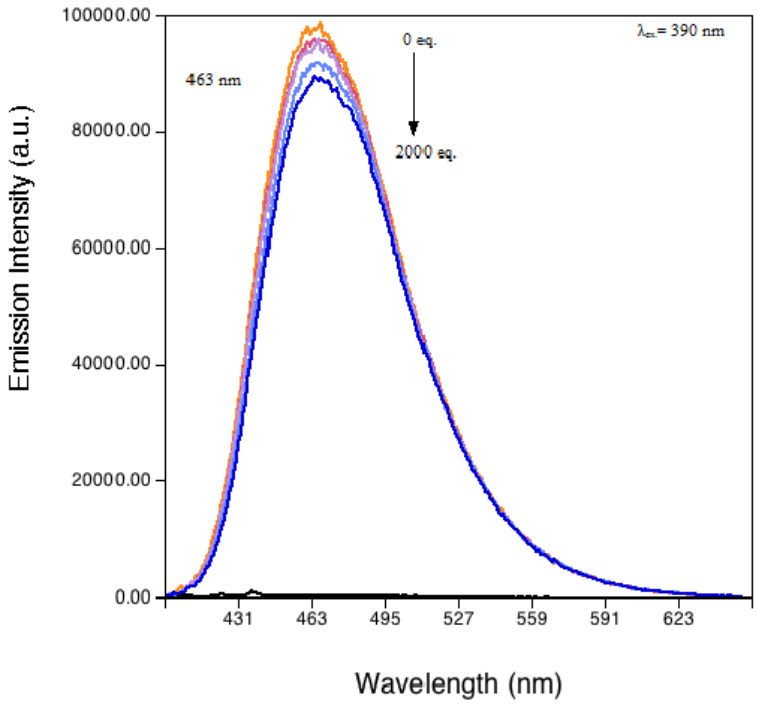
λ_{ex} = 390 nm
463 nm
0 eq.
2000 eq.
Emission Intensity (a.u.)
100000.00
80000.00
60000.00
40000.00
20000.00
0.00
431
463
495
527
559
591
623
Wavelength (nm)

2.2 + $H_2PO_4^-$

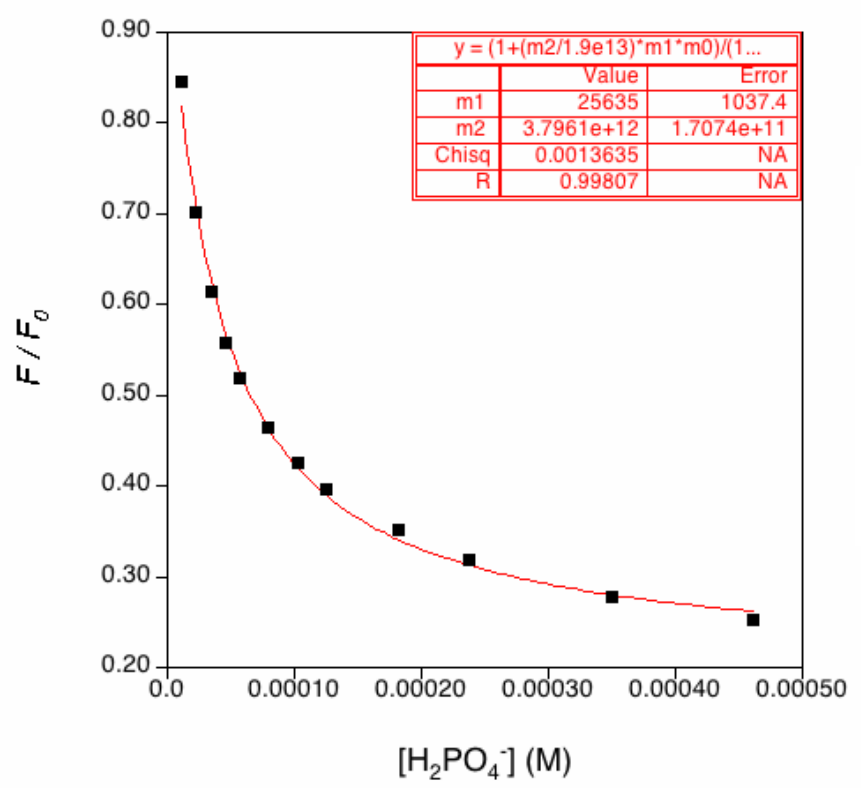
y = (1+(m2/1.9e13)*m1*m0)/(1...
Value Error
m1 25635 1037.4
m2 3.7961e+12 1.7074e+11
Chisq 0.0013635 NA
R 0.99807 NA
F / F0
0.90
0.80
0.70
0.60
0.50
0.40
0.30
0.20
0.0
0.00010
0.00020
0.00030
0.00040
0.00050
[H2PO4-] (M)

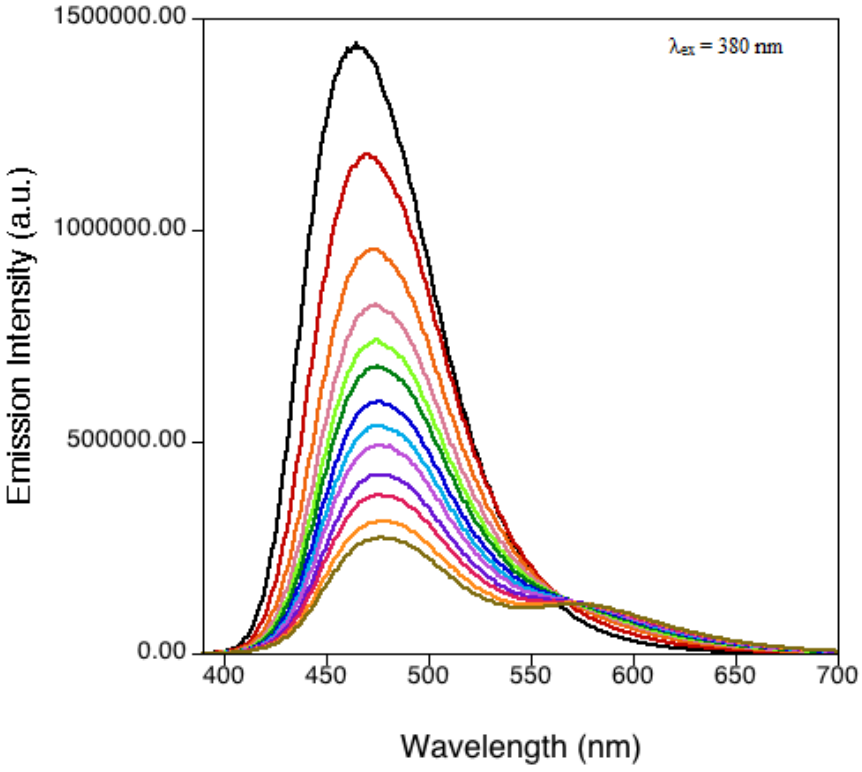
λex = 380 nm
Emission Intensity (a.u.)
1500000.00
1000000.00
500000.00
0.00
400
450
500
550
600
650
700
Wavelength (nm)

2.2 + $H_2PO_4^-$

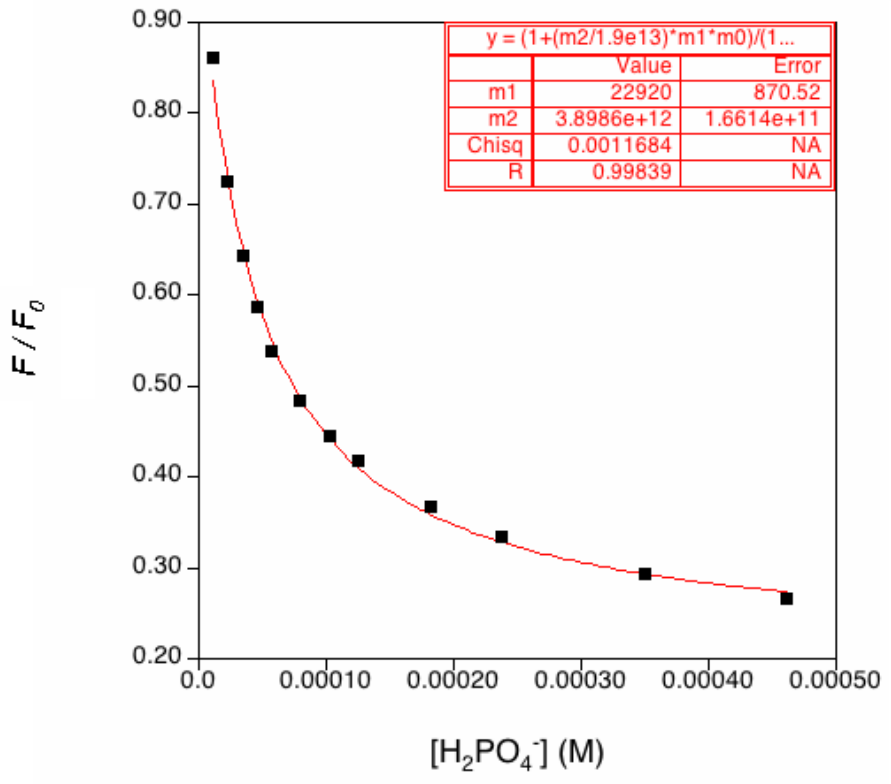
y = (1+(m2/1.9e13)*m1*m0)/(1...
Value Error
m1 22920 870.52
m2 3.8986e+12 1.6614e+11
Chisq 0.0011684 NA
R 0.99839 NA
F / F0
0.90
0.80
0.70
0.60
0.50
0.40
0.30
0.20
0.0
0.00010
0.00020
0.00030
0.00040
0.00050
[H2PO4-] (M)

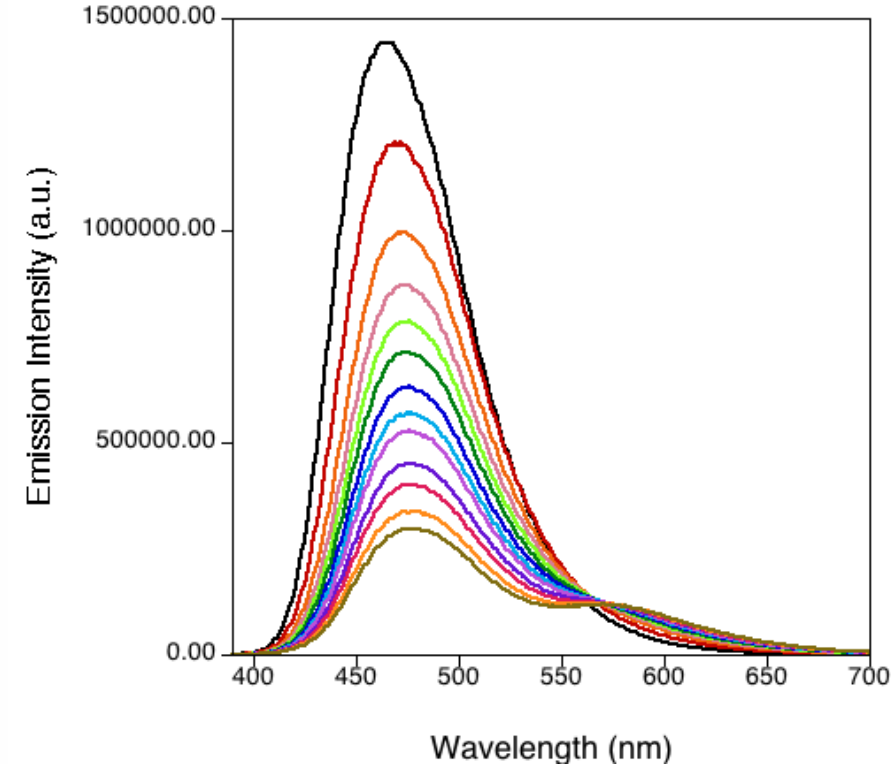
Emission Intensity (a.u.)
1500000.00
1000000.00
500000.00
0.00
400
450
500
550
600
650
700
Wavelength (nm)

2.2 + $H_2PO_4^-$

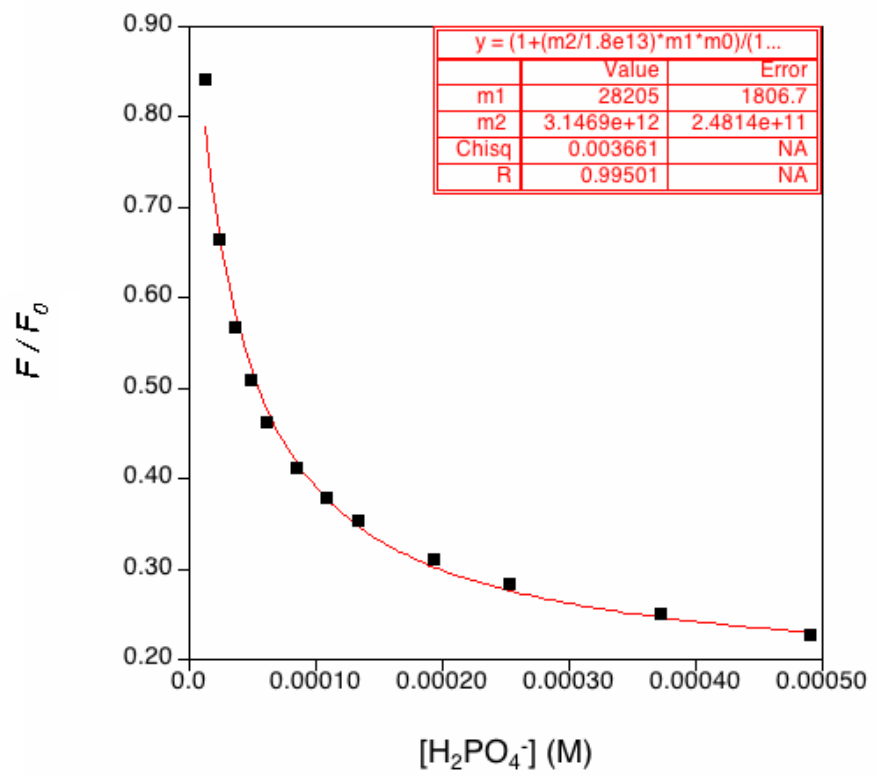
y = (1+(m2/1.8e13)*m1*m0)/(1...
Value Error
m1 28205 1806.7
m2 3.1469e+12 2.4814e+11
Chisq 0.003661 NA
R 0.99501 NA
F / F0
0.90
0.80
0.70
0.60
0.50
0.40
0.30
0.20
0.0
0.00010
0.00020
0.00030
0.00040
0.00050
[H2PO4-] (M)

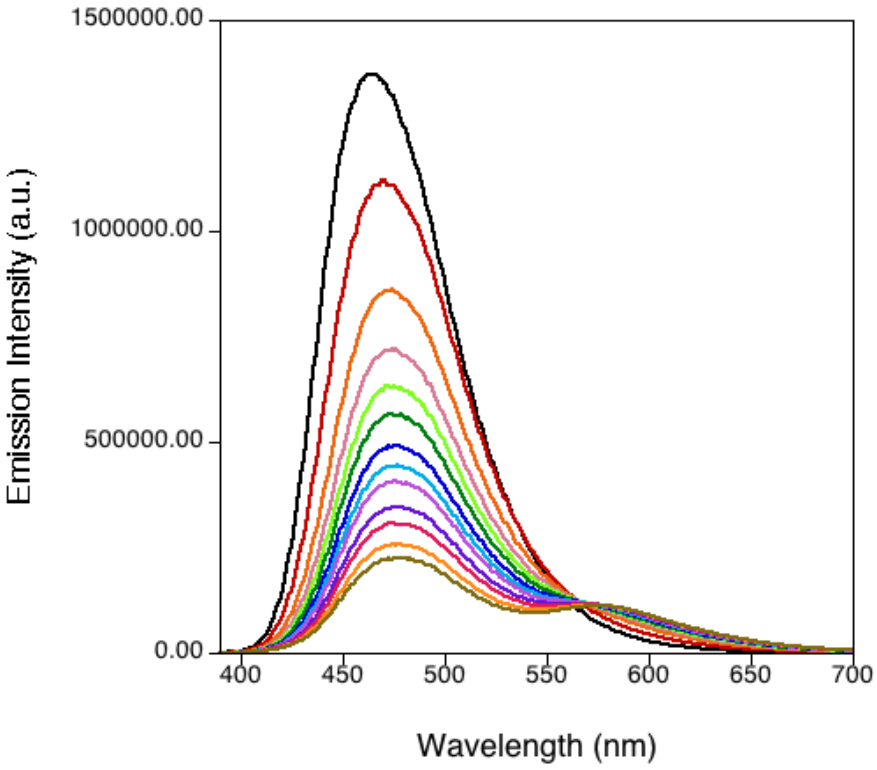
Emission Intensity (a.u.)
1500000.00
1000000.00
500000.00
0.00
400
450
500
550
600
650
700
Wavelength (nm)

2.2 + Cl^-

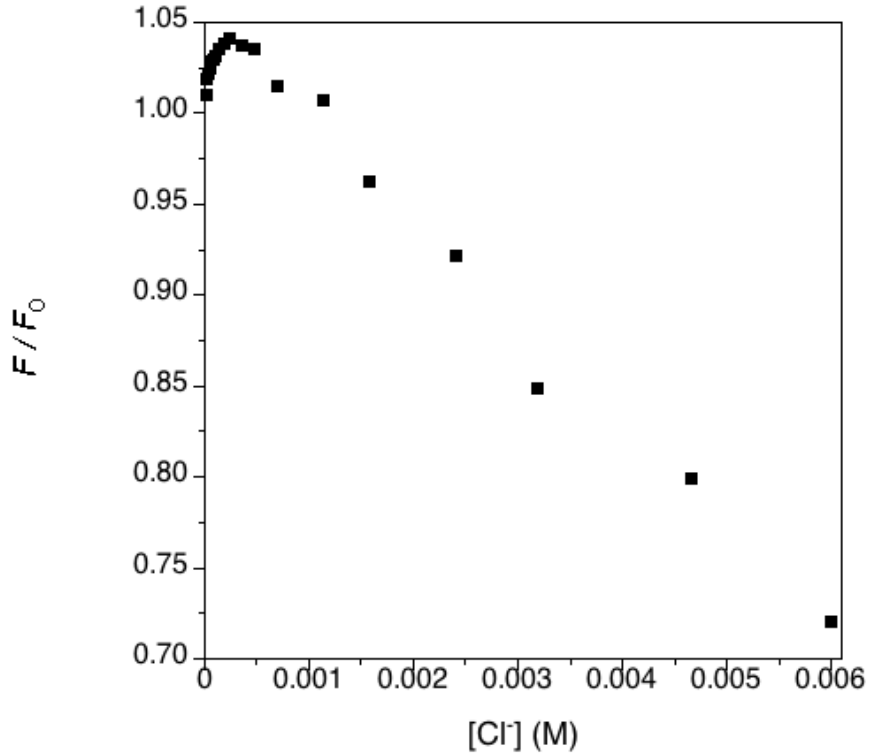
1.05
1.00
0.95
0.90
0.85
0.80
0.75
0.70
F / F0
0
0.001
0.002
0.003
0.004
0.005
0.006
[Cl-] (M)

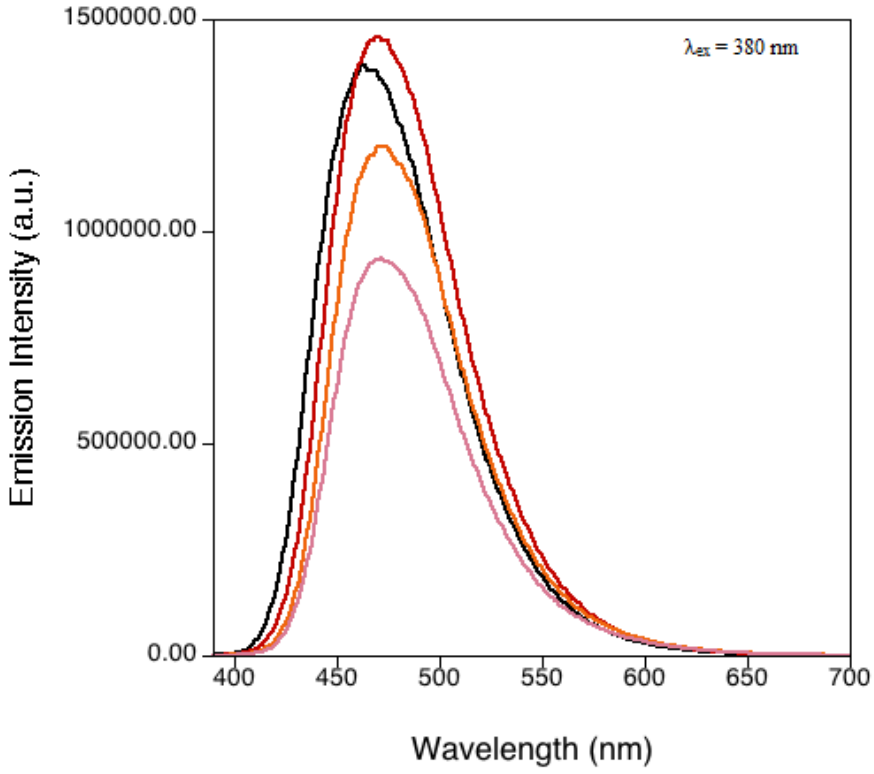
1500000.00
1000000.00
500000.00
0.00
λex = 380 nm
Emission Intensity (a.u.)
400
450
500
550
600
650
700
Wavelength (nm)

2.2 + Cl^-

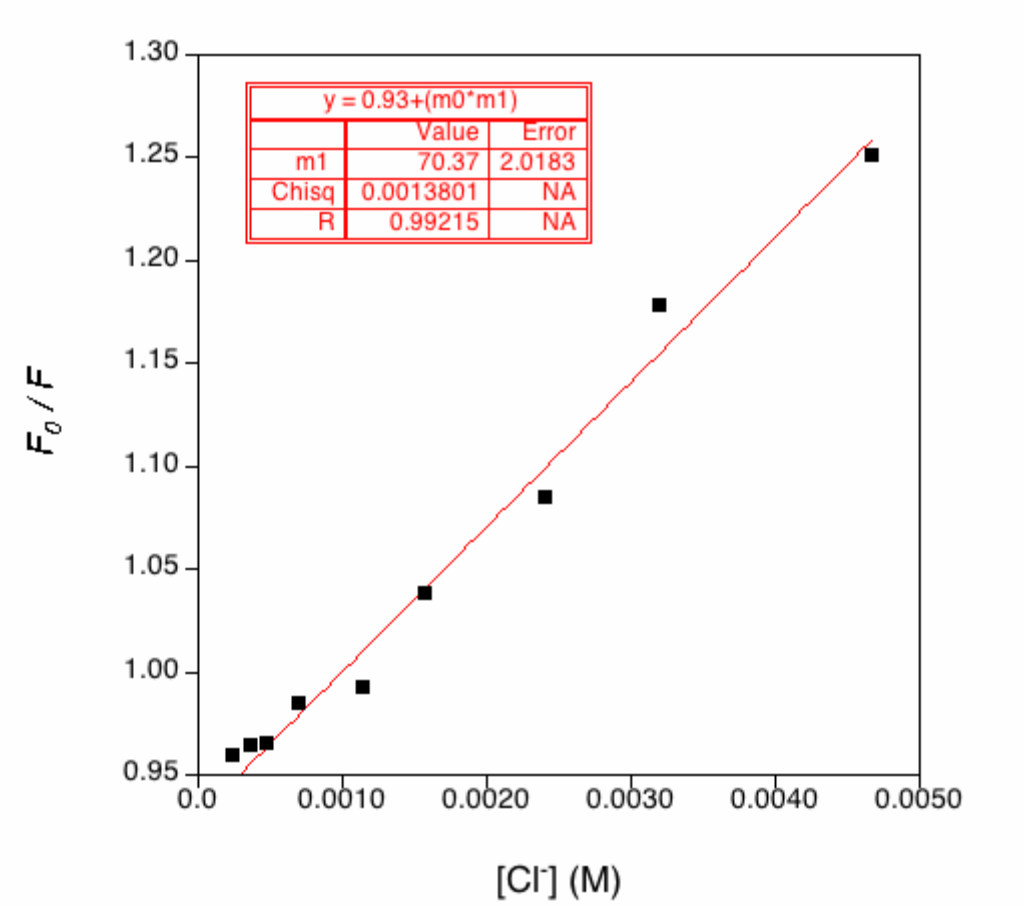
y = 0.93+(m0*m1)
Value Error
m1 70.37 2.0183
Chisq 0.0013801 NA
R 0.99215 NA
1.30
1.25
1.20
1.15
1.10
1.05
1.00
0.95
F_0 / F
0.0
0.0010
0.0020
0.0030
0.0040
0.0050
[Cl-] (M)

3.7 + Cl^-

(a)

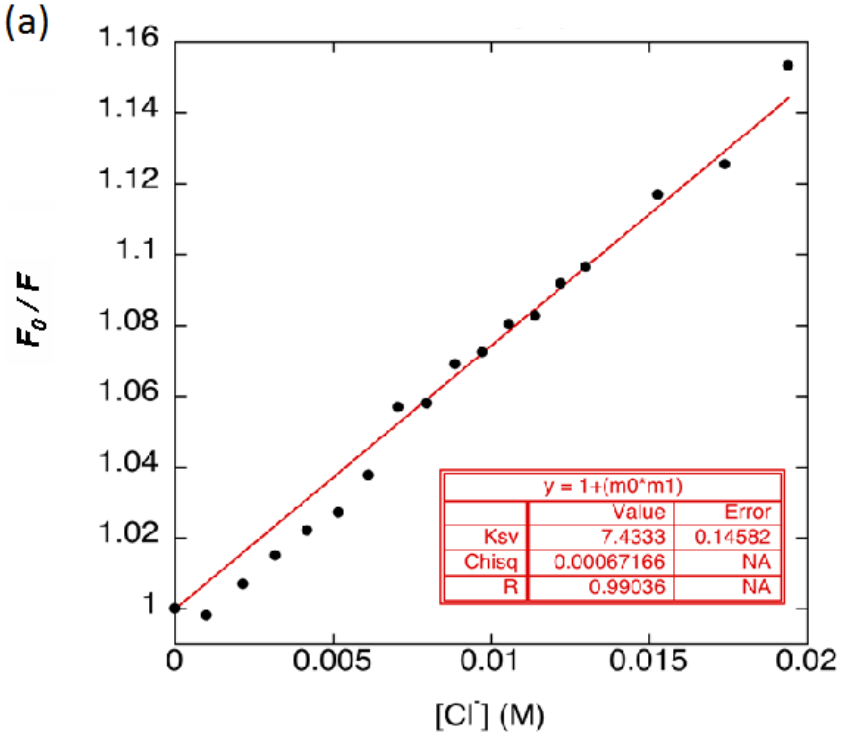
1.16
1.14
1.12
1.1
1.08
1.06
1.04
1.02
1
F_0 / F
0
0.005
0.01
0.015
0.02
[Cl⁻] (M)
y = 1+(m0*m1)
Value
Error
Ksv
7.4333
0.14582
Chisq
0.00067166
NA
R
0.99036
NA

(b)

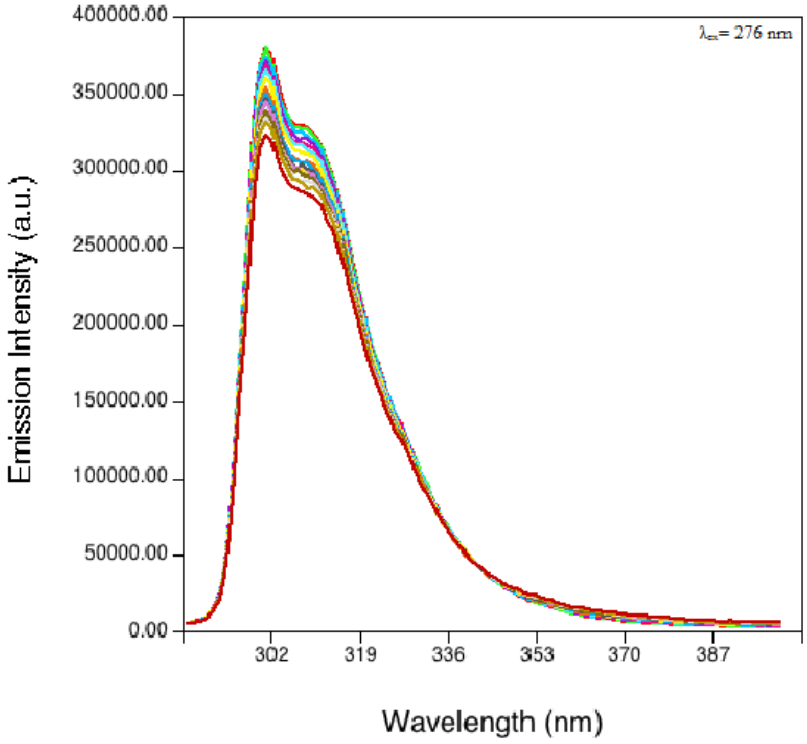
400000.00
350000.00
300000.00
250000.00
200000.00
150000.00
100000.00
50000.00
0.00
Emission Intensity (a.u.)
λ_{ex}= 276 nm
302
319
336
353
370
387
Wavelength (nm)

3.7 + CH_3COO^-

(a)

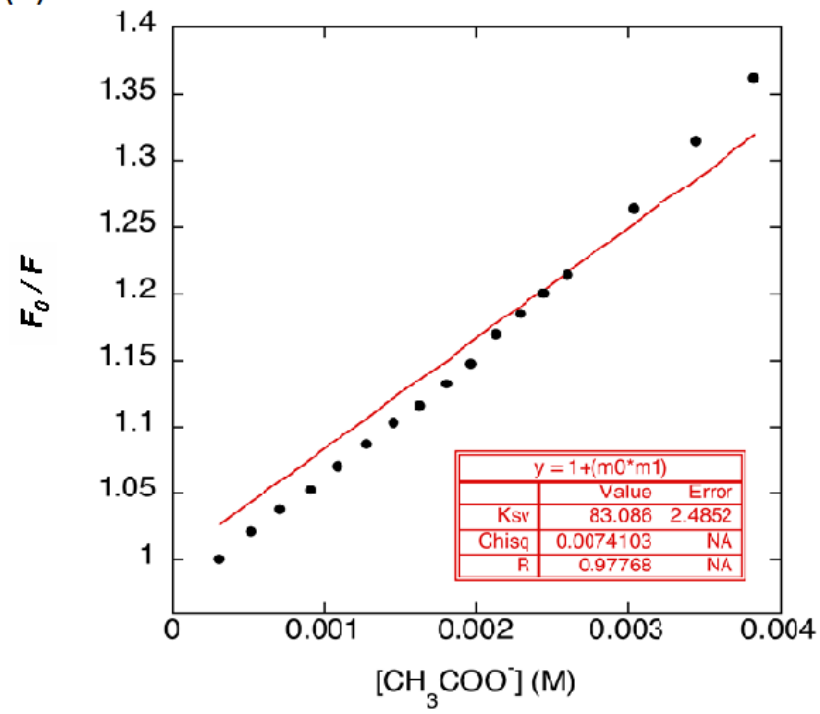
1.4
1.35
1.3
1.25
1.2
1.15
1.1
1.05
1
F0 / F
0
0.001
0.002
0.003
0.004
[CH3COO-] (M)
y = 1+(m0*m1)
Value Error
Ksv 83.086 2.4852
Chisq 0.0074103 NA
R 0.97768 NA

(b)

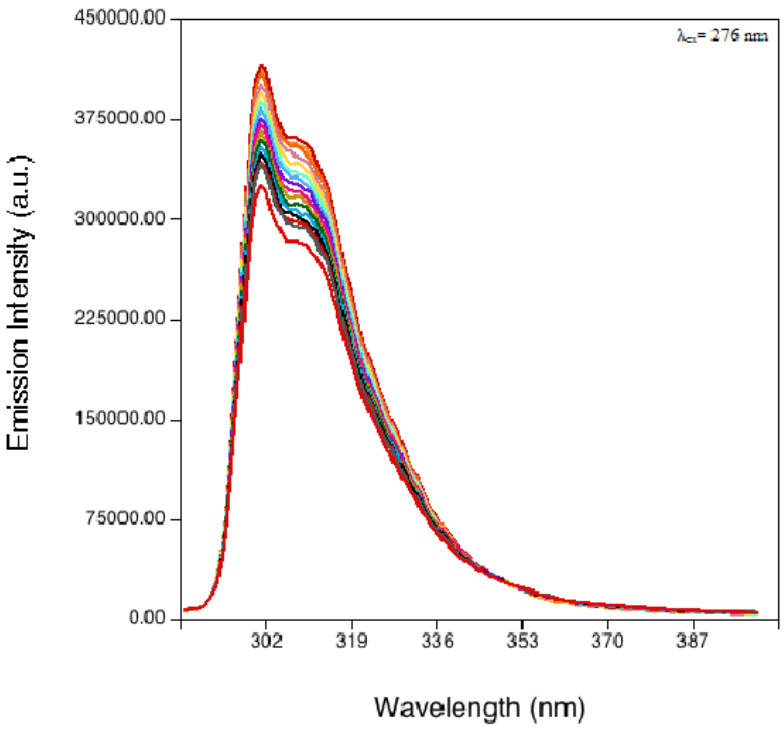
450000.00
375000.00
300000.00
225000.00
150000.00
75000.00
0.00
λex= 276 nm
Emission Intensity (a.u.)
302
319
336
353
370
387
Wavelength (nm)

3.2 + Cl^-

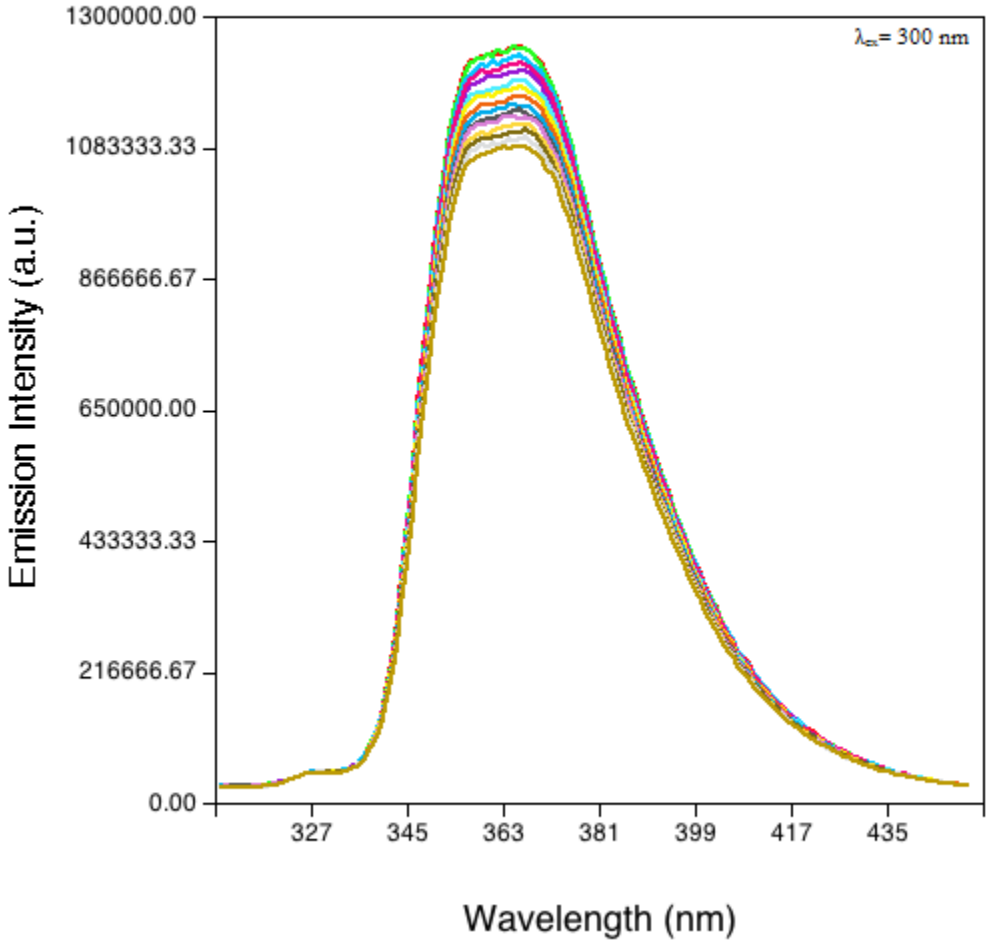
1300000.00
1083333.33
866666.67
650000.00
433333.33
216666.67
0.00
Emission Intensity (a.u.)
327
345
363
381
399
417
435
Wavelength (nm)
λex= 300 nm

APPENDIX B: ^{1}H-NMR, MASS SPECTROSCOPY, AND HPLC

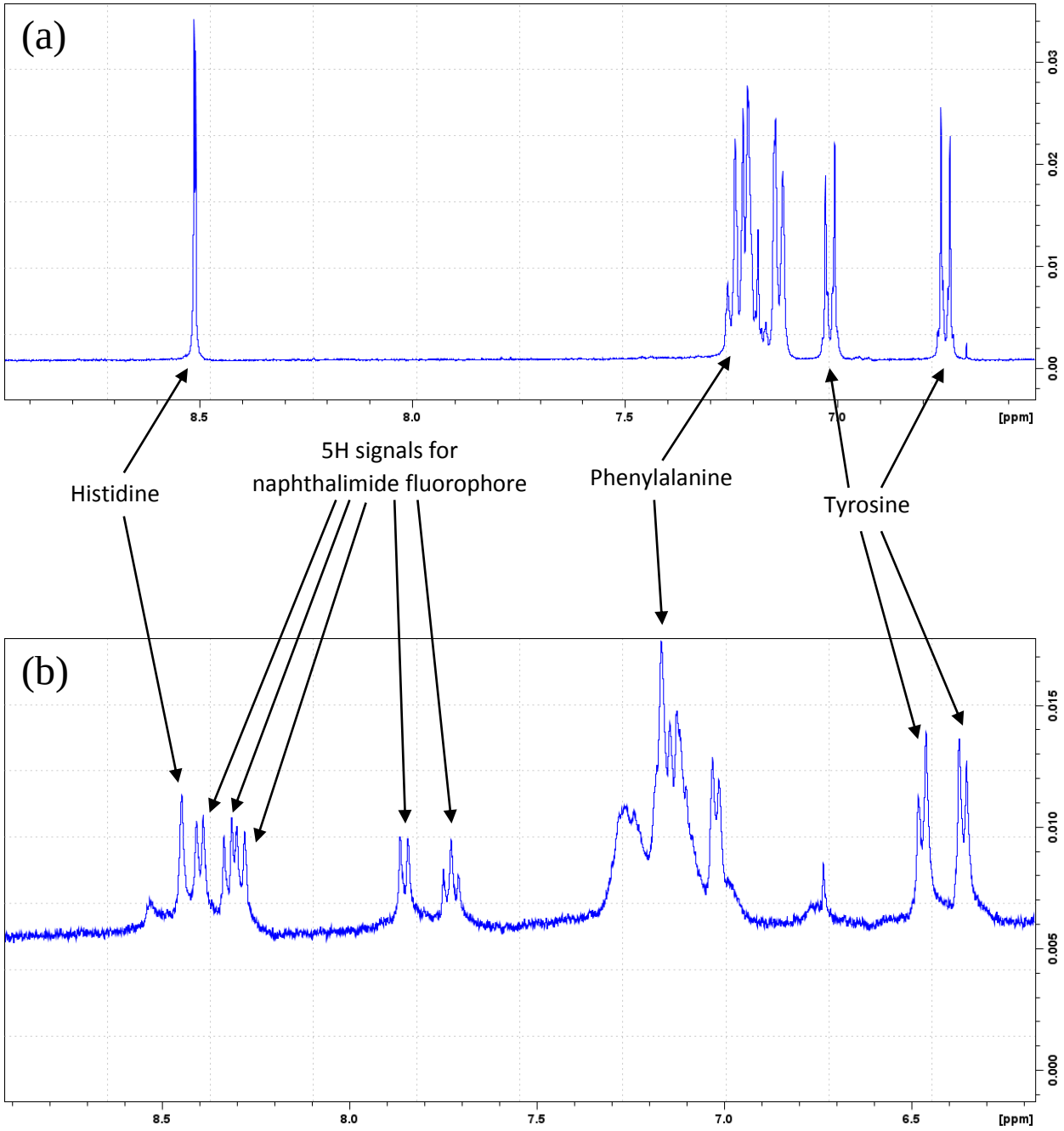

(a) YKKEIAHALFSA-NH_2 CONTROL PEPTIDE

(b) YKK-E*-IAHALFSA-NH_2 FLUORESCENT PEPTIDE WITH 2.1 DERIVATIVE

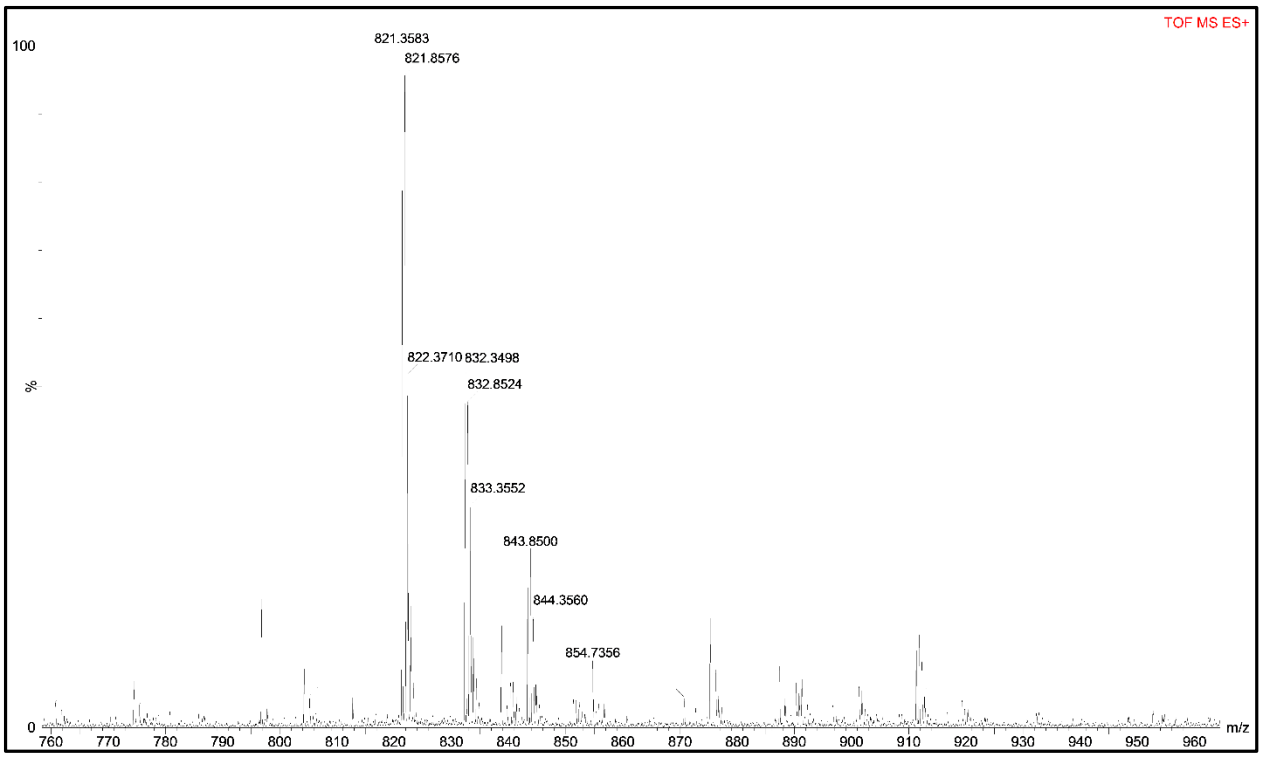

YKK-E*-IAHALFSA-NH_2 fluorescent peptide with 2.1 derivative (HRMS ESI calcd for $(M+H)^+$ 1641.8900, found 1641.6640. Calcd for $(M+2H)^{2+}$ 821.4486, found 821.3583. Calcd for $(M+Na+H)^{2+}$ 832.4396, found 832.3498. Calcd for $(M+2Na)^{2+}$ 843.4306, found 843.3474.

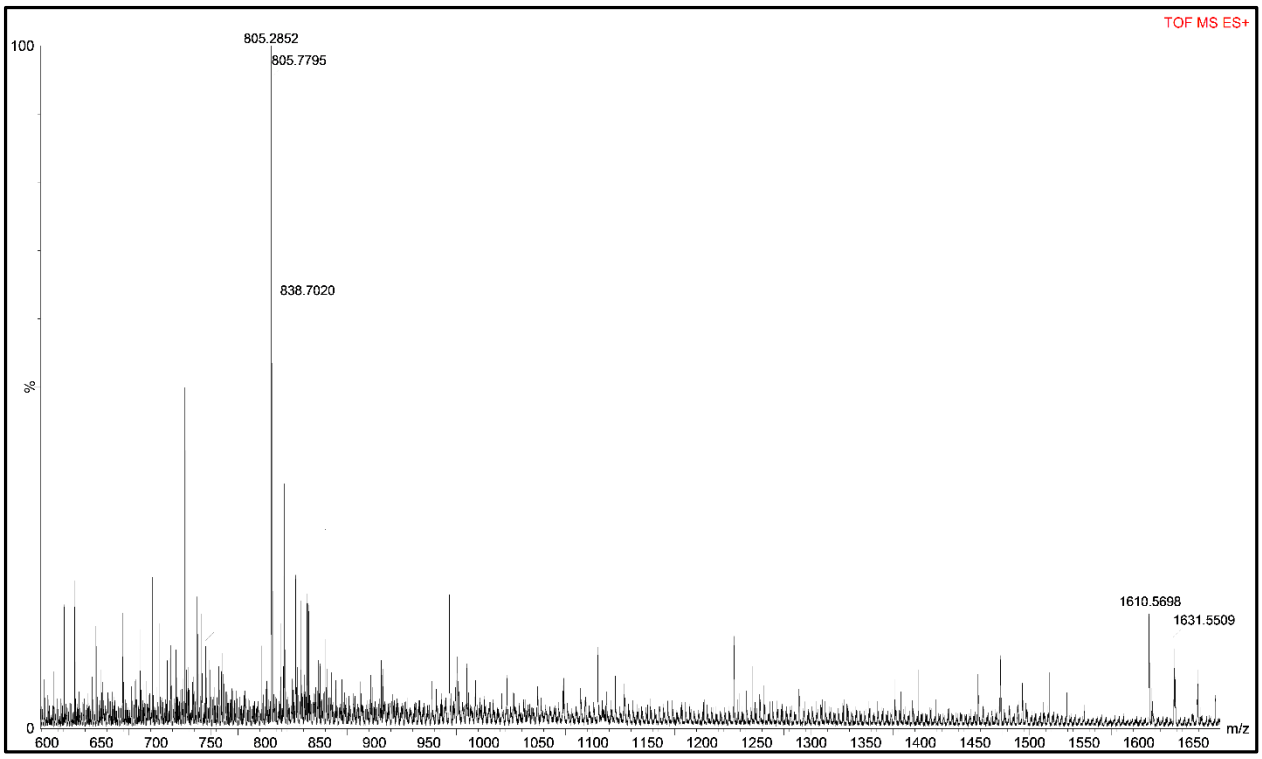

YKKEIAHAL-D*-SA-NH_2 fluorescent peptide with 2.2 derivative (HRMS ESI calcd for $(M+H)^+$ 1609.8485, found 1609.5603. Calcd for $(M+2H)^{2+}$ 805.4279, found 805.2852. Calcd for $(M+Na+H)^{2+}$ 816.4189, found 816.2787. Calcd for $(M+2Na)^{2+}$ 827.4099, found 827.2510.

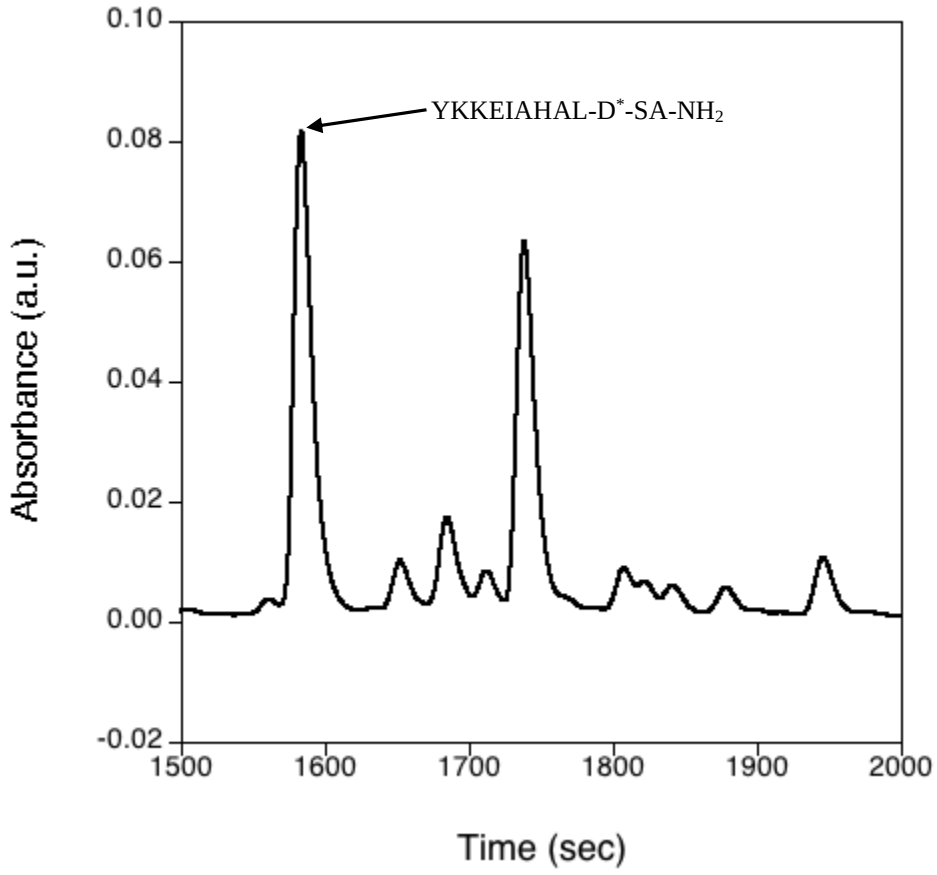

HPLC trace of YKKEIAHAL-D*-SA-NH_2 with the peak at R_t = 1584 seconds. The method used was as follows: Flow rate 1.00 mL/min, Buffer A: acetonitrile/0.1% TFA, Buffer B: Water/0.1% TFA. Start, Isocratic Flow (A:B, 10:90) 2 min, Load/Inject Sample (0.250 mL), Zero Baseline, Linear Gradient (A:B, 10:90 → 50:50) 30 min, Isocratic Flow (A:B, 50:50) 5 min, Linear Gradient (A:B, 50:50 → 100:0) 5 min, Isocratic Flow (A:B, 100:0) 3 min, Linear Gradient (A:B, 100:0 → 10:90) 5 min, Isocratic Flow (A:B, 10:90) 2 min, End of Protocol. YKKEIAHAL-D*-SA-NH_2 eluted at A:B = 42:58 detected by 375 nm light.